DISTRIBUTION OF RETRACTIVE FORCE TO ANTERIOR TEETH DURING *EN MASSE* RETRACTION

Sean Andrew Corsini
B.Sc., Dip. Hons., D.D.S.

A dissertation submitted in partial fulfillment of the
requirements for the degree of

Master of Science (M.Sc.)

in

Orthodontics,
Department of Preventive Dental Science
Faculty of Dentistry
of the
University of Manitoba
Winnipeg, Manitoba,
Canada

THE UNIVERSITY OF MANITOBA

FACULTY OF GRADUATE STUDIES

*****

COPYRIGHT PERMISSION PAGE

Distribution of Retractive Force to Anterior Teeth During *En Masse* Retraction

BY

Sean Andrew Corsini

A Thesis/Practicum submitted to the Faculty of Graduate Studies of The University of Manitoba in partial fulfillment of the requirements of the degree of

MASTER OF SCIENCE

ABSTRACT

Orthodontists have always been concerned regarding the forces they deliver to teeth during orthodontic treatment. The clinical analyses of such forces have been largely intuitive. Traditionally, it is assumed that the forces of retraction are distributed equally among the anterior teeth during frictionless *en masse* retraction. The present study was intended to elucidate the distribution of retractive force transmitted to individual teeth of the anterior segment by a semicircular archwire during frictionless *en masse* retraction. Theoretical models based in static free-body mechanics were developed for both infinitely flexible and infinitely rigid semicircular archwires to predict the distribution of retractive force on the six anterior teeth delivered by the archwire alone. The theoretical models produced similar results for the distribution of retractive force to the anterior teeth, namely, 55.0% of the retractive force is delivered to the central incisor, 31.2% to the lateral incisor and 13.7% to the canine. Using six acrylic rods to represent the anterior teeth, experimental testing produced results that were in close agreement with theoretical predictions. For each central incisor rod pair, no statistically significant difference ($p>0.05$) in the mean values of the retractive component was found. The same was true for both the lateral incisor and canine rod pairs. The mean magnitude of the retractive component was greatest for the central incisors, less for the lateral incisors, and lowest for the canines. There were also no statistically significant differences ($p>0.05$) in mean values of retractive force for a given rod when tested with flexible or rigid archwires. Statistically significant differences ($p>0.001$) in mean magnitudes of retractive force components were found between the rods representing central incisors, lateral incisors and canines during testing with both flexible and rigid archwires. The

presence of medial components which were not predicted by the theoretical models indicate that these models are incomplete in their present form. Results seem to have implications for anchorage control as well as the need for improved appliance design to effect efficient *en masse* anterior retraction.

TABLE OF CONTENTS

LIST OF FIGURES

LIST OF TABLES

CHAPTER 1

INTRODUCTION

"From the nature of things, ideas do not come from prosperity, affluence and contentment, but rather from the blackness of despair, not in the bright light of day, nor the footlight's glare, but rather in the quiet undisturbed hours of midnight, or early morning, when one can be alone to think. These are the grandest hours of all, when imagination is allowed to run riot on the problem that blocks the progress of research, when the hewn stones of scientific fact are turned over and over, and fitted in so that the mosaic figure of truth discovered by Mother Nature long ago, be formed from the chaos."

F.G. Banting

1.1 FOREWORD

Orthodontics deals with the treatment of dental malocclusion and provides a means for effecting substantial change in the positions of teeth with the goals of improving occlusion and appearance. Implicit in this is the application of forces to teeth to cause dental movement through bone and surrounding tissues. Orthodontic appliances are used to apply mechanical forces to the teeth in the direction of their desired movement. Force is transmitted from the appliance(s) to the periodontal structures via the *en face* root surface area of a tooth, which, as explained by Lee,[1] is the side of the root facing the direction of motion and is equal to approximately half of the root surface area within bone. Many orthodontic appliances exist and have been developed, often with little knowledge of the nature of the force systems they generate.

1.2 MOTIVATION FOR THIS INVESTIGATION

Although orthodontists remain interested in the forces they deliver to teeth, the clinical analysis of such force systems has correctly or incorrectly been intuitive, and myriad malocclusions have been successfully corrected, often with little knowledge of the magnitude or direction of force and moments delivered from commonly used orthodontic appliances.[2,3] Specific data on the relation between force systems and dental movement is essential not only to facilitate orthodontic treatment in a safe and timely manner, but also to establish an understanding for appropriate appliance design.[4,5] The motivation of this investigation is not to shed more light on the relation between force and dental movement, but rather to analyze the force system that is commonly delivered during *en masse* retraction and determine if an assumption that many clinicians take for granted in

appliance design and behavior are correct, specifically, if there is an equal distribution of retractive force to the individual anterior teeth.

1.3 PURPOSE OF THIS INVESTIGATION

The purpose of this investigation is two fold.

1. To mathematically model the retractive forces delivered to the six anterior teeth such that the proportion of the total retractive force to a particular tooth alone can be theoretically determined.
2. To test the validity of the mathematical model by developing a physical model of the six anterior teeth, which allows measurement of the force experienced by each anterior tooth from the archwire. The model will be designed such that the teeth can resist moments, allowing only the magnitude and direction of the applied force produced by the retractive force to be measured.

1.4 RATIONALE OF THIS METHOD OF INVESTIGATION

The approach to this investigation offers many advantages. First, a mathematical model permits easy definition and manipulation of a defined number of variables. It also provides a sound theoretical basis for any physical model of the same system. Second, a physical model of a biomechanical system allows for a limited number of variables compared to a biomechanical system which has numerous, often uncontrollable variables which cause difficulty in interpretation of results. Third, the physical apparatus is developed such that every "tooth" being examined responds homogeneously to an applied force, that is, each "tooth" in the apparatus would generally respond in the same

way to the same force. The advantage of this is simply ease of interpretation of results. Since a purpose of this investigation is to measure the proportion of total retractive force transmitted to each "tooth," a similar response of each "tooth" permits direct comparison without having to account for differences in "tooth" size and shape, etc. Fourth, and most importantly, this novel mathematical and *in vitro* approach permits analysis of an otherwise unsolvable *in vivo* force system. Difficulties of force measurement *in vivo* are described in Chapter 2, as are descriptions of various *in vitro* approaches.

1.5 NULL HYPOTHESIS

The null hypothesis of this investigation states that there is an equal distribution of the retractive force among the anterior six teeth for a posteriorly directed retractive force in *en masse* retraction.

CHAPTER 2

REVIEW OF THE LITERATURE

2.1 CONCEPT OF OPTIMAL FORCE

Two fundamental characteristics of orthodontic appliances which are paramount to their proper use are the appropriateness of the applied force (biologic force), and the distribution of this applied force to teeth. Many clinicians assume that there is an equal distribution of the retractive force to the individual anterior teeth. The essence of the present investigation is to test and determine whether this assumption about *en masse* space closure is correct. If in fact an equal distribution of retractive force exists in this situation, we would question whether a particular force that is appropriate for orthodontic movement of a central incisor would also be appropriate for a smaller-rooted tooth like the lateral incisor or a larger-rooted tooth like the canine. An examination of the literature and early experimentation may serve to illuminate the concept of appropriate force in orthodontic treatment.

2.1.1 RELATION BETWEEN BIOLOGIC RESPONSE AND APPLIED ORTHODONTIC FORCE

While tooth movement through bone is a function of the applied force from the appliance to the tooth, it is also a function of the biologic response within the supporting structures of the teeth. The first investigator to systematically investigate the biologic response to orthodontic movement was Sandstedt. In 1904 he conducted experiments involving placement of a labial bow against the incisors of a dog and tipping the canine teeth mesially by daily turns of screws (located at the termini of the labial bow). He described histologic results of the effects of various forces applied to the canine teeth, and was able to show that orthodontic movement was achieved for both low and high forces. Further,

the movement from high force involved necrosis of supporting structures in a process which he called "undermining resorption." Interpretation of his results suggests that the biologic processes involved in orthodontic movement are more acceptable, physiologically, when low forces are employed. This in turn implies that there is a maximum force which teeth can tolerate before adverse or destructive processes occur. A failing of his study is the lack of any quantitative information in regards to the magnitudes of the orthodontic forces used in his study. [6]

The earliest quantitative information of the biologic response to an applied orthodontic force is provided by Schwarz in 1932. Using finger springs to deliver calibrated forces to tip dog premolars buccally, he was able to show that, histologically, the physiologic processes of bone resorption and deposition that allowed dental movement from low orthodontic forces were less destructive than those processes which ensued when high orthodontic forces were used. Each calibrated spring exerted a tipping force to a group of three ipsilateral dog premolar teeth. He expressed these forces as pressures, and based on the results from Sandstedt, stated that dental movement was not destructive when the pressures generated were not greater than the physiologic blood pressure of the capillaries within the periodontal ligament space, which approximates an orthodontic pressure not greater than 20 to 26 grams per square centimeter of root surface for mammalian teeth. His reasoning was that if the capillaries within the periodontal ligament space were not occluded, undermining resorption would not occur. His experimental results were consistent with those of Standstedt and he determined that safe orthodontic tooth movement occurred with continuous forces of 15 to 20 grams per square centimeter of

root surface, and undermining resorption occurred when the capillaries were occluded. In his theory, the existence of an optimal force at which orthodontic dental movement is safe and efficient is implicit.[7]

2.1.2 THE WORK OF STOREY AND SMITH

Investigating the concept of optimal force in orthodontic movement, Storey and Smith set out to determine the values of forces that should be used for specific orthodontic purposes, particularly cuspid retraction in human patients.[8,9] Stating that there was a lack of generally accepted information in this regard, they worked under the assumption that a light continuous force would yield the best result, based in part on the works by Sandstedt,[6] Schwarz[7] and Oppenheim.[10,11] Storey and Smith postulated the existence of an optimum force or optimum range of forces which should be used for safe and effective orthodontic dental movement. The term "optimum force" usually describes a force that produces the most rapid and safe tooth movement.[12] Storey sand Smith were dissatisfied with Schwarz's experimental protocol, claiming that the distribution of force over the length of a calibrated spring *in situ* is impossible to assess: Schwarz measured the force of the finger spring at each site of application individually prior to application,[7] but the force system when applied to all three premolar teeth simultaneously cannot be resolved. Also, the springs were reactivated several times during the experiments. Storey and Smith were also dissatisfied with measuring forces which caused the tipping of teeth since tipping results in an unequal distribution of force along the root, as illustrated by Stoner[13] and later by Nickolai[14] and Haack.[15] Also, the findings from Oppenheim were disputed on the basis that the forces used in his study were not measured. Oppenheim

believed that no purpose was served in measuring the effect of force quantitatively due to the wide variation of response in different patients. While Oppenheim's observation that there is no force light enough to effect orthodontic dental movement without causing some damage, cannot be entirely dismissed, since the forces were not measured, it does demonstrate the general lack of understanding of the force systems delivered by orthodontic appliances of the time.

For the retraction of human canine teeth, Storey and Smith demonstrated that these teeth moved most efficiently when a force in the range of 150 to 200 grams is used. For forces between 300 to 500 grams, there was little or no movement of the canine while there was significant mesial movement of the posterior anchor unit that persisted until the force from the spring decayed to the range of 200-300 grams. Equating the orthodontic forces to the ratio of root surface areas of the cuspid and the anchorage unit, they arrived at an experimentally derived ratio of approximately 3:8. That is, the optimal force for movement of the cuspid is 3/8 that of the anchorage unit.[8] Expressed in other words, the force exerted per unit area of contact between bone and root of the cuspid required to produce the maximum rate of dental movement corresponds approximately to that of the posterior anchorage unit. Applied forces less than the so-called optimum force for a tooth will cause little or no movement of that tooth. By increasing the force above the optimum range, the comparative rate of movement decreases to zero, demonstrating a behaviour which would be expected by the initial process of undermining resorption as proposed and supported by Sandstedt[6] and Schwartz,[7] respectively.

2.2 CONCEPT AND CONTROVERSY OF DIFFERENTIAL FORCE

In 1956 Begg used the conclusions from the papers of Storey and Smith in the publication of his orthodontic technique[16] to explain an aspect of it which he called "differential force." He described differential force as a force great enough to move certain teeth, but insufficient to move others. A relatively small force will move one tooth if resisted by several teeth, with the reciprocating force distributed over anchorage teeth which he called "resistance teeth." The teeth in the anchorage unit experience a lower pressure individually and the forces generating these pressures are lower than the optimal range for movement of the individual teeth. Begg identified the optimal force for canine movement at 300 grams, while the use of orthodontic force in his technique was largely empirical.

Reviews of the relation of applied force and tooth movement by Hixon *et al,*[12,17] scrutinized much of the experimentation pertaining to optimum forces for orthodontic dental movement. For example, they pointed out that tipping introduces several variables which obscure the relation between applied force and dental movement. Tipping causes an unequal distribution of the force along the root, with the highest concentrations at the alveolar crest and apex, and the lowest adjacent to the centre of resistance.[14] Although Storey and Smith criticized Schwarz in this regard, they did not adjust their protocol accordingly in their studies. In fact, the experimental protocol used by Storey and Smith caused the canine to tip into the extraction sites, whereas the premolar and molar were prevented from tipping and were secured to an appliance that allowed a more translatory movement. While forces as light as 1.68 grams have been shown to readily tip teeth,[18]

translation of a tooth occurs slowly and requires relatively heavier forces,[1,19] in the order of hundreds of grams.

It becomes evident that a comparison of forces causing tipping of one tooth and bodily movement of other teeth is nonsensical when attempting to elucidate the relation between dental movement and applied force. In fact, Hocevar[4] suggested that the anchorage phenomenon of differential force response used in the Begg technique be explained as follows: a light force sufficient to produce tipping, by concentrating the force at the apex and alveolar crest, may cause negligible movement if the force is delivered such that it is distributed evenly over a large (root surface) area and the pressure at any point is insufficient to induce osteoclastic activity to allow the tooth to move.[4] Thus, the force which causes tipping has a reactive force applied to the posterior teeth which is too light to protract these teeth (which are not able to tip due appliance design).

The conclusions from Hixon *et al.*, following careful inspection of experimental method and variables, do not substantiate the concepts of optimal force or differential force in orthodontics. They did, however, note that higher forces (i.e., up to 300 grams) in canine retraction were generally more efficient, and rotation and tipping components associated with canine retraction were difficult to counteract when the applied force exceeded 300 grams.[12]

2.3 CONFOUNDS OF CLINICAL STUDIES RELATING ORTHODONTIC FORCE TO DENTAL MOVEMENT

Scrutiny of the literature thus far demonstrates five major problems which complicate the clinical study of the relation between magnitude of applied force and dental movement.[2] The first is an inability to control the type of dental movement effected by orthodontic appliances, i.e., tipping versus translation with or without rotation.[6,7] In earlier studies, the crown was used as a reference for measuring tooth movement; the results are difficult to interpret because the relation between the rates of crown and root movement depends on the position of the centre of resistance which is difficult to determine and changes with tipping.[20,21] The second is data that may be biased due to the nonlinear, time-dependent nature of dental movement following the application of an orthodontic force.[21-23] The third is the large variations in patient response to dental movement as well as the errors associated with measurement of such movements make statistically significant findings difficult to attain.[24,25] The fourth is the deflection of archwires that may occur during orthodontic movement,[17,26] requires energy. In clinical experimentation, measurement of energy causing wire deflection during such movement remains unaccounted for. For the most part, only the orthodontic force is measured. Also, archwire deflection adds rotation and tipping components to the dental movement. The fifth is friction in the archwire/bracket system which can inflate measurable force levels.[27,28] The contribution of friction to the total force system can be accounted for only if it has been elucidated in previous experiments, and subtracted from the force system being measured.

It becomes clear that force standards as a useful guide in appliance design thus far remain nebulous, and it is not surprising that controversy permeates discussions of optimal force, differential force and anchorage to this day.[19,27,29,30] The balance of the literature pertaining to values of optimal force derived from clinical experimentation deals with canines on one hand, and groups of posterior teeth termed "anchorage units" on the other. The determined value(s) for optimal force(s) vary widely and are, at best, only suggestions. Given that the variation between patients is likely greater than the differences between the types of dental movement for a particular force, Hixon claims that if an optimal force for a given patient is indeed a reality, it cannot be determined prior to treatment.[17] Thus we are left with no substantial idea of what optimal force values for orthodontic movement are, beyond what have been accepted as "safe" ranges of force for particular movements.[12,17,21,27,31-33]

2.4 FURTHER ATTEMPTS AT ELUCIDATION OF FORCE SYSTEMS FOR ORTHODONTIC MOVEMENT

Further attempts to elucidate the relation between orthodontic force and dental movement have generally followed one of two paths. First, attempts to analyze the clinical response to various orthodontic forces within and among individuals have been endeavoured. Second, *in vitro* or laboratory experimentation of modeled systems in attempts to minimize and control the myriad variables inherent in a biologic system.

2.4.1 INVESTIGATIONS OF CLINICAL RESPONSES TO ORTHODONTIC FORCE

Boester and Johnston[25] set out to determine if there is a force which can be regarded as optimal for a large percentage of orthodontic patients, and also to determine if there is a generalized differential response to orthodontic treatment with differential force. A group of 10 patients were studied. All patients required the removal of four first premolars and distal retraction of the canines as part of their individual orthodontic treatment. In each patient, four different retractive forces were used, one in each quadrant: 55g, 140g, 225g and 310g. Results of this experiment could not elucidate the existence of any optimum force, nor could they show any support for the concept of differential force as a mode of space closure in orthodontic treatment. Relative anchorage loss was independent of the force used. Similar findings were found (for dogs) by Pilon *et al.*[21]

2.4.2 *IN VITRO* EXPERIMENTATION

Several investigators have attempted to minimize the number of variables inherent in a biologic system by experimentally or mathematically modeling the clinical system being investigated. Clinically, the measurements and interpretation of such forces are complicated, since the measurement reflects not only the response of the physical system of the archwire in the bracket, but also the response of the entire biomechanical system which is inherently indeterminate and defies analysis. Thus, the goal of experimentation performed on laboratory models or analysis of mathematical models is to provide a rational explanation of the behaviour of the biomechanical system by controlling and

manipulating particular variables and studying the effects. It also allows investigations of other manifestations of orthodontic force which do not lend themselves to methodical analysis in clinical situations.

For example, Clifford *et al.* used a photoelastic model to demonstrate the stress distribution around an entire arch of teeth in response to a reverse curve of Spee.[34] Caputo *et al.* employed a photoelastic model to visualize the effects of orthodontic forces applied to a mandibular canine tooth by various segmental retraction springs.[35] For obvious reasons, the distribution of stress surrounding a tooth cannot be directly visualized clinically. The results of their studies suggest that excessive retractive force causes a tipping movement of the tooth, which has been shown to occur in spite of any compensatory bends placed in the spring.[36] This in turn demonstrates that even a simple spring or sectional arch can involve unexpected forces with concurrent undesired dental movement during retraction. Photoelastic studies have been criticized as a method for determining force and stress levels due to the crudeness of modeling and interpretation.[37]

White *et al.* developed an experimental apparatus consisting of a metal framework, a strain gauge and a Wheatstone bridge to model the mandibular incisors and measure the forces and moments delivered to these teeth by a mandibular utility arch.[38] This work by White *et al.* is significant as this method of measurement addressed the complex problem of force system analysis from a continuous archwire by individually measuring the strain at each dental position (represented by stainless steel posts) by the utility arch. In essence, the system was reduced to a series of determinate systems and the data from

each was compiled to allow interpretation of a force system that was otherwise unsolvable. A similar technique was used by Murphy *et al.* to analyze the force system generated by a contraction utility arch.[39] The authors cited several reasons such as voltage variation, electrical heating, humidity, inconsistent wire bending, positioning of orthodontic brackets and placement of the utility arch which may have inflated the resulting measurement error to over 20%. The strain gauges did not provide information which would allow resolution of the forces into their mesiodistal or buccolingual components; only the magnitudes were registered. Refinements to their experimental apparati could include a means to allow determination of the direction of the applied force. Also, the force measurements were accomplished in a static situation which may not necessarily represent the force system existing in a dynamic environment such as the oral cavity.[21-23] However, the development of this measurement technique was a major advance in the analysis of force from continuous archwires using models of clinical situations.

2.5 MATHEMATICAL ANALYSES OF ORTHODONTIC FORCE SYSTEMS

2.5.1 MATHEMATICAL AND COMPUTER MODELING

A mathematical analysis using generalized field equations for arbitrary curved and twisted beams in space, allowed Koenig and Burstone to develop a computer modeling system capable of predicting the force systems delivered by complex orthodontic appliances.[40] This model used a finite-difference matrix technique which is different from a finite element analysis (to be discussed later). This work was undertaken with the

expectation that it could be employed in the analysis and determination of force systems of orthodontic appliances prior to their clinical use. The extension of this analysis to the clinical situation involves Burstone's segmented arch treatment technique, which was designed to deliver light constant forces to the tooth or teeth being moved, while maintaining reasonable control over the anchor teeth.[3,41]

Eden and Waters[42] investigated the force characteristics of the Type 2 PG canine retraction spring by breaking down the spring into its component spring elements and modeling each mathematically according to complementary (strain) energy method described by Timoshenko.[43] The theoretical behavior of this spring was verified experimentally using strain gauges to measure the forces and couples produced. They obtained good agreement between the theoretical and experimental behaviors of this spring. This implies the following: a) the assumptions presented in Timoshenko's mathematical model are valid, b) this mathematical analysis could be used with confidence to theoretically compare the Type 2 PG retractor with other springs, c) this mathematical model may be used to predict the characteristics of other springs, and d) mathematical modeling may be a valid method to model springs for the purposes of force system analysis.

2.5.2 FINITE ELEMENT ANALYSIS

Finite element analysis (FEA) is a mathematically-based technique used to examine the physical characteristics of an object. If the object being examined in an orthodontic spring of arbitrary geometry, the spring is first broken down into a finite number of

straight segments called elements.[44] A stiffness is set for each element via an equation analogous to Hooke's law[45] for a spring.* The idea of FEA is to determine how the behavior of one element effects the behavior of adjacent elements. The results of, for example, bending of one element becomes the initial condition for the next element, and the equations are solved sequentially for all elements to determine the behavior of the entire object. This method of analysis is commonly preformed on computer.

FEA has been used in several studies to analyze retraction springs and the effects of retraction springs[46,47] alone and in the human dentition.[37] Advantages of FEA include the ability to create and analyze complex configurations before placement and after placement with deformation, and to envision activations while obtaining data on forces, moments and rate of movement. The disadvantages of FEA include its absolute dependence on initial conditions and the procedure of modeling, and it's being commonly done only in two dimensions.

2.5.3 CONCEPTS OF EQUILIBRIUM AND STATICS

Knowing the force systems allows the use of the concept of equilibrium; it may be assumed that an activated orthodontic appliance *in situ* is in equilibrium since its elements are not accelerating. Statics is that area of engineering which uses Newton's first law of motion to describe equilibrium or balance of forces, and it implies a non-

* Hooke's law is F=kx, where F is the applied force, k is the spring constant, and x is the displacement. This is a linear equation. In finite element analysis, the analogous equation is non-linear and is written symbolically as {F}=[K]{Q} in which {F} is the applied force, [K] is the stiffness matrix which is dependent on the initial axial force F_o which in turn is a function of joint displacement {Q} between adjacent elements.

accelerating system. The application of the equations of static equilibrium to orthodontics has been described by Haack[48] and Burstone *et al.*[3]

2.5.4 DETERMINATE SYSTEMS

Analysis of a force system distributed over two bodies is a solvable system as long as the force system on one of the bodies is known. Such a system is called a determinate system, since technically, the number of equations required to solve the system is the same as the number of unknowns, and the equations of static equilibrium may be employed to elucidate the force system. Burstone treated a group of anchor teeth as one large tooth by placing a large dimension stainless steel wire in the brackets and/or tubes and tying them together, thereby treating the group as one of the bodies in a two-body determinate system.[41] Thus, Koenig and Burstone's aforementioned computer analysis[40] could be used to analyze the force system developed by a particular orthodontic appliance, and the segmented arch technique allowed its application to a solvable, determinate orthodontic system.

2.6 FORCE SYSTEMS IN ORTHODONTIC SPACE CLOSURE

A fundamental step in a considerable number of orthodontic treatments is retraction of the upper anterior teeth. This stage of treatment remains one of the most challenging to orthodontists, and the evolution of several techniques and appliances to accomplish anterior retraction is reflective of a lack of understanding of the force system required for effective controlled space closure. Examples of various techniques include the K-SIR archwire,[49] finger springs,[50] the PG retraction loop,[51,52] magnetic repulsion,[53] Nickel-

Titanium springs,[54,55] elastomeric auxiliaries,[55,56] J-hook headgear,[57] *en masse* retraction,[58,59] anterior headgear,[59] and the universal appliance,[60] only to name a few.

The correct force system may not necessarily be the one that merely results in closed intraarch spaces, and the majority of designs of various orthodontic retraction appliances have not been analyzed to determine if they provide the required force system. As described above, analysis involving the principles of engineering and physics is preferred to trial and error for guidance in the development of orthodontic appliances.[61-67]

2.6.1 FORCE SYSTEM REQUIRED FOR SPACE CLOSURE

The force system required for controlled space closure consists of a minimum of two equal and opposite forces plus a moment on either end of the retraction appliance.[42,47,64,66,68] Moments are required since force cannot be directly applied at the centre or resistance of a tooth (required for bodily movement), and they are applied to the tooth through a couple at the bracket.[66] The two forces serve to draw the teeth together. The combinations of moment and force on either side of the space are intended to cause a translatory or a controlled tipping movement of teeth, rather than uncontrolled tipping, into the space. This is intended because it has been shown that root parallelism of teeth result in greater long term stability following orthodontic dental movement.[69] The moment-to-force ratio is an important mechanical characteristic of a particular appliance since it is this ratio that will determine how much translation and/or tipping will occur. In conjunction with biologic variables, the force system ultimately dictates the type and amount of dental movement.

2.6.2 MECHANICS OF SPACE CLOSURE

Several techniques are involved in current methods of space closure. With fixed orthodontic appliances, the retraction mechanics can be classified as either sliding or frictionless.

In both sliding and frictionless retraction mechanics, the appliances are relied upon to deliver what is deemed an appropriate moment to force ratio to the tooth or teeth. *In situ*, the moment-to-force ratio is *in situ* impossible to maintain, since the force deactivation characteristics of retraction appliances and the biologic response of the surrounding tissue change with time.[21-23] Hence the thrust to develop and analyze models is a sensible method to elucidate the behaviour of clinical situations through utilization of engineering principles, as demonstrated by, for example, the aforementioned works by White *et al.*,[38] Murphy *et al.*[39] and Koenig and Burstone.[40]

2.6.2.1 SLIDING MECHANICS

In sliding mechanics, teeth are moved along the archwire into the space being closed. In such situations, the applied force causes some tipping of the tooth being moved, but with the archwire being sufficiently stiff to resist significant deformation, the bracket will be permitted to slide along the archwire without becoming markedly tipped (relative to the wire) to cause significant friction.[70] Effective translatory dental movement is the intended result. A major advantage to sliding mechanics is that complex archwire configurations are not required, making initial wire placement less time-consuming.

2.6.2.2 FRICTIONLESS MECHANICS

In frictionless mechanics, the basic principle is to cause the archwire to move, taking the tooth or teeth with it.[71] Teeth are moved without the brackets sliding along the archwire, and the problem of friction between the archwire and the bracket as seen in sliding mechanics is not an issue; hence the name "frictionless" mechanics. The archwire (either segmental or continuous) is caused to move in several ways. For example, the archwire may have loops placed in it that store energy and release it when they are activated, or elastic elements can be engaged on hooks between sections of an arch to draw them together. Moments may be applied through bends in the archwire, or by expression of torque via engagement of a rectangular archwire in the bracket slot. It is felt that frictionless mechanics offers more controlled dental movement and taxes the anchorage teeth less than sliding mechanics does.[70,71]

2.7 SUMMARY

A review of the literature demonstrates that there is no real guide for what may be considered optimal forces for dental movement, and that what many people regard as optimal forces for a particular dental movement vary wildly. Also, the wide variability of response to orthodontic force within and among individuals obscures the idea of an optimal force further.

Many appliances and techniques exist for space closure, illustrating a lack of consensus for what may be an ideal method. Also, the majority of these appliances were developed without appreciation of the force system that is generated, beyond what has anecdotally

or experimentally been considered a safe force and that it eventually closed the space. Further, use and behavior of these appliances may have involved assumptions on the part of the clinician which may not be correct.

Numerous analytic techniques exist for the testing of various appliances, spanning a spectrum from clinical *in vivo* testing to mathematical computer-driven analyses. Review of the literature in these regards was not preformed to determine the best technique or analysis. Rather, it was preformed with the hope that the wide ranges of opinions, assumptions, techniques and experimental results in these regards is appreciated by the scholar and skeptic alike.

CHAPTER 3

MATERIALS AND MEHODS

3.1 MATERIALS USED IN THIS INVESTIGATION

3.1.1 ACRYLIC RODS

Acrylics (e.g., Plexiglas™, Rohm and Haas, West Philadelphia, PA; Lucite™, Du Pont Corporation Canada, Mississauga, ON.) are a wide ranging family of plastics notable for clarity, light weight, colour-fastness and rigidity. Of the homopolymers, copolymers and monomers included in this group, the majority of modern acrylics use methyl methacrylate (MMA) monomers in its polymers (polymethyl methacrylate, or PMMA).[72] Thus, the basic chemical structure of acrylics is as follows:[73]

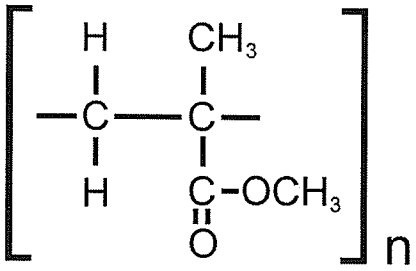

Figure 3.1 Chemical structure of polymethyl methacrylate (acrylic).

Acrylic is a derivative of natural gas. Production of acrylic results from a two-stage process in which acetone and hydrogen cyanide are reacted to form acetone cyanohydrin. This compound is reacted with sulphuric acid to produce methacrylamide, which is then heated with methanol to produce MMA monomer.

Natural gas → propane → propylene → isopropyl alcohol → acetone

Acetone + hydrogen cyanide → acetone cyanohydrin

Acetone cyanohydrin + sulphuric acid → methacryolamide

Methacrylamide + methanol → ***Methyl methacrylate***

Polymerization of the MMA monomers to produce the PMMA polymer can occur by one of several methods, among which are bulk, solution, emulsion and suspension systems. Molecular weight and physical properties can be adjusted depending on the type of process and process conditions.[72]

The flexural yield strength of acrylic is 103.5 MPa,[74] depending on the molecular weight of the particular acrylic.[72] Alloying constituents may be added to provide as much as 20 times the impact strength of the general acrylic amorphous polymer.[75]

Acrylic behaves elastically up to its elastic limit, and there is a linear relation between load (stress, σ) and deflection (strain, ε) of acrylic up to its proportional limit. Below this value unloading will occur with no permanent deformation.[72] For the most part, energy required for deflection is stored in the amorphous structure of acrylic and is released totally when the load is removed, provided that the load is below the elastic limit for acrylic. The deflection process is not 100% efficient, and there is a negligible portion of this energy which is dissipated as heat.

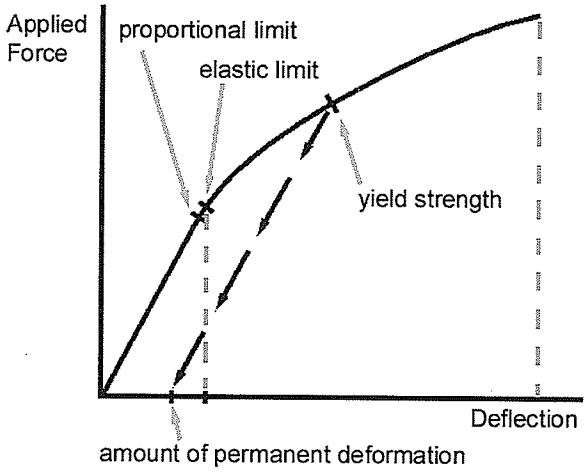

Figure 3.2 Example of a load-deflection plot.

For loads in excess of its elastic limit, acrylic will behave inelastically, and unloading will result in permanent deformation, as a portion of the energy required for deformation has been used to alter its structure.

The large and linear elastic range and suitable strength of acrylic, coupled with its safe and easy handling characteristics, make it an ideal material for this investigation. The rods used are 6.35 ± 0.03mm (1/4 inch) in diameter, and 175.5 ± 0.1mm (approximately 7 inches) long. They are fixed at one end in the experimental apparatus (see **Section 3.2.3.1**). A pilot study showed that rods of these dimensions were found to deflect a suitable amount when the light loads used in this investigation were applied.

3.1.2 LIGHT EMITTERS

"Laser" pointers (wavelength 650 nm, power <5mW; Sean & Stephen Corporation, Yung-Kang City, Taiwan) used for, e.g. teaching purposes, were disassembled to attain the light-emitting components. The light emitted by these pointers is a monochromatic focused beam, very similar to a laser beam. The total pointer, prior to disassembly, weighed 32.05 ± 0.07g.

The emitter components consist of a light emitting diode (LED) fused to a brass heat sink, a small printed circuit board, and a lens to focus the light. These components were reassembled on an acrylic base and leads to a power supply were soldered to the printed circuit board.

Collimators were placed on the lenses and the emitter components were covered with a section of white styrene tube for protection. The entire reconstructed light emitter (minus the power leads) had dimensions 23.5x10x8mm, and complete with power supply leads, weighed approximately 5.7 ± 0.05g (see **Figure 3.3**, below).

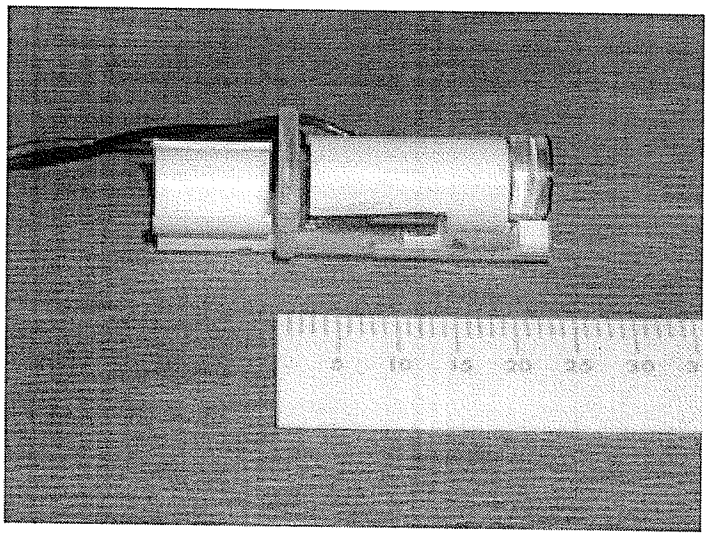

Figure 3.3 A light emitter used in this investigation.

The light emitters were clipped onto the ends of the rods with C-shaped styrene tube sections, and immobilized with small elastic bands and/or Weld-On™ #4 Acrylic Solvent (IPS Corporation, Gardena, CA) (see **Section 3.1.3**, below). The emitters were connected to a common power supply consisting of 3 size AA alkaline batteries.

3.1.3 ACRYLIC SOLVENT

The acrylic solvent used in this investigation is Weld-On™ #4 Acrylic Solvent (IPS Corporation, Gardena, CA) and is composed of approximately 50% methylene chloride, CH_2Cl_2 (CAS No. 75-09-2),[76] approximately 50% trichloroethylene, C_2HCl_3 (CAS No.

79-01-6)[77] and trace amounts (<1%) MMA monomer, $CH_2C(CH_3)COOCH_3$ (CAS No. 80-62-6).[78] This product is a clear fluid with a viscosity less than that of water and a specific gravity of approximately 1.37.[79]

Figure 3.4 Weld-On™ acrylic solvent.

Acrylic solvents act by temporarily breaking the secondary bonds in the PMMA polymer, producing an amorphous mixture of MMA monomers and oligomers. Since the components of the solvent are highly volatile, evaporation of this substance occurs readily. The monomers and oligomers repolymerize to form PMMA as evaporation proceeds. A bond strength between 85-100% of the parent components may be attained, that is, the bond is between 85-100% as strong as a single piece of acrylic.[73]

3.2 EXPERIMENTAL METHOD

3.2.1 THEORETICAL MODELS

The purpose of the theoretical models was to determine the expected or theoretical distribution of retractive force to each of the six anterior teeth during *en masse* retraction. The results of this model were compared with those of the laboratory experimentation.

The theoretical models are described in detail in **CHAPTER 4**.

3.2.2 LABORATORY EXPERIMENTATION

3.2.2.1 APPARATUS

The apparatus consists of six acrylic rods arranged in a semicircle (refer to **Figure 4.12**). One end of each rod is fixed in a robust jig made of 12.7mm (1/2 inch) thick acrylic and is fused in place with Weld-On™. Each rod has a light emitter (as shown in **Figure 3.3**) clipped to the other end with a styrene split-tube clip. The power supply wires of each emitter are coiled to prevent any significant deflection of the rod(s) which may result from tension in the wires. These leads are connected to a power supply consisting of 3 size AA batteries.

Near the emitter end of each rod are two small styrene tabs, fused to the rod with Weld-On™, to prevent the archwire from sliding off the rod when weights are applied. Also included in the apparatus are two independent light emitters (one on the top and one on the bottom of the apparatus) used for orientation of successive measurements (see **Section 3.2.2.5**).

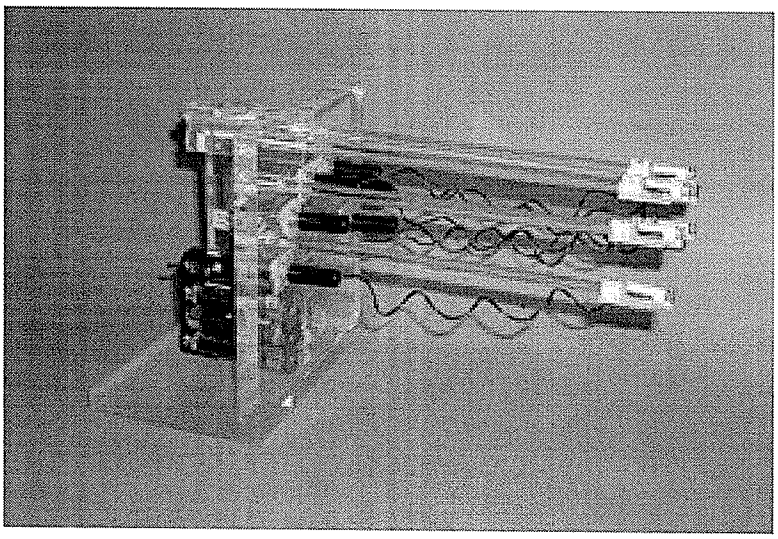

Figure 3.5 The experimental apparatus.

3.2.2.2 ARCHWIRES

3.2.2.2.1 FLEXIBLE ARCHWIRE

Dental floss was used to model an infinitely flexible archwire. The floss was laid over the emitter ends of the rods, between the two plastic tabs, and weights were suspended from the ends of the floss (see **Section 3.2.2.3**).

To minimize friction between the floss and the rods, the floss was lubricated with a commercially available lubricant (WD-40®; WD-40 Products Canada Ltd., Etobicoke, ON). Methylmethacrylate has good chemical resistance to oils.[80]

To prevent medial collapse of the canine rods, the apparatus was modified to include guides for the floss at positions that approximated a premolar tooth, located directly behind the canine rods, beneath the point(s) of application of the floss archwire. This minimized the collapse and insofar as direction of retractive force is concerned, was a

better representation of the clinical situation this apparatus is intended to model. A picture of the apparatus with the guide is shown in **Figure 3.6** below.

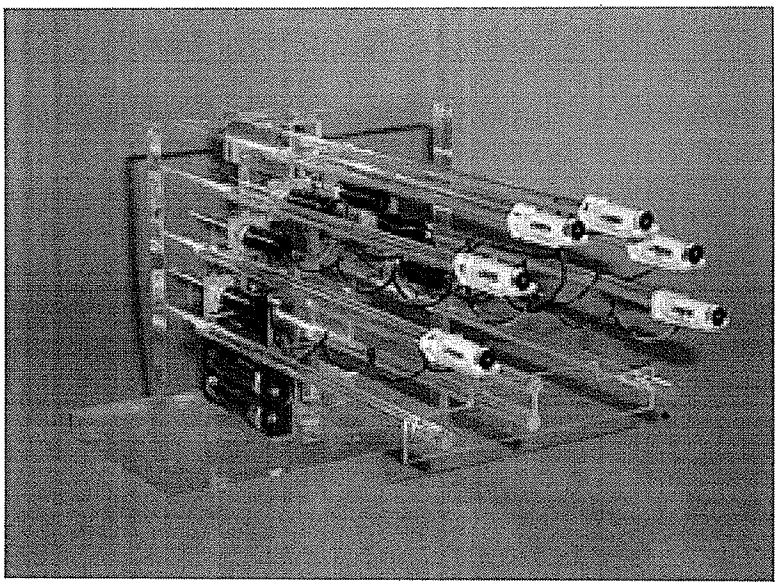

Figure 3.6 Experimental apparatus with guides attached to minimize medial collapse of the canine rods during testing with the infinitely flexible archwire (dental floss).

3.2.2.2.2 RIGID ARCHWIRE

To model an infinitely rigid archwire, a solid piece of acrylic, approximately 1.5mm in thickness, had a semicircular section machined into it such that it passively contacted each rod at the emitter end (between the styrene tabs). Weights were suspended in a similar manner as described in **Sections 3.2.2.2.1** and **3.2.2.3**. "Zero" positions (see **Section 3.2.2.5**) were those with no load, and the first weight applied was actually the acrylic alone (i.e., without weights).

To minimize friction between the rigid archwire and the rods, WD-40® was applied to the rigid archwire.

3.2.2.3 WEIGHTS USED TO PROVIDE RETRACTIVE FORCE

Weights used were ¼ inch (6.25 mm) #8 nuts tied with dental floss in groups of five. The weights of 20 groups of five nuts were measured three times each on a scale (Harvard Trip Balance, Ohaus Scale Corporation, Union, NJ). The weight of each group of five nuts, presented as a mean ± standard deviation was found to be 16.16 ± 0.05g. These weights were suspended from the ends of the archwires and deflections of the rods were measured (see **Section 3.2.2.5**).

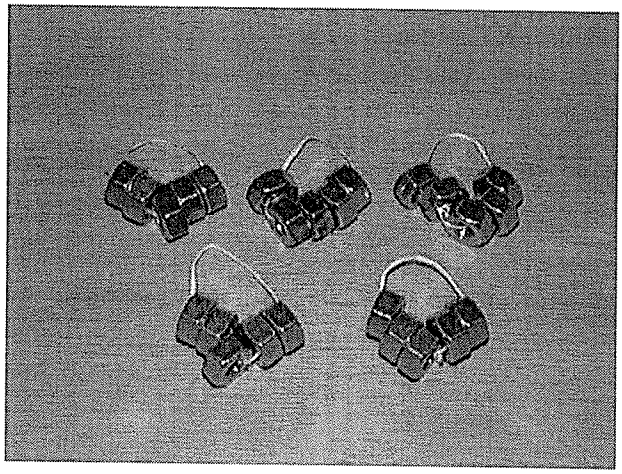

Figure 3.7 Weights used in this investigation.

3.2.2.4 CALIBRATION

Each rod was calibrated in the following manner:

1. A zero-point was marked on the screen for the rod under no load.
2. Deflection resulting from a particular weight was measured as the linear distance in millimeters of the light point from the emitter away from the zero point, and also as horizontal and vertical components of this deflection.

3. The weight was removed and the next measurement was taken after a duration of 3 minutes.
4. Deflection for each weight was measured 10 times to ensure repeatability, and the deflection for a particular weight was expressed and plotted as a *Mean ± Standard Deviation.*

3.2.2.5 METHOD OF MEASUREMENT

Deflections of each rod in the apparatus were marked on a screen at a distance of 2.50 ± 0.005 m away from the lens of the light emitters. Deflections were charted on graph paper which was oriented according to the two orientation pointers on the top and bottom of the apparatus. This provided excellent comparison of successive measurements since the orientation pointers were fixed in place and did not move.

The deflections were measured immediately once the rods steadied themselves. Once a data point was acquired, the load was removed and a duration of 3 minutes was allowed to elapse between successive measurements to allow for any viscoelastic recovery of the acrylic rods to occur.

Vertical displacement of the light points from their zero positions were measured to the closest 1/4mm using a mm-scale ruler (China, ACME #R-405-30) for the calibration data because the large deflections prohibited the use of digital calipers. For the experimental data, horizontal and vertical displacements of the light point from its zero position for each measurement were taken with a CE Electronic Digital Caliper (Lee Valley Tools Ltd., Ogdensburg, NY). Determination of the distribution of retractive force to each rod

was determined using the calibration plot for each individual rod, since a particular amount of deflection results only from one particular applied force.

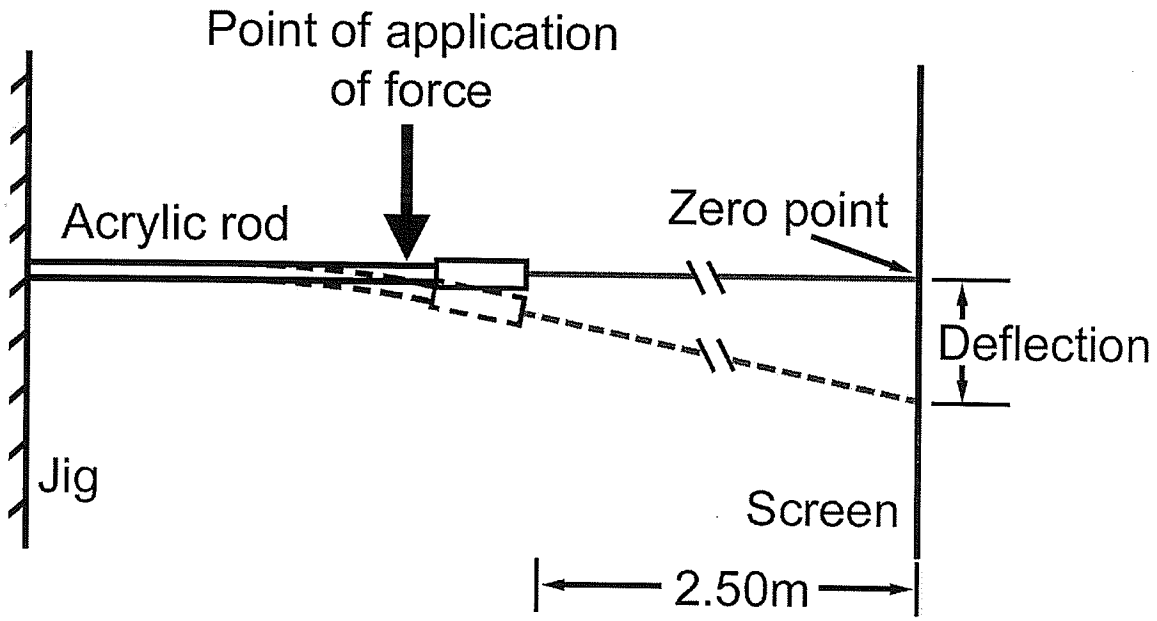

Figure 3.8 Schematic diagram of apparatus and testing method.

3.2.2.6 CREEP TESTING

Creep is defined as a slow flow over time that occurs in materials under stress below their proportional limits, or a time-dependent strain in a material as a result of application and maintenance of a stress at a set level.[81] To determine whether or not the acrylic rods experienced creep during the measurements (described in **Section 3.2.2.5**), successive measurements were taken 3 minutes apart. Following a measurement, the rod was given 3 minutes to return to its original position. At the end of 3 minutes, a new zero point was measured and compared to the original zero point. Any discrepancy between the two zero points would indicate that creep had occurred during the loading of the rod during the measurement.

To validate the use of acrylic rods in this investigation, it is important to determine whether or not creep *could* occur during the measurement phase. To test creep of the acrylic rods, a load of 96.96 ± 0.3g was suspended from each of a group of six rods for 30 minutes. This load was used as it was slightly greater than the greatest load applied during testing: with the rigid archwire, it was 86.94 ± 0.25g. The duration of 30 minutes was chosen since it is far in excess of any duration during the measurement phase described in **Section 3.2.2.5.** To evaluate the viscoelastic recovery of the rods, measurement continued for a further 15 minutes after the load was removed. Deflections were measured at **Time** = 0, 2, 20, 30 (removal of load), 31, 33, 35, 40 and 45 minutes. At the end of 45 minutes, a new zero point was measured and compared to the original zero point. Any discrepancy between the two zero points would indicate that creep had occurred.

3.2.2.7 TESTING OF ELASTIC LIMIT OF THE ACRYLIC RODS

Apparatus similar to that shown in **Figure 3.5** was constructed to hold 3 acrylic rods of the same dimensions as those used for measurements. Light emitters (see **Figure 3.3**) were mounted on the end of each rod.

The rods were subjected to successively heavier loads, and deflections of the light point from its zero position were measured using a mm-scale ruler (China, ACME #R-405-30) because the large deflection prohibited the use of digital calipers. Permanent deformation of the acrylic rods was indicated when the light point failed to return to its zero point following removal of the load.

CHAPTER 4

THEORETICAL MODELS

4.1 REVIEW OF TRIGONOMETRY[82,83]

4.1.1 ANGLES

Angles can be measured in degrees or radians (the latter abbreviated as rad). The angle given by a complete revolution contains 360° or 2π rad. Therefore:

π rad = 180°

so, 1 rad = (180°/π),

or, **1 rad ≈ 57.3°**

and **1° ≈ 0.017 rad.**

The standard position of an angle θ is that which occurs when we place its vertex at the origin of a coordinate system and its initial side on the positive x-axis as illustrated in the following figure.

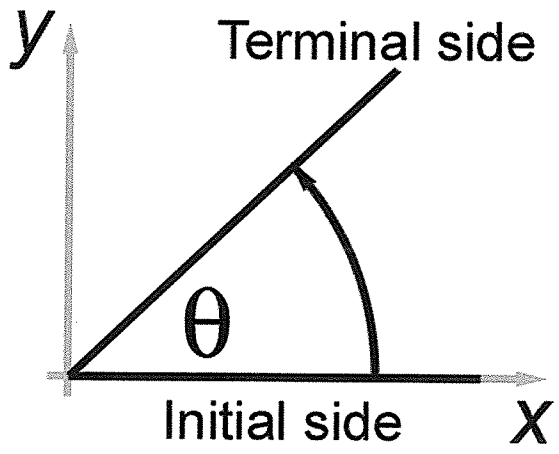

Figure 4.1 Standard position of an angle.

Angles are measured from initial side to terminal side. Provided that the positive x-axis is defined as directed to the right, a positive angle is obtained by measuring the angle in a counterclockwise way, that is, the angle sweeps in a counterclockwise rotation beginning at the initial side and ending at the terminal side. Similarly, negative angles are obtained by measuring in a clockwise rotation.

4.1.2 TRIGONOMETRIC FUNCTIONS

For a positive acute angle θ, six trigonometric functions are defined as ratios of lengths of sides of a right triangle as illustrated in **Figure 4.2**. The sides of a triangle are defined in relation to the angle. The side *opposite* θ is abbreviated as **opp**, the side which makes a 90° angle to **opp** is **adj** or *adjacent* to θ (which is equivalent to the initial side of θ), and the *hypotenuse* is the remaining "slanted" side and is abbreviated as **hyp** (which is also equivalent to the terminal side of θ).

Sine of θ	**sinθ = opp/hyp**
Cosine of θ	**cosθ = adj/hyp**
Tangent of θ	**tanθ = opp/adj**
Cosecant of θ	**cscθ = hyp/opp**
Secant of θ	**secθ = hyp/adj**
Cotangent of θ	**cotθ = adj/opp**

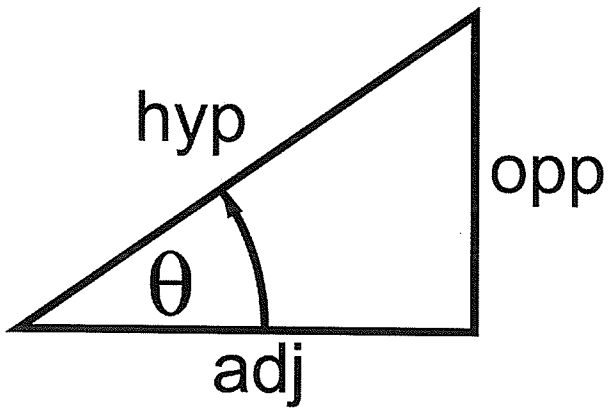

Figure 4.2 Relation of an angle θ to the sides of a right angle triangle.

The functions *sine* and *cosine* are called circular functions because they can be used to describe coordinates of a point on a circle with radius $\mathbf{r = 1}$ centred on the origin of a coordinate system through the following equation:

$$\mathbf{\sin^2\theta + \cos^2\theta = 1}$$

The equation $\mathbf{\sin^2\theta + \cos^2\theta = 1}$ is analogous to that of Pythagoras,

$$\mathbf{x^2 + y^2 = r^2} \qquad \text{where } \mathbf{x = r\cos\theta} \text{ and } \mathbf{y = r\sin\theta}$$

Pythagoras' Theorem states that the square root of the sum of the squares of a right triangle equals the hypotenuse of the triangle. The above equations allow determination of the lengths of the sides of a triangle contained within a circle, provided that the hypotenuse is the radius of the circle and the angle to either x- or y-axis is known.

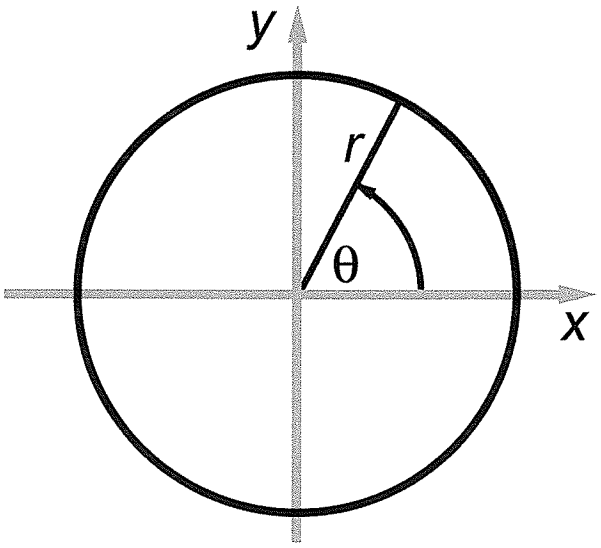

Figure 4.3a Circle of radius **r**, where $\mathbf{r^2 = x^2+y^2}$.

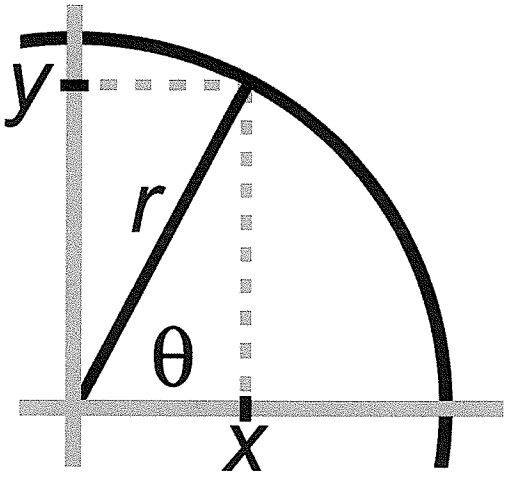

Figure 4.3b Circle, $\mathbf{\sin^2\theta+\cos^2\theta=1}$, where $\mathbf{x=r\cos\theta}$ and $\mathbf{y=r\sin\theta}$.

Sine and cosine functions of θ are also known as *periodic functions of θ* with a period of 2π. Expressed mathematically,

$$\sin(\theta + 2\pi) = \sin\theta$$

$$\cos(\theta + 2\pi) = \cos\theta$$

This periodicity of the sine and cosine functions are illustrated graphically in the following figures.

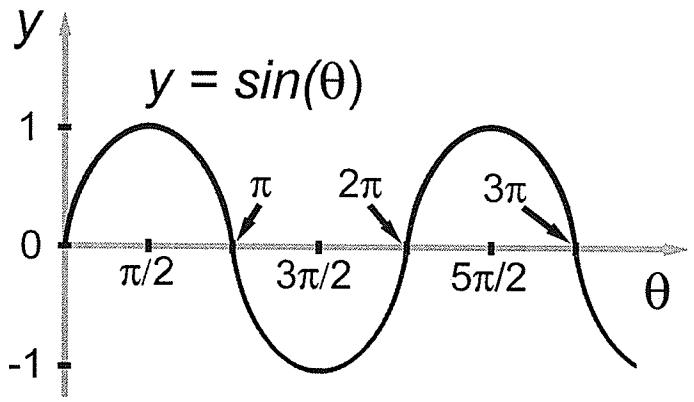

Figure 4.4a Sine wave, **y = sin(θ)**.

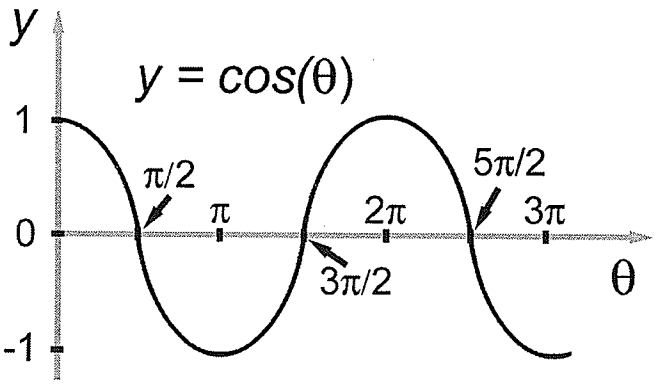

Figure 4.4b Cosine wave, **y = cos(θ)**.

4.2 REVIEW OF VECTORS[84]

A vector is a quantity that has magnitude and direction and follows certain rules of combination. Some physical quantities that can be expressed by vectors are:

Displacement
Velocity
Acceleration
Force
Fields: Electric, Magnetic, etc.

Straight-line arrows are typically used to graphically illustrate vector quantities. For different vectors representing force, a comparison of magnitudes is accomplished graphically by using arrows of different lengths. The greater the magnitude, the longer the arrow.

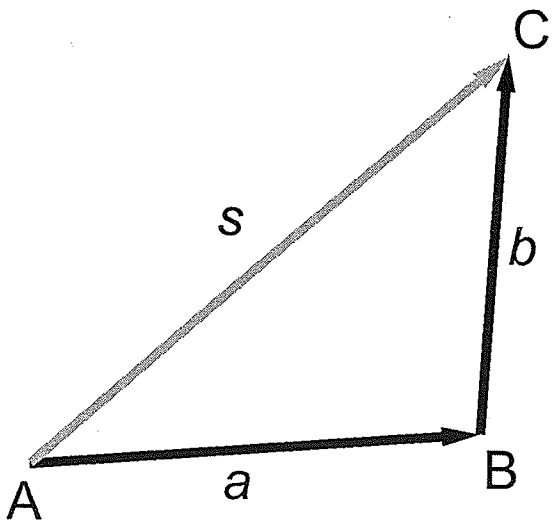

Figure 4.5 Example of vectors representing displacement of a body from Point A to Point B then to Point C.

4.2.1 ADDITION OF VECTORS

In **Figure 4.5**, suppose that a body starts at position **A** and moves to position **B**, then to position **C**. The individual displacement vectors are labeled **a** and **b**. The net effect of

these two displacement vectors is a single displacement vector from **A** to **C**, which is labeled **s**, which is the *vector sum* of vectors **a** and **b**. Note that the vector **s** is not an algebraic sum. Vectors can be added graphically by placing them in a tip-to-tail fashion.

$\mathbf{s = a + b}$ **vector addition**

Defined this way, addition of vectors has two important properties. First, the order of the addition is irrelevant, and is known as the commutative law of vector addition:

$\mathbf{a + b = b + a}$ **commutative law**

Second, for more than two vectors being added, it does not matter how they are grouped as they are added. This is known as the associative law of vector addition:

$\mathbf{(a + b) + c = a + (b + c)}$ **associative law**

There also exists what is called the parallelogram law of vector addition. For the two vectors in **Figure 4.6**, the magnitude of the resultant vector $\boldsymbol{C}$ can be determined if the ends of the two initial vectors $\boldsymbol{A}$ and $\boldsymbol{B}$ are placed together and represent two sides of a parallelogram. Dashed lines are extended from the tips of vectors $\boldsymbol{A}$ and $\boldsymbol{B}$ and intersect at a common point, thereby forming the adjacent sides of a parallelogram.

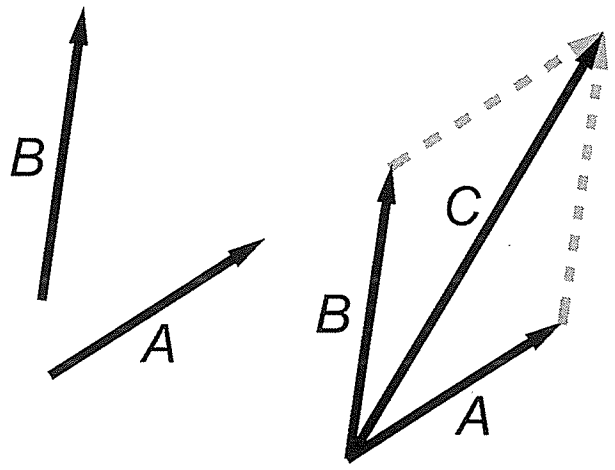

Figure 4.6 Parallelogram Law of vector addition of vectors $\boldsymbol{A}$ and $\boldsymbol{B}$.

The resultant vector ***C*** is the diagonal of the parallelogram, which extends from the tails of the initial vectors to the intersection of the dashed lines. This law is essentially an extension of the commutative law, since the magnitude of the resultant vector is the same independent of how the vectors are added. The parallelogram law may provide a means of easier visualization of the addition of two vectors, depending on the situation.

4.2.2 VECTOR COMPONENTS

Thus far, vectors have been represented in the absence of coordinate axes. The application of coordinate axes to the analyses of vectors allows the analyses to be performed algebraically. As such, vectors need to be resolved into components that are parallel to the orthogonal axes of the coordinate system.

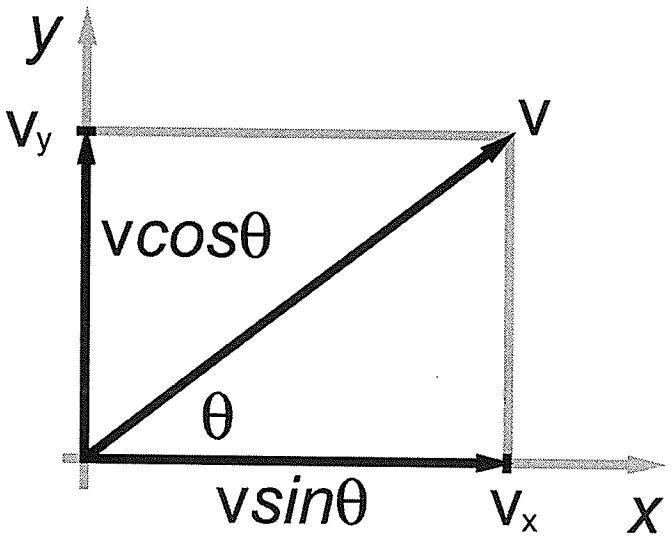

Figure 4.7 Orthogonal components of a vector **v**.

For example, consider the vector **v** in **Figure 4.7**. Perpendicular lines from the ends of the vector to the coordinate axes indicate the magnitudes of the orthogonal components

of **v**, namely $\mathbf{v_x}$ on the x-axis and $\mathbf{v_y}$ on the y-axis. This is the same as determining the x- and y- components of the radius **r** of the circle depicted in **Figure 4.3b**. The magnitude of **v** is given by the vector addition of $\mathbf{v_x}$ and $\mathbf{v_y}$. Using the sine and cosine trigonometric functions, numerical values for the components can be determined with the following equations:

$$\mathbf{v_x = v\cos\theta}$$

$$\mathbf{v_y = v\sin\theta}$$

Thus, the values of the orthogonal components of a given vector depend on the angle the vector makes with the coordinate axes. The components of vectors can be represented by a scalar quantity, since only a number (magnitude), a unit and an algebraic sign are required to define them. This allows the algebraic addition of vector components as long as it is recognized that they can only exist in the direction parallel to their respective axes.

To extend the concept of vector addition into the realm of coordinate axes for algebraic component addition, the equivalent required equations would be:

Vector addition	**Algebraic addition of components**	
$\mathbf{v = a + b + \ldots + n}$	$\mathbf{v_x = a_x + b_x + \ldots + n_x}$	
	$\mathbf{v_y = a_y + b_y + \ldots + n_y}$	
	$\mathbf{v = (v_x^2 + v_y^2)^{1/2}}$	(magnitude)
	$\mathbf{\theta = \tan^{-1}(v_y/v_x)}$	(angle to x-axis)

4.3 INTEGRATION AS IT IS APPLIED TO THIS INVESTIGATION

This investigation is designed to determine the amount of retractive force applied at a point or range of points on a semicircular archwire. The retractive force that pulls the archwire directly posteriorly exerts a radially directed force at all points on the archwire that can be resolved into horizontal and vertical components (see **Section 4.4.3.1**). An applied force **F** at any point can be resolved into its horizontal or vertical forces, or components (as illustrated in **Figure 4.8**), according to the following equations:

$$\mathbf{F}_x = \mathbf{F}\cos\theta$$

$$\mathbf{F}_y = \mathbf{F}\sin\theta$$

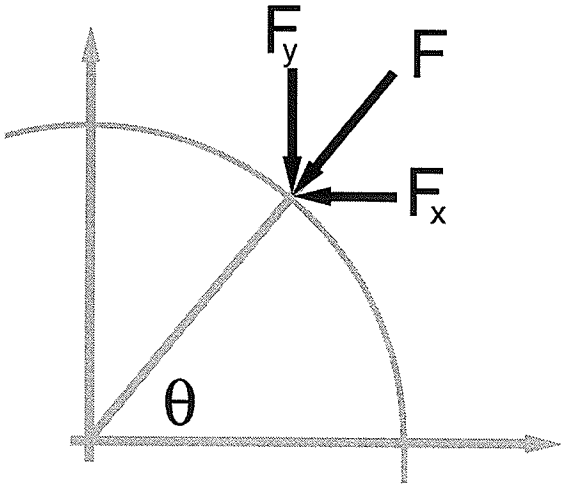

Figure 4.8 Force applied to a schematic archwire, resolved into its components.

In **Figure 4.8**, $\mathbf{F}_x$ is the horizontal component and $\mathbf{F}_y$ is the vertical component of the applied force **F**, and θ is the angle between vector and the horizontal axis.

The retractive force applied at the ends of the archwire exerts a retractive component at any point along the circumference of the anterior segment of that archwire. The magnitude of that component depends on the angle at which it is measured, with the apex of the angle located at the centre of the semicircle. For example, $\mathbf{F}_y$ will be greatest when it is measured at $\theta = 90°$, that is, when it is measured on the y-axis. Also, $\mathbf{F}_y$ will be minimum when it is measured at $\theta = 0°$. That is, when it is measured on the x-axis; the magnitude of $\mathbf{F}_y$ will in fact be zero at $\theta = 0°$. The magnitude of $\mathbf{F}_y$ will increase as a function of θ for all angles measured from $\theta = 0°$ to 90°.

Analysis would be simple if the decrease of $\mathbf{F}_y$ occurred in a linear fashion. Recall that the magnitude of $\mathbf{F}_y$ is given by $\mathbf{F}_y = \mathbf{F}\ \mathbf{sin}\theta$. Thus, the decrease in $\mathbf{F}_y$ as measured from 90° and 0° is not linear, but rather follows a sine wave, as explained graphically in the following figure.

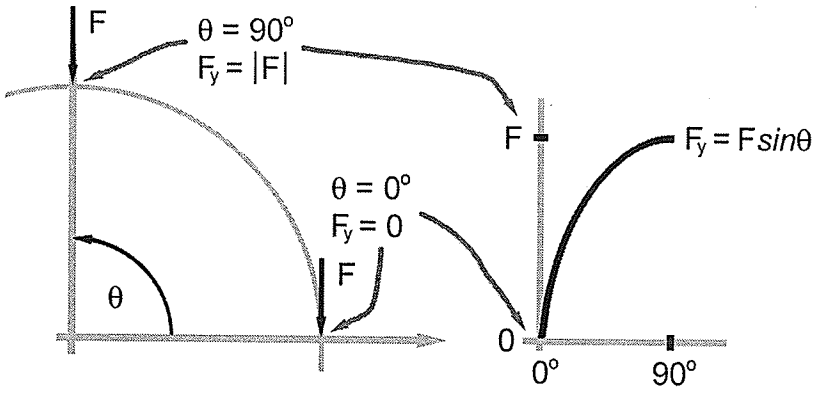

Figure 4.9 Decrease in $\mathbf{F}_y$ is a function of sinθ, greatest at $\theta = 90°$ and zero at $\theta = 0°$.

As illustrated and explained later (see **Sections 4.4.2** and **4.5**), the analysis is preformed over *angular ranges* corresponding to individual teeth rather than at individual points. If the decrease in $\mathbf{F}_y$ were linear, then the amount of the retractive force to the section of archwire corresponding to a tooth could be calculated by taking the difference in retractive components at the beginning and end of the section. Since the decrease in $\mathbf{F}_y$ follows a sine relation, which is dependent on the angle at any point, simple differences calculated using values of $\mathbf{F}_y$ at the termini of the section would yield an incorrect result. The individual retractive components at every point within the section must be summed to yield the actual amount of retractive force applied to that section.

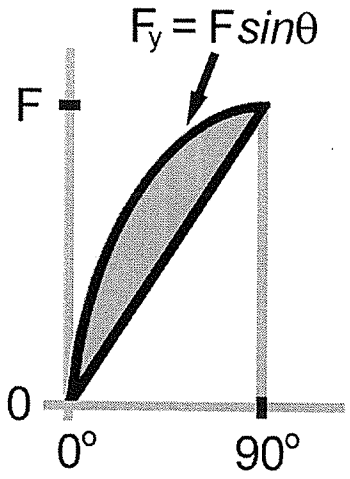

Figure 4.10 Linear and sine-dependent decreases in $\mathbf{F}_y$ as a function of the angle, θ. Shaded area indicates the amount of error.

An approximate value of retractive force over a section of archwire could be arrived at by dividing the section into **n** smaller subsections, where **n** is a finite number. Consider a semicircular archwire which opens downward as an example, depicted in **Figure 4.11**.

The section of that archwire, also called an angular range between θ_1 and θ_2, would be divided into **n** smaller angles, each called θ, given by the formula:

$$\theta = (\theta_1 - \theta_2) / \mathbf{n}$$

The required assumption is that each section has a linear decrease in $\mathbf{F_y}$. As such, a less inaccurate value of retractive force is arrived at, that is, the value would still be incorrect, but would better approximate the actual value. If the number is subsections is increased, that is as **n** increases, the calculated value of the retractive force approaches the actual value. The sum of the differences between the subsections is the approximation of the retractive force applied to the entire section.

Sum of differences,

$$S = \sum_{i=1}^{n} \left(F\sin\theta_i - F\sin\theta_{i-1} \right)$$

$$= F\sum_{i=1}^{n} \left(\sin\theta_i - \sin\theta_{i-1} \right)$$

$$= F\sum_{i=1}^{n} \Delta\sin\theta_i$$

for **n** subsections

If the number **n** of subsections was increased to infinity, then the sum of the differences in the $\mathbf{F_y}$ for all the subsections would yield the actual amount of the retractive force applied to the entire section. Also, as **n** approaches infinity, the value of θ diminishes to an infinitesimal amount $\mathbf{d\theta}$.

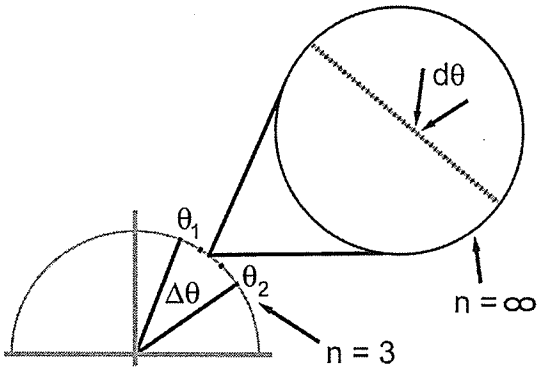

Figure 4.11 Infinitesimal angular subsections, **dθ**, contained within the angular range θ.

The limit of the sum of the differences in the retractive components as the number of subsections approaches infinity and the angular subsection becomes infinitesimal becomes the **integral** of the retractive components for every infinitesimal angular subsection **dθ** over the entire angular range defined between θ_1 and θ_2:

$$\lim_{n\to\infty} F\sum_{i=1}^{n} \Delta\sin\theta = F\int_{\theta_2}^{\theta_1} \sin\theta d\theta$$

An integral is essentially a sum of infinitesimal divisions over a particular range. In the context of this investigation, the integral will be used to calculate the theoretical value of the amount of retractive force applied to a particular section of a semicircular archwire.

4.4 DEVELOPMENT OF THE THEORETICAL MODELS

4.4.1 SEMICIRCULAR ARCH FORM

The mathematical model is based on a semicircle for the following reasons:

1. Although there are myriad number of naturally occurring arch forms, a semicircular arch form represents a "midpoint" between square and tapered arch forms.
2. Circles (and semicircles) have a constant radius and permit analysis with simple trigonometric functions of an angle and radius as measured from the centre of the circle (or semicircle).
3. Forces directed tangentially to a circle have orthogonal "normal" forces which are directed at the centre. For the laboratory experimentation which is to follow (which is based on and compared to this mathematical model), retractive forces will be easiest to produce if they are directed to the right and left termini of a semicircle. Directed as such, it will permit the investigator to produce retractive forces using the force of gravity, with the base of the semicircle parallel to the ground. The retractive forces will be parallel to each other, and the normal forces which are directed to the centre will be antiparallel.* The importance of parallel tangential retractive forces is that they *a)*allows experimentation to be carried out in a manner that minimizes variables and confounders, and *b)* makes interpretation of the results easier to understand.
4. Previously published articles have demonstrated that the spatial relation of the maxillary anterior six teeth are arranged on a semicircle.[85,86]

---

* Antiparallel vectors are vectors which are parallel to each other but point in opposite directions. They may or may not be of equal magnitude, and may or may not be collinear. By definition, if two antiparallel vectors of equal magnitude are added by the law of vector addition, the resultant vector will have zero magnitude. Vectors of equal magnitude are added by the law of vector addition, and the resultant vector will have zero magnitude.

5. Any other single arch form would suffer from being equally arbitrary.

Two separate models were developed to predict the behavior of the system at the extremes of the spectrum of archwire stiffness: one model for an infinitely flexible archwire, and another model for an infinitely rigid archwire. Since, in the real world, no such archwires exist, the actual stiffnesses of archwires used clinically lie somewhere within the spectrum of stiffness between infinitely flexible and infinitely rigid. Determining the theoretical behavior of the system under the extremes serves as a guide in experimental design.

4.4.2 DISTRIBUTION OF THE TEETH AS FREE BODIES

For the purposes of analysis in the mathematical models, each tooth in the group of six anterior teeth was represented as a free body. Free-body mechanics refers to a method of analysis which represents a body (in general) by its centre of mass. The term "body" refers to mass (which in turn refers to a collection of matter). Any body which experiences an applied force not applied to its centre of mass will rotate about its centre of mass. A free-body analysis "frees" the body of any physical characteristics that may be difficult to represent. Newton's laws of motion govern free-body mechanics.

Clinically, a central incisor, a lateral incisor and a canine all have different mesiodistal widths. Representing teeth as free bodies in a mathematical analysis ignores such dimensions by definition, but since the motivation of this investigation is to determine the distribution of retractive force over an archwire (which is modeled as a two-dimensional

object), we must arrange the free body "teeth" similarly to that which is evident clinically.

Average mesiodistal widths for central and lateral incisors and canine teeth were taken from Moyer's tables for a North American Caucasian male.[86] Moyer's tables were used because they are widely recognized in orthodontics. The average dimensions of mesiodistal width for the maxillary central incisor, lateral incisor and canine are 8.8mm, 6.9mm and 8.0mm respectively. If one central, lateral incisor and canine are laid next to each other in a straight line, the sum of their mesiodistal widths is 23.7mm. The central incisor occupies 37.1% of this measurement, the lateral incisor occupies 29.1% and the canine occupies 33.7%. For ease of apparatus construction, the semicircle had a diameter of 115 ± 0.5mm.

To arrange the "teeth" in a semicircular pattern, the measurement of 23.7mm along the circumference would equal half the semicircle, or 90°. Thus, for example, one side of the semicircle represents one side (right or left) of the anterior segment and would have a central incisor that occupied 37.1% of 90°, which is 33.4°. The lateral incisor would occupy 29.1% of 90°, which is 26.2°, and the canine would occupy 33.7% of 90°, which is 30.4°. The other side of the semicircle would be the mirror image.

In the theoretical model, the distribution of the free bodies representing the rods which are to be tested experimentally is such that a free body is located in the middle of each section corresponding to a tooth, as illustrated in **Figure 4.12** below.

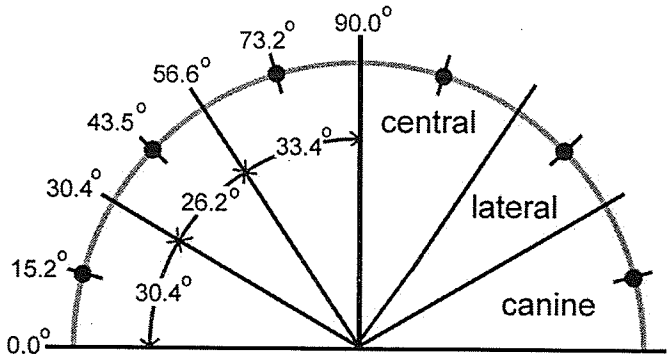

Figure 4.12 Distribution of the rods as free bodies.

4.4.3 ASSUMPTIONS

4.4.3.1 ASSUMPTIONS OF THE FLEXIBLE MODEL

The theoretical model of an infinitely flexible archwire is based on the following assumptions:

Assumption #1: For a semicircular archwire of infinite flexibility, the magnitude of the tension vectors on either side of any point on that archwire is the same. Further, the tension between any two points is the same and directed on a straight line connecting those two points.

Assumption #2: For a semicircular archwire of infinite flexibility, the resultant force at any point resulting from the tension in the archwire is directed radially towards the centre of the semicircle.

4.4.3.2 RATIONALIZATION OF ASSUMPTIONS – FLEXIBLE MODEL

Rationalization of Assumption #1:

To explain the first assumption, consider **Figure 4.13**. This figure depicts a semicircle divided into several linear sections of equal length, each occupying an angular range θ. At the junction of two adjacent sections, vectors representing tension in the archwire are collinear with the sections.

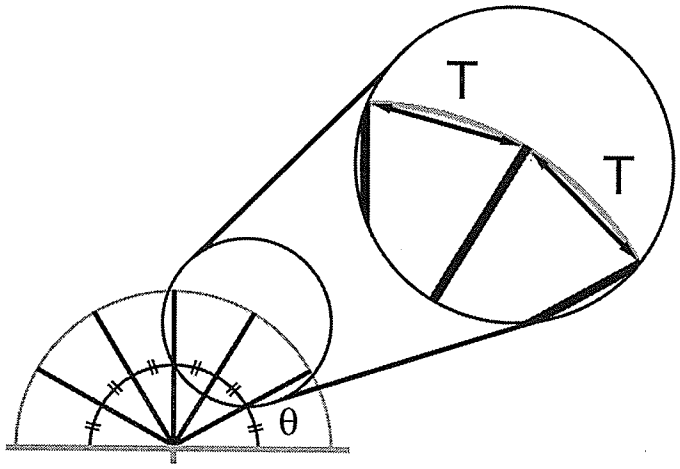

Figure 4.13 Semicircle divided into sections, showing vectors representing tension in each section.

Newton's first law of motion states that a body at rest will tend to stay at rest and a body in motion will continue in motion in a straight line unless it is acted upon by a net external force. Forces may be acting on a body, but if that body is in a state of equilibrium (that is, it is not accelerating in any direction), then the forces are balanced, and there is no net force acting on the body. The application of Newton's first law of motion to any section of the archwire allows one to draw the following conclusions about the archwire:

1. If the archwire is not accelerating or rotating, then there is no net external force acting on the archwire.

   Rationalization: Newton's first law of motion.

2. If the archwire maintains its semicircular form, then every point on the archwire must be in a state of equilibrium with each other.

   Rationalization: If two points were not in equilibrium, then there should be acceleration of these two points towards or away from each other, indicating the presence of a net external force, which would manifest itself as a change in shape or distortion of the archwire.

3. Since no two points on the archwire are accelerating towards or away from each other, and the archwire maintains its semicircular form, the tension force between any two adjacent points must be equal in magnitude and opposite in direction since an equilibrium exists between these two points.

   Rationalization: If the forces were not balanced, then one of the points would accelerate, and/or a distortion of the archwire would occur.

4. The tension between any two points in the archwire is collinear with a line joining these two points.

   Rationalization: By definition, tension is defined as a force between two points. The forces of tension must be directed towards each other on a line joining two points.

Rationalization of Assumption #2:

The parallelogram law of vector addition can be used to explain the second assumption. Consider the junction of two adjacent sections of the archwire as depicted in **Figure 4.14**. If the parallelogram law is applied, the resultant vector is directed inwards.

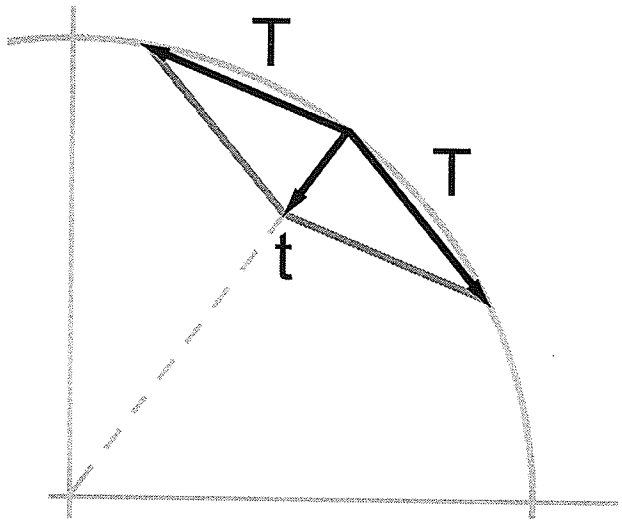

Figure 4.14 Parallelogram law for tension vectors, showing the resultant vector directed at centre of the semicircular archwire.

Since it has been demonstrated that the magnitudes of the two tension vectors **T** are the same, then the resultant vector **t** must bisect the angle between the two vectors. Further, since the archwire maintains a semicircular form, and the sections are assumed to be of equal size, and the points where any two segments meet lie on the semicircle, the resultant vector must be directed towards the centre of the semicircle.

The resultant force vector inwards will exist only if the two tensile vectors of equal magnitude are not antiparallel, but make an angle with each other that is not 180°.

Collinear vectors directed towards each other will cancel each other and no resultant vector will exist.

This resultant inward force has been demonstrated here using an approximate model of the archwire using linear sections, each with an angular range θ. If the angular range is decreased to an infinitesimal size $\mathbf{d\theta}$, then the length of each linear section becomes negligible and the polygonal approximation of a semicircle actually becomes a true semicircle. Also, for each $\mathbf{d\theta}$ there still exist infinitesimal tension vectors **dT** which still yield an infinitesimal resultant **dt**.

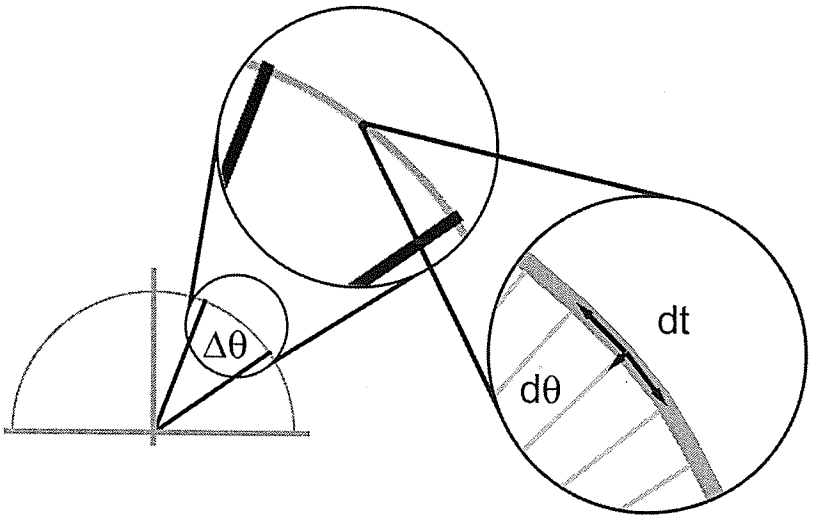

Figure 4.15 For every infinitesimal $\mathbf{d\theta}$, there exist tension vectors of infinitesimal magnitude, **dT**, the resultants of which, **dt**, are directed towards the center of the circle.

The contribution of these infinitesimal resultants individually is negligible, but when they are integrated over the entire semicircle, their contribution is significant as they serve to maintain the semicircular shape of the infinitely flexible archwire.

Thus, for a semicircular archwire of infinite flexibility, the resultant force between any two points resulting from the tension in the archwire is directed towards the centre of the semicircle.

4.4.3.3 ASSUMPTIONS OF THE RIGID MODEL

The theoretical model of an infinitely rigid archwire is based on the following assumptions:

Assumption #1: For a semicircular archwire of infinite rigidity, the archwire does not distort or use any of the energy of the system; it simply applies a force to the free bodies representing the teeth.

Assumption #2: For a semicircular archwire of infinite rigidity, the retractive force at any point along the archwire is uniform and in the same direction as that of the retractive force applied to the archwire.

4.4.3.4 RATIONALIZATION OF ASSUMPTIONS – RIGID MODEL

Rationalization of Assumption #1:

For an infinitely rigid body to distort in any fashion, an infinite amount of energy is required to accomplish the distortion. Conversely, to cause distortion of any solid body requires energy. For example, consider a lever being used to move a heavy object. A small amount of bending of the lever is noticed as the force is applied. A very small percent of the total energy required to move the object is "used" by the lever as it bends (because it can bend), while the overwhelming majority of the energy is still used in moving the object. If the lever was incapable of bending, it would be incapable of using that small percentage of energy in the system. The law of Conservation of Energy states

that energy can neither be created nor destroyed. A corollary of that law would be that energy that exists in a closed system must be constant. If there are two objects physically interacting in a closed system and one of those objects is infinitely rigid, then the amount of energy exerted by that infinitely rigid object on the other is the total amount of energy associated with that interaction.

Thus, for a theoretically infinitely rigid object, no distortion of any form is expected.

Rationalization of Assumption #2:

The behaviour of a theoretically infinitely rigid archwire is different from that of a theoretically infinitely flexible archwire in that it does not exert any tension between adjacent points. (Rather, it probably exerts an infinite amount of tension between adjacent points, but for the purposes of this discussion, the tension cannot be scrutinized in the way it was in **Section 4.4.3.2.**) Since there is no tension in the archwire, it cannot direct a resultant tensile vector **dt** towards the centre of the circle. Also, since it is also incapable of distorting, any resultant force would be in the same direction of the applied force.

Thus, the application of the law of Conservation of Energy to a theoretically infinitely rigid archwire allows the following conclusions to be drawn:

1. Any energy associated with the archwire is 100% transferred to the object it is interacting with.

   Rationalization: Energy would otherwise be used in distorting the archwire.

2. No tension exists between any two adjacent points along the archwire.

   Rationalization: The presence of tension would indicate the ability of two adjacent points to be moved apart from each other. Such an event cannot occur in an object defined as infinitely rigid.

3. Any retractive component of the applied retractive force is equal in magnitude and direction to the applied retractive force at any point along the archwire. See **Figures 4.16a** and **4.16b**.

   Rationalization: If the wire could be distorted, then its tension between any two points could exist, and a resultant force would exist in a different direction from that of the applied force. This event would be contrary to the above two conclusions.

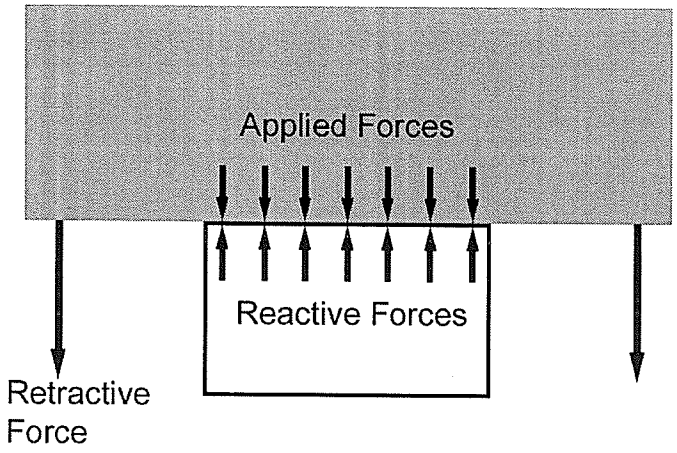

Figure 4.16a Consider a flat rigid body applying a force directly downward. The force at any point along this object is directed downward, in the same direction as the applied force. Any object resisting this force does so with reactive force(s) antiparallel to the applied force.

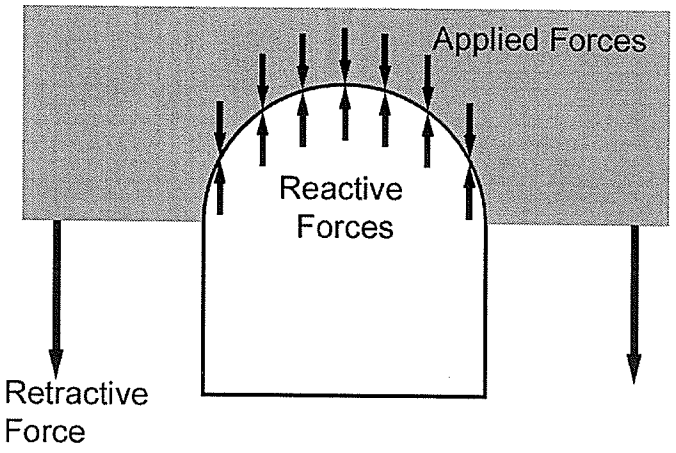

Figure 4.16b If the flat rigid body were to have a downward-facing semicircle carved into it, and it, too, were to apply a force directly downward, any object resisting this force also does so with reactive force(s) antiparallel to the applied force.

Thus, logic dictates that since the infinitely rigid archwire does not distort, no tension could exist in any part of the archwire, and the magnitude and direction of the retractive force at any point along the archwire is constant and equal to that of the applied retractive force.

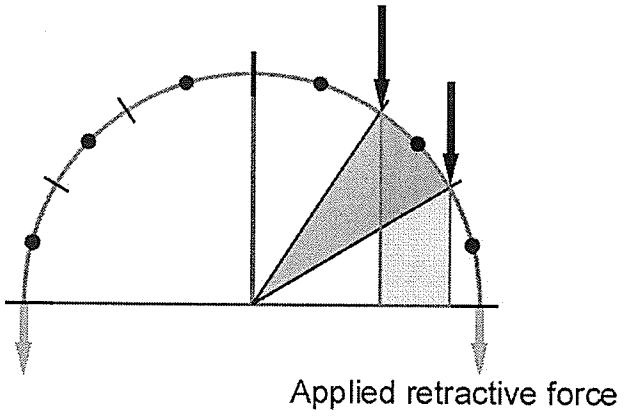

Figure 4.17 The magnitude and direction of the retractive force at any point along the archwire is constant and equal to that of the applied retractive force.

4.5 THEORETICAL MODELS

4.5.1 FLEXIBLE MODEL

It has been demonstrated that for a semicircular theoretically infinitely flexible archwire, resultant forces exist which are directed towards the centre of the semicircle. Further, there are retractive components of these inwardly directed resultant forces which are dependent upon the sine function of the angle at which they are measured.

To determine the total retractive force exerted on a section of infinitely flexible archwire, the retractive components of the resultant vectors must be integrated over the entire angular $\Delta\theta$ range defined between θ_1 and θ_2.

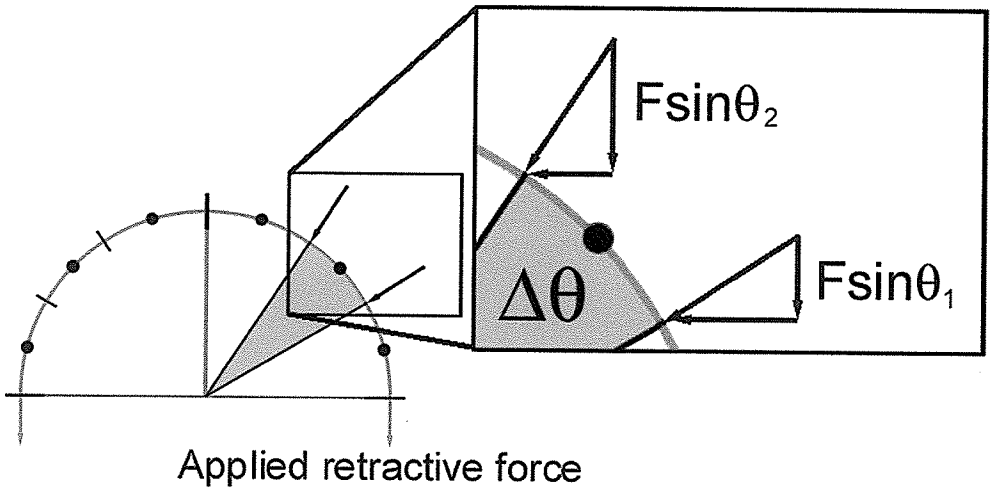

Figure 4.18 Components of the retractive force at the termini of an angular range corresponding to a tooth.

The theoretical value of the retractive force applied to any section of infinitely flexible archwire is determined by integrating the components (**Fsinθ**) over the entire range between θ_1 and θ_2.

Theoretical value for any range on an infinitely flexible archwire:

$$F\int_{\theta_2}^{\theta_1} \sin\, d\theta$$

$$= F\cos\theta\Big|_{\theta_2}^{\theta_1}$$

$$= F(\cos\theta_1 - \cos\theta_2)$$

4.5.2 RIGID MODEL

It has been demonstrated that for a semicircular theoretically infinitely rigid archwire, any force applied to any section of the is equal in magnitude and direction to that of the applied retractive force. The theoretical value of the retractive force to any section of infinitely rigid archwire depends on the horizontal projection of that section of archwire between θ_1 and θ_2. This value is equal to the difference of the x-components of the retractive force at θ_1 and θ_2. Consider **Figure 4.19**.

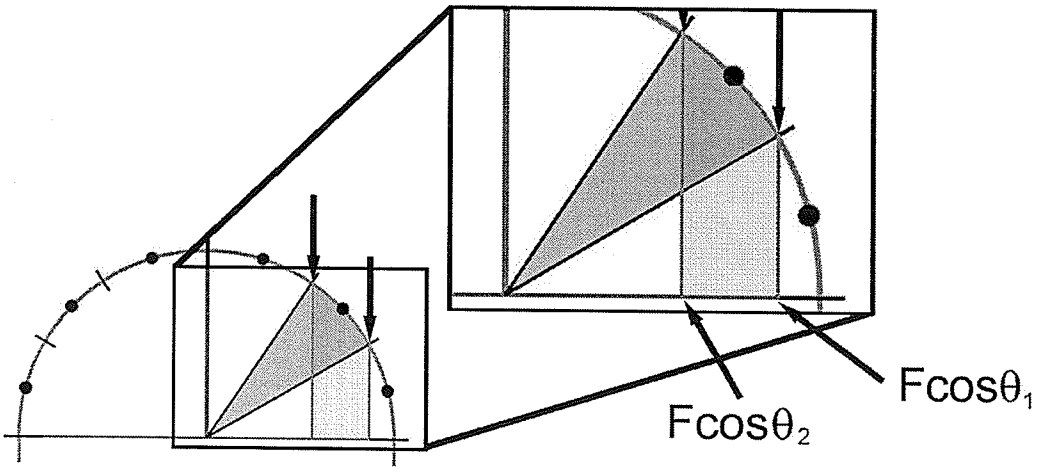

Figure 4.19 The theoretical value of the retractive force to any section of infinitely rigid archwire depends on the horizontal projection of that section of archwire between θ_1 and θ_2.

Theoretical value for any range on an infinitely rigid archwire:

$$F\cos\theta_1 - F\cos\theta_2$$

$$= F(\cos\theta_1 - \cos\theta_2)$$

This general mathematical result is identical to that of the model of the infinitely flexible archwire.

4.6 RESULTS OF THE THEORETICAL MODELS

Tooth	θ_1	θ_2	θ
Central Incisor	56.6°	90.0°	33.4°
Lateral Incisor	30.4°	56.6°	26.2°
Canine	0.0°	30.4°	30.4°

Table 4.1 Angular ranges and termini of ranges for teeth distributed as free bodies along the archwire.

Using the values for θ_1 and θ_2 in **Table 4.1**, the theoretical models yield the same results for both infinitely flexible and infinitely rigid archwires, displayed as follows:

Central Incisor:

$\theta_1 = 56.6°$

$\theta_2 = 90.0°$

$$F(\cos\theta_1 - \cos\theta_2)$$

$$= F(\cos 90.0 - \cos 56.6)$$

$$= 0.550F$$

Thus, the theoretical proportion of the total retractive force transmitted to the section corresponding to the central incisor is **55.0% of the total**.

Lateral Incisor:

$\theta_1 = 30.4°$

$\theta_2 = 56.6°$

$$F(\cos\theta_1 - \cos\theta_2)$$

$$= F(\cos 56.6 - \cos 30.4)$$

$$= 0.312F$$

Thus, the theoretical proportion of the total retractive force transmitted to the section corresponding to the lateral incisor is **31.2% of the total**.

Canine:

$\theta_1 = 0.0°$

$\theta_2 = 56.6°$

$$F(\cos\theta_1 - \cos\theta_2)$$

$$= F(\cos 30.4 - \cos 0.0)$$

$$= 0.137F$$

Thus, the theoretical proportion of the total retractive force transmitted to the section corresponding to the canine is **13.7% of the total**.

Therefore, the results of the theoretical models for the distribution of retractive force to anterior teeth for both infinitely flexible and infinitely rigid archwires are the following:

Tooth	Percentage of applied retractive force
Central Incisor	55.0%
Lateral Incisor	31.2%
Canine	13.7%

Table 4.2 Results of the theoretical models.

4.7 Summary

Thus, the theoretical models show that approximately half (55%) of the retractive force is concentrated at the central incisor, approximately one-third (31.2%) is concentrated at the lateral incisor, and approximately one-eighth (13.7%) is concentrated at the canine.

CHAPTER 5

RESULTS

5.1 CALIBRATION OF ACRYLIC RODS

The calibration plots for the acrylic rods used in this investigation are presented in **Figures 5.1 – 5.7**. They are presented as *Mean ± Standard Deviation*. All rods except *rod 23* (**Figure 5.6**) had slopes of similar statistical magnitude ($p>0.05$), and all rods except *rod 13* (**Figure 5.3**) had y-intercepts of similar statistical magnitude ($p>0.05$). However, these findings have little effect on the results and analysis of this investigation since, for example, even though the y-intercept value for *rod 13* (**Figure 5.3**) lies 0.0057mm or 5.7 m outside the 95% confidence limit, it still falls well within the limit of measurement error of deflection. Also, since there is no direct interaction of the rods, the rods are essentially behaving independently during measurements, and any deflection depends on the bending behaviour of an individual rod, and the concepts of mean values of slopes and y-intercepts of the group acrylic rods have no bearing on this investigation.

Rod	Slope	Y-intercept
Rod 11	1.668	0.0120
Rod 12	1.625	0.0111
Rod 13	1.669	0.0264*
Rod 21	1.610	0.0040
Rod 22	1.679	0.0078
Rod 23	1.586*	0.0147

Table 5.1 Slopes and y-intercepts of the calibration lines for the acrylic rods used in this investigation. Values with an asterisk (*) lie outside the 95% confidence limit(s).

Rod 22 had the highest slope and *rod 23* (**Figure 5.6**) had the lowest slope, showing that *rod 22* was the most flexible rod of the group and *rod 23* (**Figure 5.6**) was the stiffest.

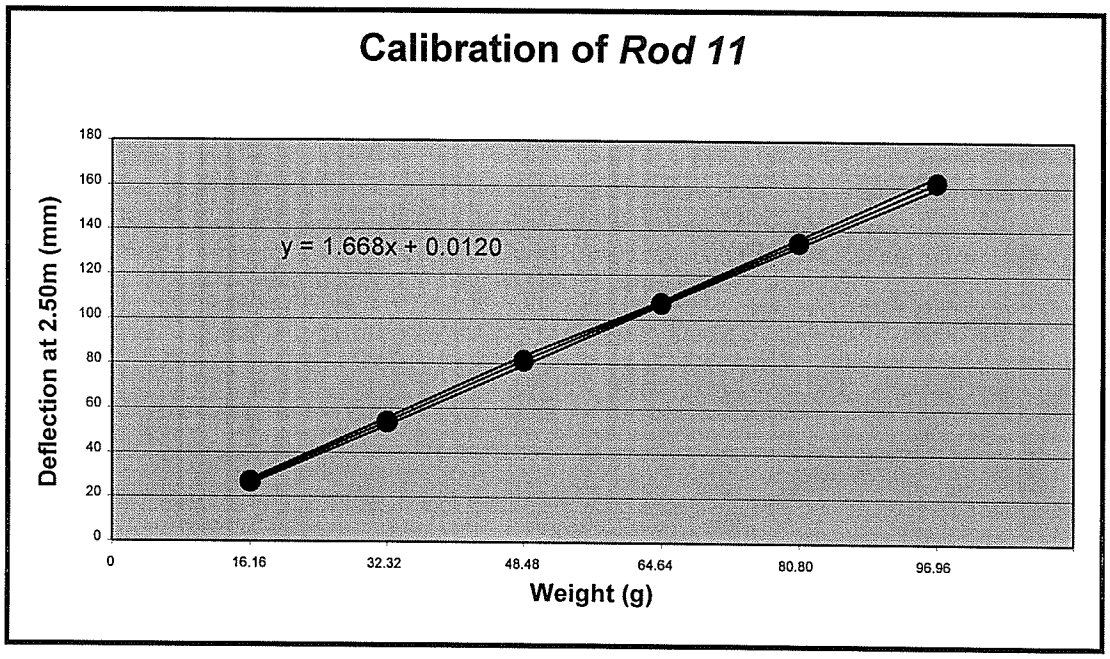

Figure 5.1 Calibration plot of *Rod 11. Mean ± Standard Deviation.*

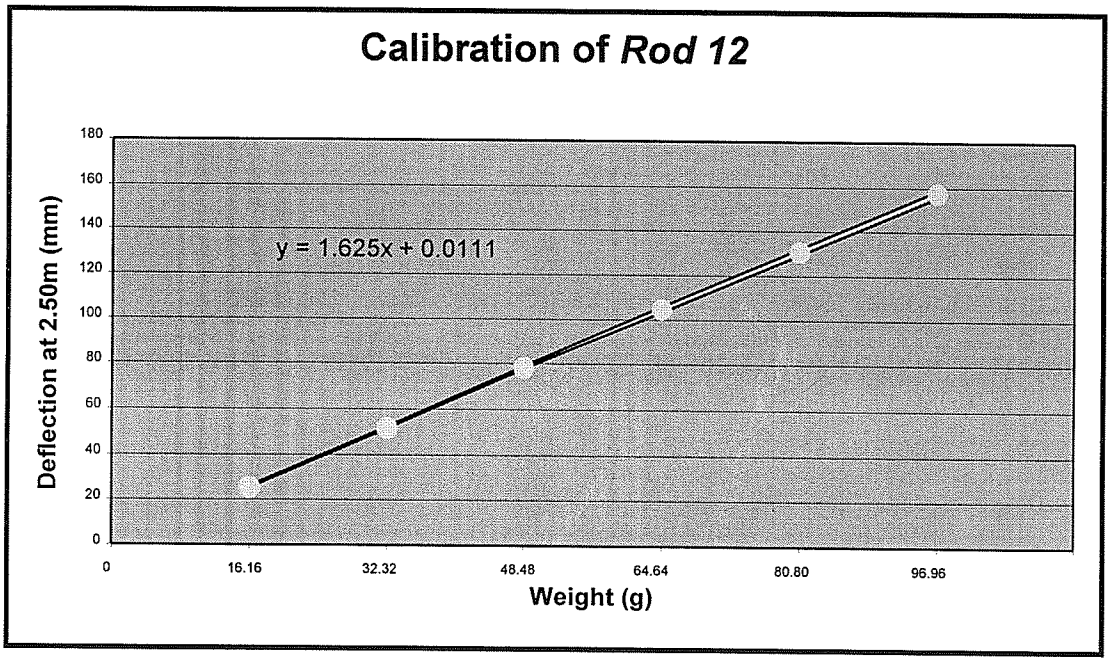

Figure 5.2 Calibration plot of *Rod 12. Mean ± Standard Deviation.*

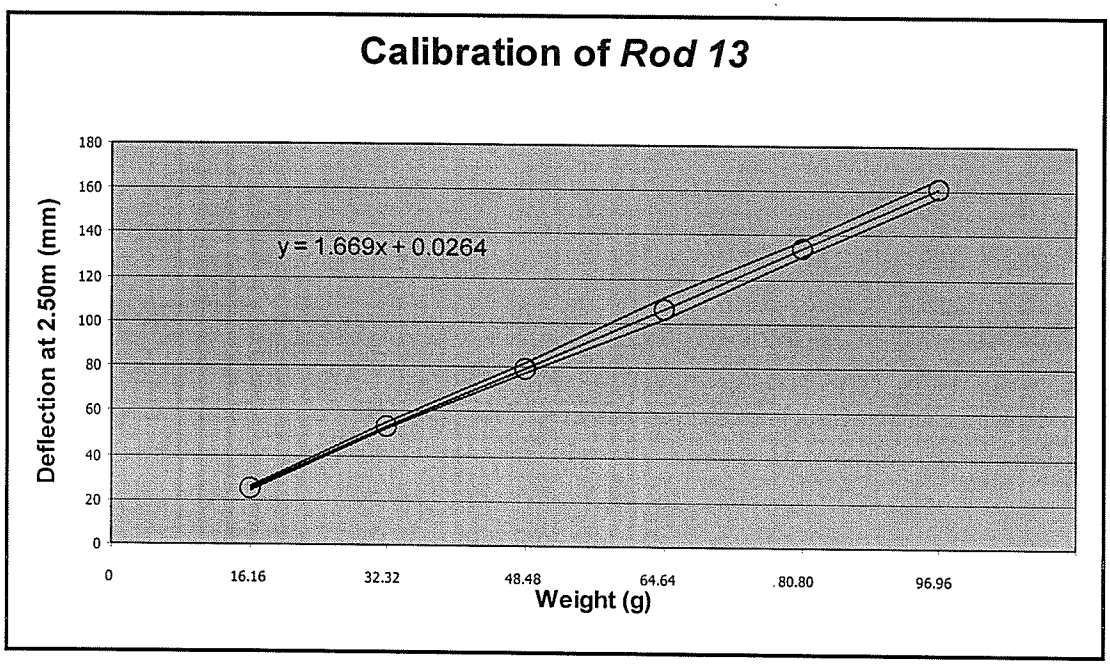

Figure 5.3 Calibration plot of *Rod 13. Mean ± Standard Deviation.*

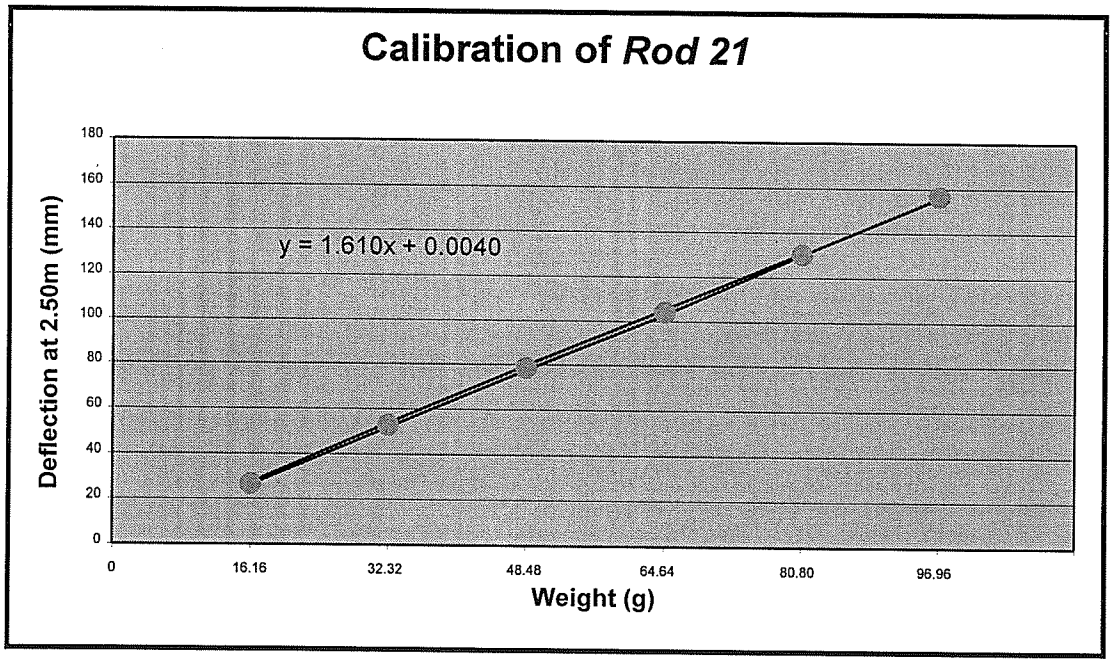

Figure 5.4 Calibration plot of *Rod 21. Mean ± Standard Deviation.*

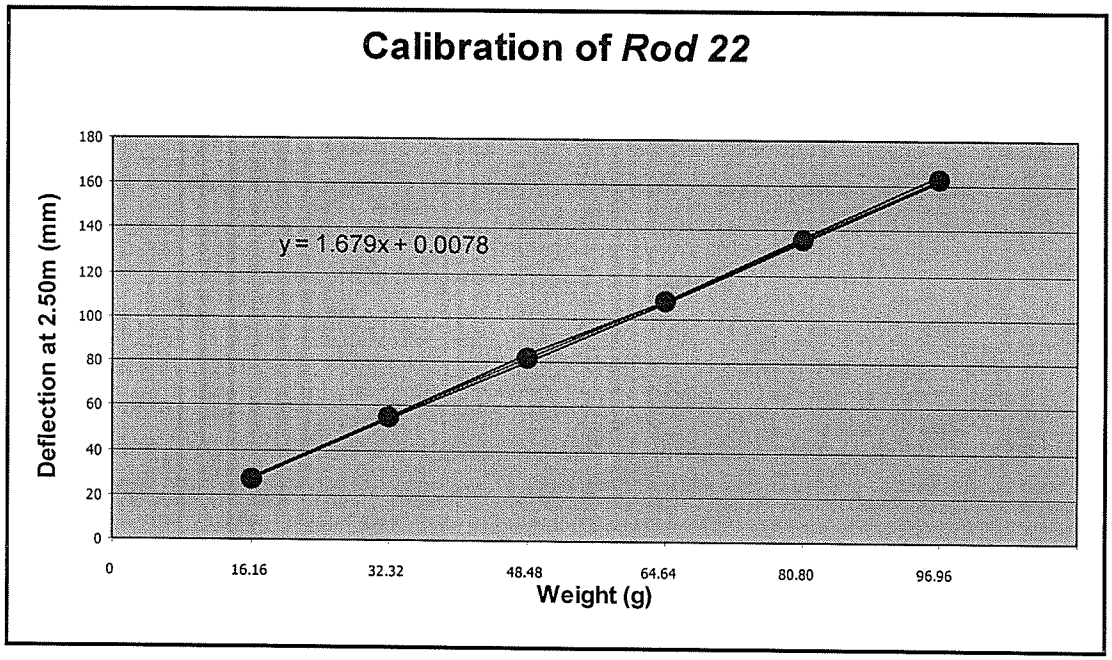

Figure 5.5 Calibration plot of *Rod 22. Mean ± Standard Deviation.*

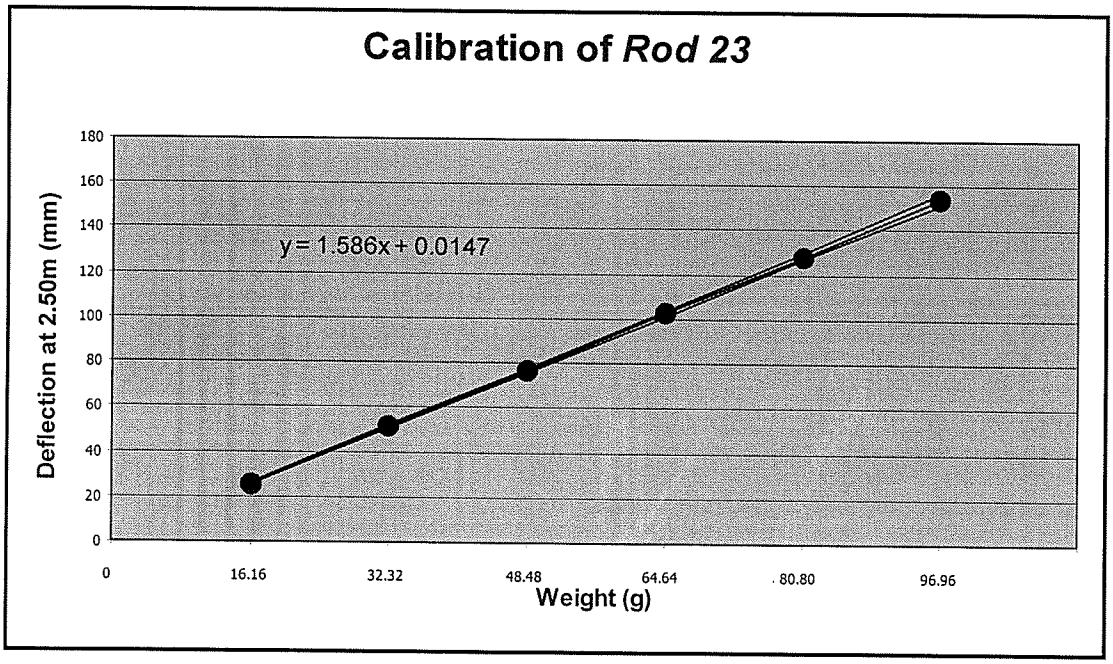

Figure 5.6 Calibration plot of *Rod 23. Mean ± Standard Deviation.*

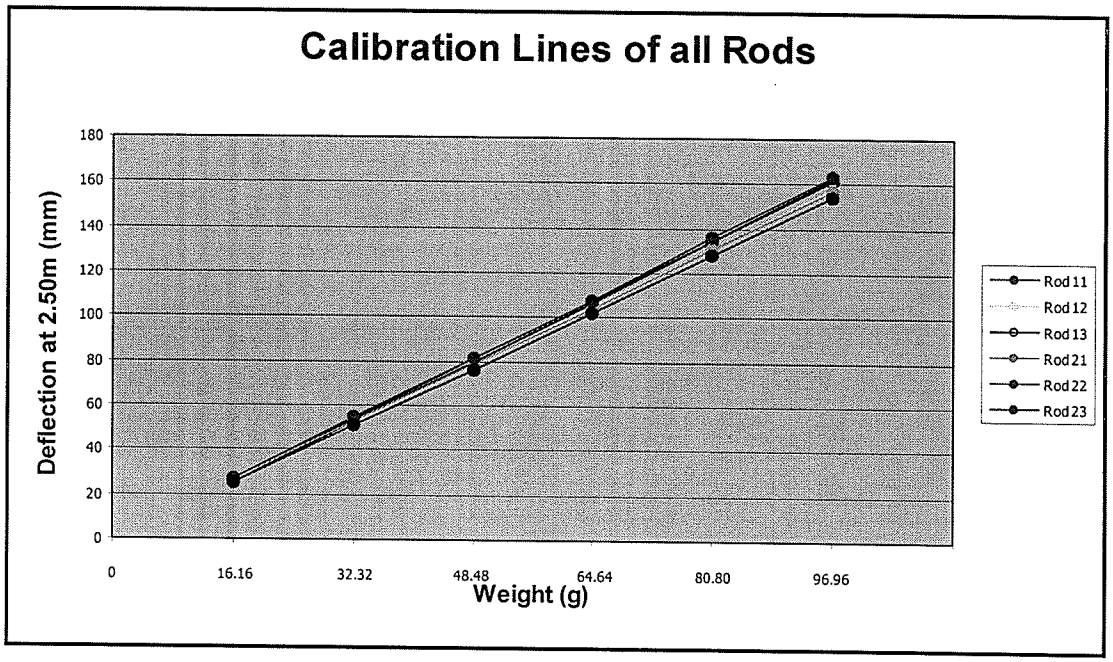

Figure 5.7 Composite of calibration plots of all rods used in this investigation.

The individual deflections of each rod, as well as mean deflection, maximum, minimum and standard deviations are listed in **Appendix 1.**

5.2 PLASTIC DEFORMATION OF ACRYLIC RODS

Results of successively higher weights applied to three acrylic rods identical to the ones used in testing in the present study (see **Figure 3.5**) revealed that the elastic range ended and permanent plastic deformation was noticed between 900.0g and 916.2g. The timing of each measurement followed the same protocol as that specified for testing with the archwires: three minutes were allowed to elapse between successive measurements to permit viscoelastic recovery of the rods (the occurrence of viscoelastic deformation was

unlikely at these loads), and the load was removed from the rod as soon as each data point was acquired (See **Section 3.2.2.5.**).

A standard load-deflection plot was not generated for this data, since deflections on the screen (2.50 ± 0.005m away from the lens of the emitter) would have been in the order of one meter or more for loads of 900g. These measurements would have been difficult and inconvenient to acquire. Instead, any deviation from the zero point was charted after a weight was removed. Failure to coincide with the zero point after a measurement would indicate that plastic deformation of the rod has occurred for that weight.

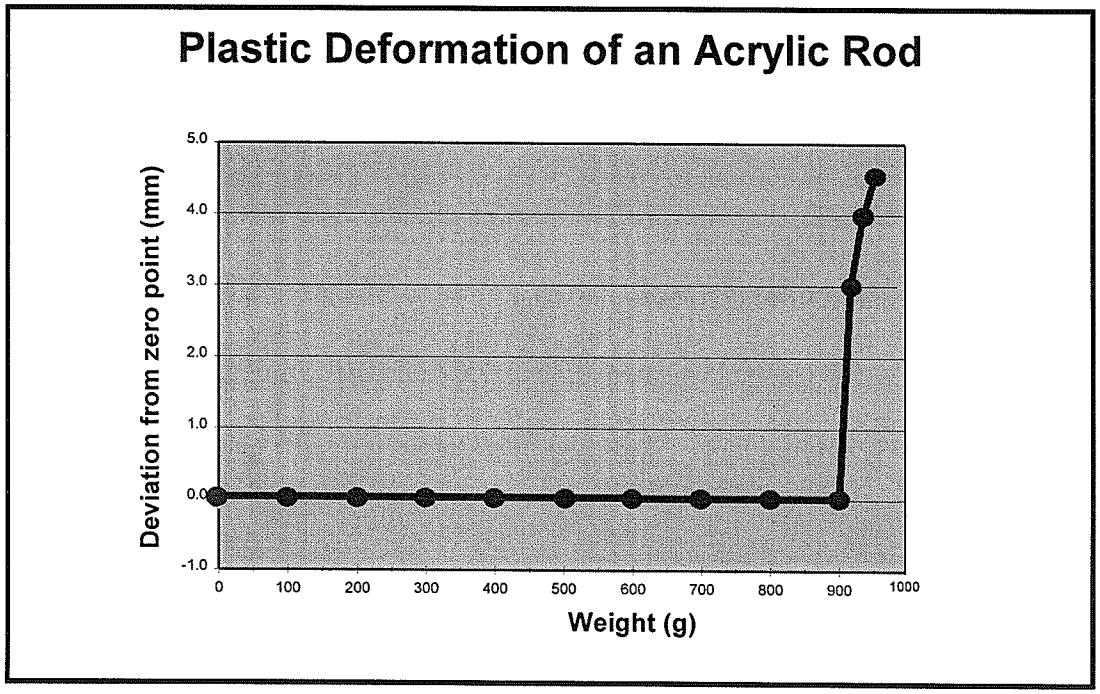

Figure 5.8 Subjecting an acrylic rod (similar to ones used in testing) to successively higher weights indicates that plastic deformation occurs between 900.0g and 916.2g.

Since the maximum weight applied to the group of rods during testing was 86.94 ± 0.25g, it is highly unlikely that any plastic deformation of any rods occurred during testing, as

the maximum applied weight was well below 900g. All deflections were observed to return to the zero point after the load was removed.

5.3 CREEP OF ACRYLIC RODS

To determine whether or not creep of the acrylic rods had occurred during testing, a load of 96.96 ± 0.3g was applied to a group of six rods similar to ones used in experimental testing and left for 30 minutes. This duration was chosen since it was far in excess of any duration during the measurement phase described in **Section 3.2.2.5.** Deflections were measured at **Time** = 0, 2, 20, 30 (removal of load), 31, 33, 35, 40 and 45 minutes. The results of this test for one of those rods are displayed in **Figure 5.9** below.

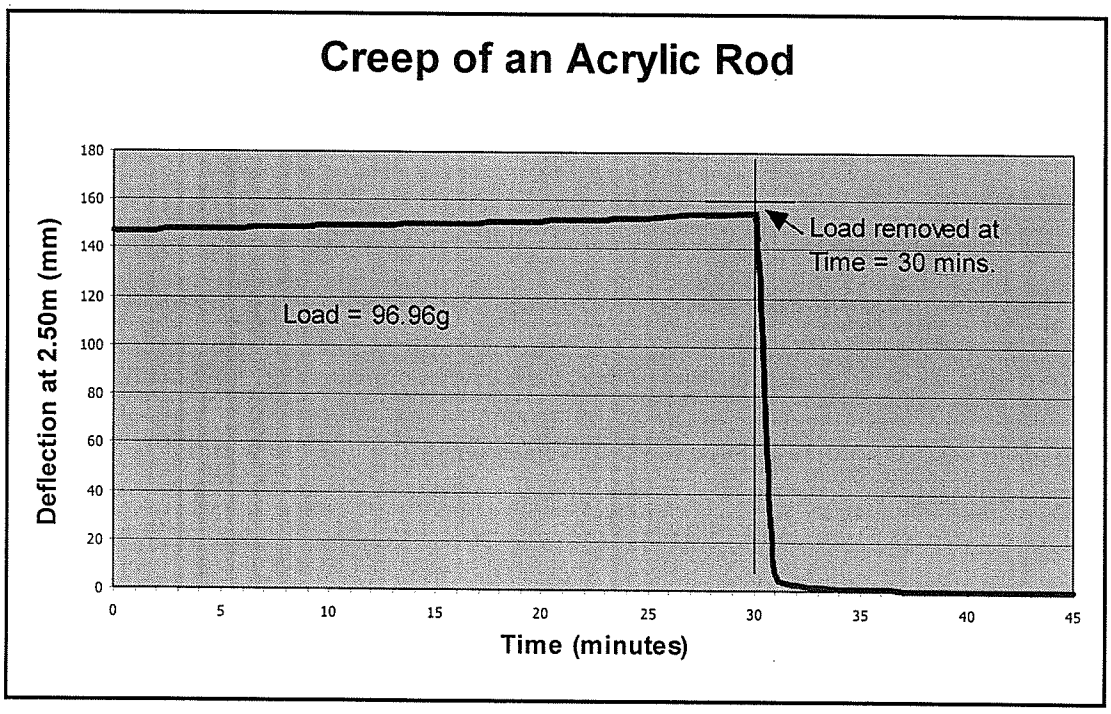

Figure 5.9 Creep testing of an acrylic rod identical to ones used in experimental testing. (Results for *rod #1* of a group of six rods is presented.)

Results show that no measurable creep of the acrylic rod had occurred. The deflection did return to the zero point after approximately 5 minutes after load removal. Also, since all deflections were observed to return to zero following load removal during the measurement phase (**Section 3.2.2.5**), it is apparent that any measurable viscoelastic deformation had recovered within the 3 minutes following load removal. No measurements were taken unless the light point(s) returned to their zero position(s).

5.4 FLEXIBLE ARCHWIRE

Mean proportions of retractive force for each rod are presented as percent-totals of the applied retractive force. These results for testing with the flexible archwire are presented in **Figure 5.10** and **Tables 5.2** and **5.3**. Values are presented as *Mean* ± *Standard Deviation*. The sum of the distribution (for each side) is greater than 100% of the applied left and right loads (102.7% for the left, and 101.8% for the right). Since this would violate the Law of Conservation of Energy, it is assumed that these seemingly erroneous results can be attributed to measurement error.

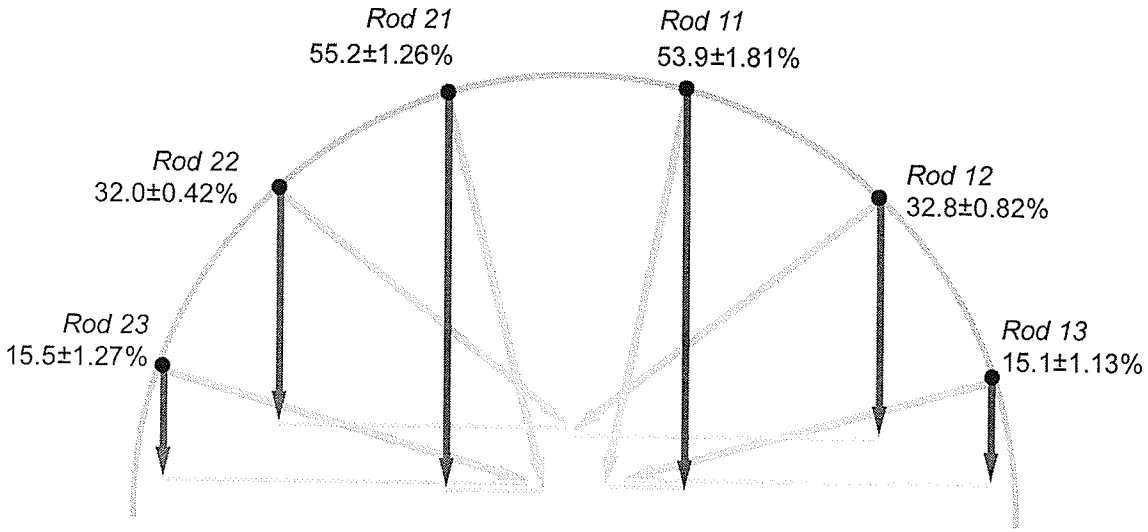

Figure 5.10 Results showing average deflection paths (gray vectors) of rods during testing with a flexible archwire (dental floss). Magnitudes of the retractive components are highlighted in red, and the proportion of the retractive force applied to each rod, expressed as percent-total of the applied retractive force, are shown adjacent to the initial position of each rod.

Central Incisors	Rod 11	Rod 21	Proportion to Central Incisors	Minimum value	Maximum value	Coefficient of Variance (%)
	53.9 ± 2.15%	55.2 ± 2.07%	54.5 ± 2.18%	50.4%	60.7%	4.01
Lateral Incisors	**Rod 12**	**Rod 22**	**Proportion to Lateral Incisors**	**Minimum value**	**Maximum value**	**Coefficient of Variance (%)**
	32.8 ± 1.49%	32.0 ± 1.63%	32.4 ± 1.61%	29.6%	38.3%	4.96
Canines	**Rod 13**	**Rod 23**	**Proportion to Canines**	**Minimum value**	**Maximum value**	**Coefficient of Variance (%)**
	15.1 ± 2.06%	15.5 ± 1.59%	15.3 ± 1.85%	11.8%	21.9%	12.04

Table 5.2 Results of testing with flexible archwire. Results of percentage of applied load to each rod are presented as *Mean ± Standard Deviation.*

Tooth	Measured Value	Theoretical Value	Absolute Difference
Central Incisor	54.5 ± 2.18%	55.0%	-0.5%
Lateral Incisor	32.4 ± 1.61%	31.2%	+1.2%
Canine	15.3 ± 1.85%	13.7%	+1.6%

Table 5.3 Comparison of measured and theoretical values of retractive components for testing with flexible archwire.

5.5 RIGID ARCHWIRE

Results for testing with the rigid archwire are presented in **Figure 5.11** and **Tables 5.4** and **5.5** below. Values are presented as *Mean ± Standard Deviation.* The sum of the distribution (for each side) is less than 100% of the applied left and right loads (95.6% for the left, and 91.5% for the right). Again, it is assumed that these seemingly erroneous results can be attributed to measurement error (in particular for the rigid archwire, refer to **Section 6.5.4**).

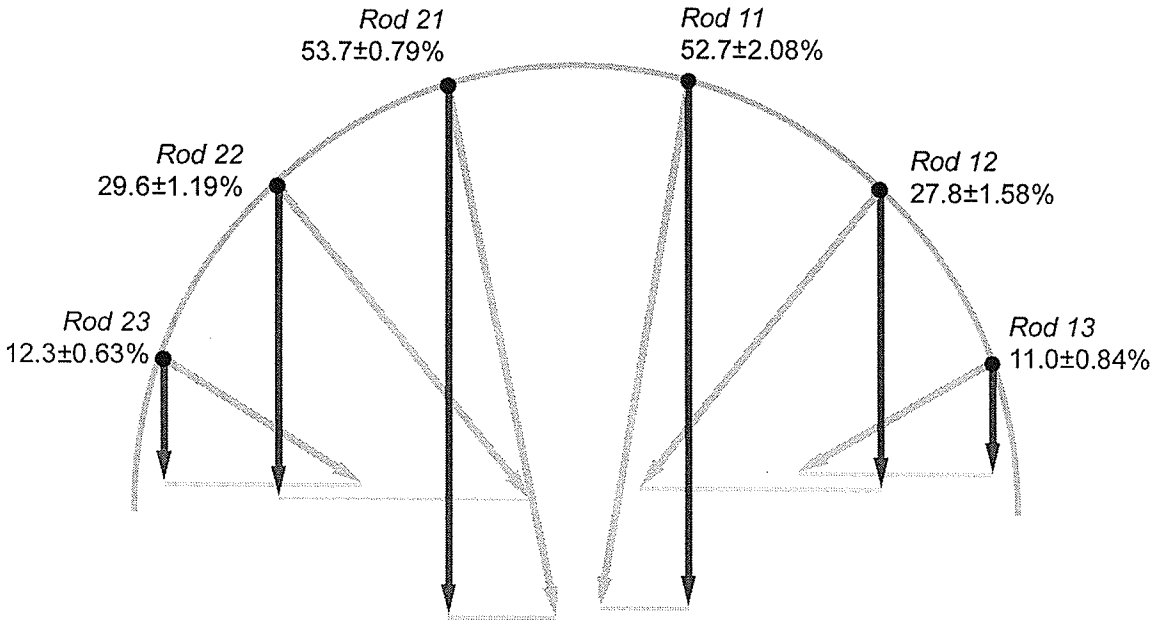

Figure 5.11 Results showing average deflection paths (grey vectors) of rods during testing with a rigid archwire (solid acrylic, 1.5mm thick). Magnitudes of the retractive components are highlighted in red, and the proportion of the retractive force applied to each rod, expressed as percent-total of the applied retractive force, are shown adjacent to the initial position of each rod.

Central Incisors	Rod 11	Rod 21	Proportion to Central Incisors	Minimum value	Maximum value	Coefficient of Variance (%)
	51.6 ± 3.12%	53.3 ± 1.89%	52.5 ± 2.71%	42.2%	58.8%	5.16
Lateral Incisors	Rod 12	Rod 22	Proportion to Lateral Incisors	Minimum value	Maximum value	Coefficient of Variance (%)
	29.3 ± 1.94%	28.7 ± 2.29%	28.9 ± 2.14%	23.3%	32.2%	7.38
Canines	Rod 13	Rod 23	Proportion to Canines	Minimum value	Maximum value	Coefficient of Variance (%)
	10.6 ± 1.38%	11.7 ± 1.85%	11.2 ± 1.71%	6.46%	14.1%	15.27

Table 5.4 Results of testing with rigid archwire. Results of percentage of applied load to each rod are presented as *Mean ± Standard Deviation.*

Tooth	Measured Value	Theoretical Value	Absolute Difference
Central Incisor	52.5 ± 2.17%	55.0%	-2.5%
Lateral Incisor	28.9 ± 2.14%	31.2%	-2.3%
Canine	11.2 ± 1.71%	13.7%	-2.5%

Table 5.5 Comparison of measured and theoretical values of retractive components for testing with rigid archwire.

5.6 SUMMARY OF RESULTS AND NULL HYPOTHESIS

For each central incisor rod pair, no statistically significant difference ($p>0.05$) in the mean values of the retractive component was found. The same was true for both the lateral incisor and canine rod pairs. The mean magnitude of the retractive component was greatest for the central incisors, less for the lateral incisors, and lowest for the canines. There were also no statistically significant differences ($p>0.05$) in mean values of retractive force for a given rod when tested with flexible or rigid archwires.

Statistically significant differences ($p>0.001$) in mean magnitudes of retractive force components were found between the rods representing central incisors, lateral incisors and canines during testing with both flexible and rigid archwires.

The null hypothesis that there is an equal distribution of retractive force among the anterior six teeth for a posteriorly directed retractive force in *en masse* retraction is therefore rejected.

CHAPTER 6

DISCUSSION

6.1 FLEXIBLE ARCHWIRE

The distribution of retractive force during testing with the flexible archwire was in close agreement with the theoretical results. In the present investigation, only the posteriorly directed, or "downward" component of the retractive force was analyzed. No analysis was preformed on the "horizontal" or medially directed components as it was outside the scope of this study (since we were only interested in determining the distribution of retractive force).

As an increasing number of weights were suspended from the termini of the flexible archwire, the light deflection points moved downward (as expected) and inward; see **Figures 5.10** and **6.4**. The amount of inward or medially directed deflection of the points is not entirely unexpected due to the nature of the flexible archwire. Indeed, if progressively stiffer strings or wires were used, there would be progressively less medial "collapse" of the deflection points at the same weight.

Interestingly, in **Figure 5.10**, the magnitudes of the gray displacement vectors associated with the central incisor rods are only slightly greater than those of the lateral incisor rods, which are slightly greater than those of the canine rods. What differs most between these displacement vectors is their direction, which reflects an increasing retractive component and a decreasing medial component as the midline is approached.

In the clinical situation, it is assumed that the effects of these medial components would be minimized or negated through interproximal contact (similar to the way a Roman arch

resists collapse by distributing its own weight amongst the individual bricks) and subsequent resistance of adjacent teeth. Since interproximal contacts were not modeled in this investigation, the rods had no resistance to medial collapse with the flexible archwire, thus the relatively large medial components of the retractive force(s) were allowed to express themselves.

Interestingly, testing with the flexible archwire in the absence of the guide rods ("distal" to the canine rods) produced results that did not appear to be significantly different from measurements of testing with the guide rods in place. (A sample large enough for statistical evaluation was not taken since doing so was not included in the protocol, and was only performed for interest's sake.) In the absence of guide rods, the magnitudes of the displacement vectors were greatest for the central incisor rods, slightly less for the lateral incisor rods, and less still for the canine rods, whereas compared to the results with the guide rods in place, the distribution of retractive force was lower for the central incisor rods, higher for the lateral incisor and canine rods.

6.2 RIGID ARCHWIRE

Results of testing with the rigid archwire produced results for the distribution of retractive force which was not statistically significantly different from that of testing with the flexible archwire. The proportion of retractive force to each rod was lower than those values for the flexible archwire, likely due to error in measured weight of the rigid archwire and the problems of friction (discussed below in **Section 6.5.3**).

Comparison of **Figure 5.10** (flexible archwire) and **Figure 5.11** (rigid archwire) reveals striking differences in magnitudes of (gray) displacement vectors for the various teeth, and also in the magnitudes of the medially directed components. The displacement vectors are largest for the central incisor rods, less for the lateral incisor rods, and least for the canine rods.

It is expected that there would be less medial collapse of the deflections of the rods (and light points) with the rigid archwire. Unlike the flexible archwire, the rigid archwire retains its shape when applying a load and does not conform to the configuration of the rods.

As a result, the amount of the medial collapse of the rods is defined by the archform and corresponds to medially directed force due to the curvature of the archwire as loads were applied. These medially directed forces were not predicted by the theoretical model. This phenomenon will be discussed further in **Section 6.3.2**. The amount of medial displacement was greatest for the lateral incisor rods, less for the canine rods and least for the central incisor rods.

6.3 CORRELATION OF EXPERIMENTAL AND THEORETICAL RESULTS

6.3.1 FLEXIBLE ARCHWIRE

For an infinitely flexible archwire, the theoretical model was based on an assumption that the tension in the archwire produced a resultant vector that was radially directed, toward

the centre of the semicircle. The results of this model were statistically similar to those attained by experimentation. Thus, it would be expected that the gray displacement vectors depicted in **Figure 5.10** would all pass through a common point, which should be the centre of the semicircle. Examination of **Figure 5.10** reveals that this is clearly not what happened. In fact, the gray vectors for each rod pair are relatively symmetric and do not appear to be random. The theoretical model also predicts that the magnitude of each gray vector should be equal, where **Figure 5.10** reveals that they are not (the vectors associated with the central incisor rods are slightly greater than those of the lateral incisor rods, which are slightly greater than those of the canine rods). This leads to two questions being asked:

1. Can the difference between the theoretical and actual displacement paths (the gray vectors of **Figure 5.10**) be explained?
2. Is the mathematical model for the infinitely flexible archwire valid?

To address these questions, it must be emphasized that the development of the theoretical models are based in static situations. As such, an assumption that the rods remain stationary seems implicit. Extending the theoretical model to the physical world necessitates certain additional assumptions. However, not all assumptions can be supported. In experimentation, the measurements were taken after the rods had deflected under load. There is movement of the rods in relation to each other as this occurs, and the static situation becomes a dynamic situation during the time that the rods take to steady themselves (i.e., reach equilibrium) under loading. Exactly how the rods interact

with each other during this movement is unclear (see **Section 6.5.1**) and the theoretical model cannot predict the effects that such movement has on the system.

During the dynamic situation of the rods deflecting under load, the distance between the tips of the rods decreases as the dental floss used to model the flexible archwire exerts the applied load and slides at the points of contact with the rods. Even though a lubricant was used to minimize friction, there will always be some friction present in the system. This friction may serve to prevent the gray displacement vectors from passing through the centre of the semicircle. Consider the displacement vectors for the central incisor rods. To pass through the centre, these vectors need to be directed medially to a greater extent than they are. Resistance of these rods to medial deflection (which is directed laterally), and friction of the dental floss with the rods (also directed laterally since the rods actually do displace medially to an extent) may add up to an amount great enough to prevent the displacement vector from actually passing through the centre, and present as they do in **Figure 5.10**.

Referring back to the way in which the theoretical model for the flexible archwire was developed, the archwire was subdivided into an infinite number of sections $\mathbf{d\theta}$. Assuming that each subsection $\mathbf{d\theta}$ was of equal (albeit infinitesimal) length, then the subsections are each separated by the same distance. Therefore, each subsection in the infinitely flexible archwire is associated with an infinitesimal tension vector **dt**. Since each subsection $\mathbf{d\theta}$ is equidistant from adjacent subsections, then each **dt** between adjacent subsections must have equal magnitude and each resultant vector from each **dt**

(see **Figure 4.15)** *must* be directed along the radius toward the centre of the semicircle and not in any other direction. Thus, the resultant vector from two adjacent tension vectors points toward the centre of a semicircle *only* if the tension vectors are of equal magnitude.

For the purposes of making the spatial relation of the rods representing the anterior teeth in the experimental apparatus more clinically relevant, they were placed particular distances apart which corresponded to average clinical values of the mesiodistal crown widths of central incisors, lateral incisors and canine teeth for a Caucasian male, distributed over a range of 180°. That is, they *were not* spaced equidistantly.

Following this line of thinking, for rods that are not spaced equidistantly, is it safe to assume that there would be different tension vectors on either side of each rod? As the diagram on the left of **Figure 6.1** demonstrates below, for the arrangement of rods used in this investigation, bisection of the angles made by joining the dots of the initial positions of the rods produces lines which pass through the centre of the semicircle. What does this say of the tension vectors on either side of each initial position? Perhaps they are unequal, but there is no way of actually knowing without measuring these tensions. Again, this is a static situation. As a load is applied, the rods deflect in different amounts, and the spatial relation to each other changes. The diagram on the right of **Figure 6.1** demonstrates that because of the differing amounts of deflection, bisection of the angles between adjacent points produces lines that *do not* pass through the centre of the semicircle or any common point. This is reflective of the numerous

variables that exist in the experimental apparatus that cannot be accounted for in the theoretical model. While the diagram on the right of **Figure 6.1** is not representative of the actual data (the gray vectors of **Figure 5.10**), it does demonstrate that there is a fault with the theoretical model in its present form.

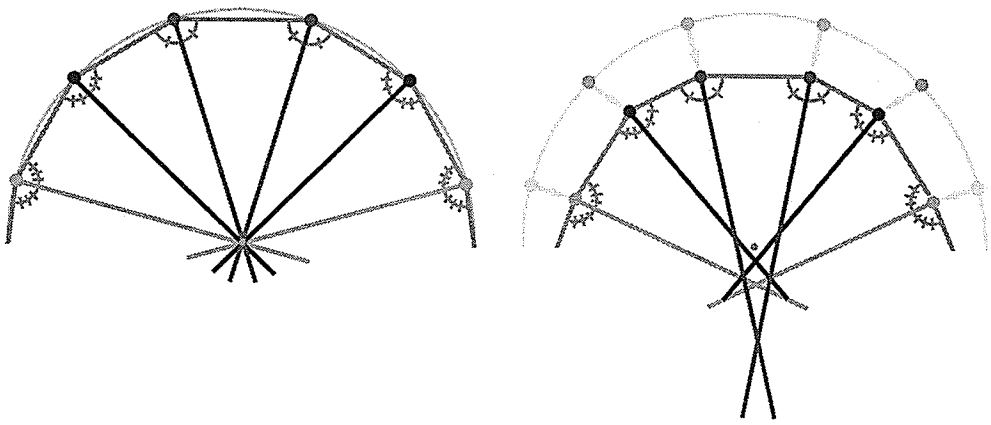

Figure 6.1 Bisection of the angles between adjacent initial position of the rods shows that lines representing resultant vectors from tension in the archwire pass through a common point at the centre of the semicircle. On the right side, deflection of the rods under load produces more deflection of the central incisor rods, less of for the lateral incisor rods, and the least for the canines. There is also medial displacement. Bisection of the angles between the points of their new positions shows that the resultant vectors do not pass through the centre or any common point. This occurs at the moment the archform is distorted from a semicircular form with constant radius, and points to a fault of the theoretical model for the flexible archwire. The distortion of the archwire during rod deflection is exaggerated merely for sake of example.

Thus, failure of the theoretical model for a flexible archwire to accommodate the dynamics during rod deflection, the associated friction, the resistance of the rods to deflection and the non-equidistant placement of the rods leads one to conclude that this model may be incomplete or perhaps even *invalid* in its present form. The variables mentioned above all have horizontal components of forces (which may have significant magnitude), and since the theoretical model for the flexible archwire did predict the

amount of retractive force that would be applied (which was validated by experimentation), perhaps the approach taken to generate this theoretical model needs further improvements. Perhaps an approach which incorporated assessment of dynamic changes in the spatial relation of the rods with each other during deflection, resistance to deflection in horizontal and vertical directions, as well as friction in the system would produce a result which arrived at the same results as the present model did for the force distribution in the vertical direction, but also may account for the failure of the gray displacement vectors to pass through the circle of the semicircle. Perhaps the theoretical model worked in the vertical direction since the greatest forces during experimentation acted vertically. (Clearly, the magnitude of applied retractive force was greater than that of friction between the floss and the rod.)

Clearly then, a new theoretical model for force distribution from a flexible archwire which will address these confounders is desired. Further, it is expected that a new theoretical model will arrive at the same results with respect to the distribution of retractive force as the present model.

6.3.2 RIGID ARCHWIRE

For an infinitely rigid archwire, the theoretical model was based on the assumption that any retractive component of the applied retractive force is equal in magnitude and direction to the applied retractive force at any point along the archwire. The difference in the amount of retractive force over any range is tied in to the geometry of the rigid archwire and the initial positions of the rods. This model predicts that the rods should

have deflected downward only; there is no prediction of any amount of medial deflection whatsoever.

However, from the experimental model, we know that there is some amount of medial deflection. Consider **Figure 6.2**, which illustrates a moving wedge contacting a stationary body. If there were an infinite amount of friction between the wedge and the object, the object would be displaced in the same direction as the wedge. If there was an absence of any friction between the wedge and the object, the object would seek the position that would allow it to be at its lowest energy level; in this case, it would be the position corresponding to the least amount of flexure of the rod.

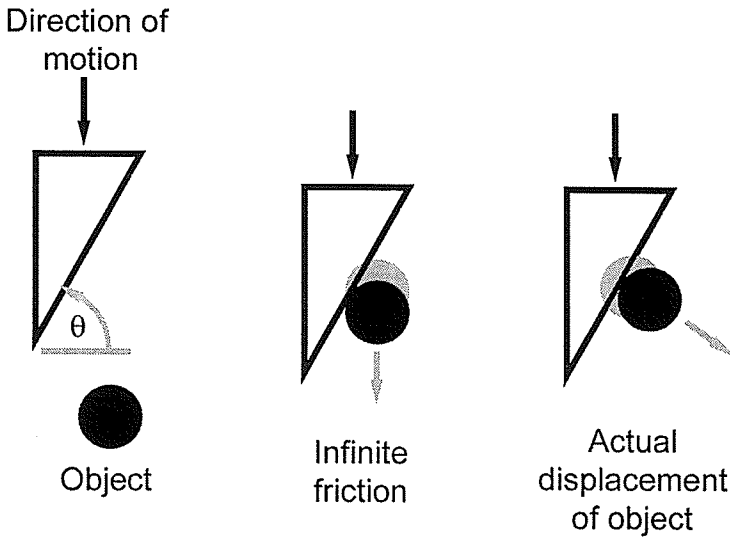

Figure 6.2 Displacement of an object in contact with a moving wedge depends on variables such as the geometry of the wedge and the amount of friction between the wedge and the object. The angle of contact, θ, is taken from a line parallel with horizontal to the side of the wedge facing the object.

If there were a degree of friction that was not infinite but greater than zero, then there would be a component of displacement of the object in both the direction and perpendicular to the direction of motion of the wedge. The resulting direction of displacement would represent the path of least resistance of the object, and would depend on variables such as the friction between the wedge and the object (and other objects), the geometry of the wedge, etc.

The rigid archwire would be analogous to a wedge contacting a rod, the geometry of which is different at the points of contact with the various rods. If the angle of contact is taken as the tangent to the archwire at the point of contact (measured with the initial side parallel with horizontal), then the canine rod would have the greatest angle of contact, the lateral incisor rod angle of contact would be less, and the smallest angle of contact is associated with the central incisor rod. One may expect that the paths of deflection of the rods at each contact point would be perpendicular to this tangent (i.e., would be radially directed), but other variables such as friction and degree of contact between the rod and archwire, resolution of the force at each point of contact, the distance each rod "slides up" the inside of the rigid archwire during deflection and other variables cause the paths of deflection to be deviated from what one may expect and actually present as those shown in **Figure 5.11**. It is not entirely unexpected that the central incisor rod would experience a greater proportion of retractive force than that experienced by the canine rod since the force applied at the central incisor rod is more-or-less "straight on" whereas the force applied at the canine is "oblique."

Thus, failure of the theoretical model for the infinitely rigid archwire to accommodate rod deflection, geometry and friction of the archwire at points of contact with the rods leads one to conclude that this model may be *invalid* in its present form and requires improvements. The fact that the experimental results for the distribution of retractive force were in close agreement with theoretical results of this model is not entirely serendipitous, but also not completely unexpected since the forces of greatest magnitude during measurement were generated by the retractive force and therefore were in same direction as the retractive force. Considering the "wedge" example of rod deflection (**Figure 6.2**), it is also not entirely unexpected that the central incisor, lateral incisor and canine rods would each experience a different amount of retractive force which is dependent on the geometry of the archwire at the points of contact. It is therefore not unexpected that the distribution of retractive force in a semicircular rigid archform may be in some way *related* to (i.e., not entirely *dependent* on) the horizontal projections of the angular ranges corresponding to each rod (see **Figure 4.19**).

Thus, a new theoretical model for force distribution from a rigid archwire which will address the aforementioned confounders is desired. It is also expected that a new theoretical model for a rigid archwire will arrive at similar results with respect to the distribution of retractive force as the present model.

6.4 COMPARISON OF RESULTS WITH PREVIOUS STUDIES

Statistically significant differences in magnitudes of retractive force delivered by the archwires alone were found between the rods representing central incisors, lateral incisors

and canines. The mean magnitude of this force was greatest for the central incisors, less for the lateral incisors, and lowest for the canines. Results were similar for testing with both flexible and rigid archwires.

Review of the literature shows that no standardized protocol exists for measurement of forces developed from archwires. As a result, most reported studies have numerous variables that differ from each other and essentially affect the way data is collected and interpreted. Of 27 papers reporting on force from orthodontic appliances (either magnitude only or magnitude and direction), seven dealt with effects on the canine exclusively,[1,9,14,21,36,42,51] eleven included evaluation of reciprocal effects on anchorage units,[8,12,13,19,27,30,35,49,52,63,87] only two dealt with force distribution,[38,39] seven were theoretical/computer-based,[37,44,46,47,61,62,65] and the overwhelming majority had markedly different protocols. Of the two papers regarding force distribution,[38,39] both had similar protocols: one paper reported testing of a regular utility arch, and the other reported testing of a contraction utility arch. Both investigations had two of three investigators in common.

The purpose of this study was to discern the forces applied to the biologic system *in vitro*. How the biologic system reacts to these forces is outside the scope of this thesis. As such, numerous variables that exist in a biologic system were eliminated. For example, Hixon *et al.*[17] pointed out that canine tipping which occurs clinically during retraction introduces several variables which obscure the relation between applied force and dental movement; the experimental protocol used by Storey and Smith caused the canine to tip

into the extraction sites, thereby obscuring the very relation they attempted to elucidate. Clinical experimentation is fraught with confounders such as inability to control the type of dental movement, biased data due to the nonlinear, time-dependent nature of dental movement following the application of an orthodontic force,[21-23] variations in patient response,[24,25] unaccounted potential energy in archwire deflection (e.g., energy stored in a spring or loop) and friction in the bracket/archwire system, only to name a few. These confounders might imply that differences in method of force measurement are significant, and makes it clear that methodical analysis in clinical situations may prove to be exceedingly difficult due to these variables. The goal of experimentation using laboratory or mathematical models is to provide data to make rational explanations of the behaviour of the biomechanical systems. An extensive Medline search and review of published literature from 1904 to present revealed that, to the best of our knowledge, the present research is the only one to demonstrate the distribution of retractive force to anterior teeth due to the archwire alone. As such, it makes comparison of this investigation to previous investigations exceedingly difficult.

6.5 ERRORS IN THIS INVESTIGATION

6.5.1 ERRORS ASSOCIATED WITH MISPLACEMENT OF THE RODS

Placement of the rods on the semicircular archform in positions different from those specified in **Section 4.4.2, Figure 4.12**, is a source of error in this investigation. For a semicircle of diameter = 115 ± 0.5mm, any deviation of 1° from the ideal location for any rod results in a difference of 1.00mm from that position along the circumference. If one or more rods are not placed in their ideal positions, the distance (angular and linear) will

be different, and the interactions of the rods in the system will produce measurements which are different from expected results.

The purpose of this section is to demonstrate that even though it is assumed that each rod is behaving independently under load, it is very likely that there is an interaction between the rods that cannot be elucidated. The following discussion is merely an educated guess as to how the interaction of the rods in the system may work.

Even though the force was measured at a particular point on the archwire, it was assumed that the retractive force acted over a specified angular range, as specified in the theoretical model. For example, if the central and lateral incisor rods are placed ideally, and the canine rod is misplaced 1.0° higher (that is, closer to the midpoint of the semicircle, along the circumference), then the angular range of the canine will increase 2.0° from 30.4° to 34.2°, the angular range of the lateral incisor would decrease from 22.2° and the lateral rod would no longer be located at the midpoint of its range. Therefore, the measurement of the lateral incisor would be affected. It is not unreasonable to assume that the central incisor rod would also be affected. Thus, misplacement of one rod from its ideal position propagates error throughout the entire system. Refer to **Figure 4.12** and to **Figure 6.3**

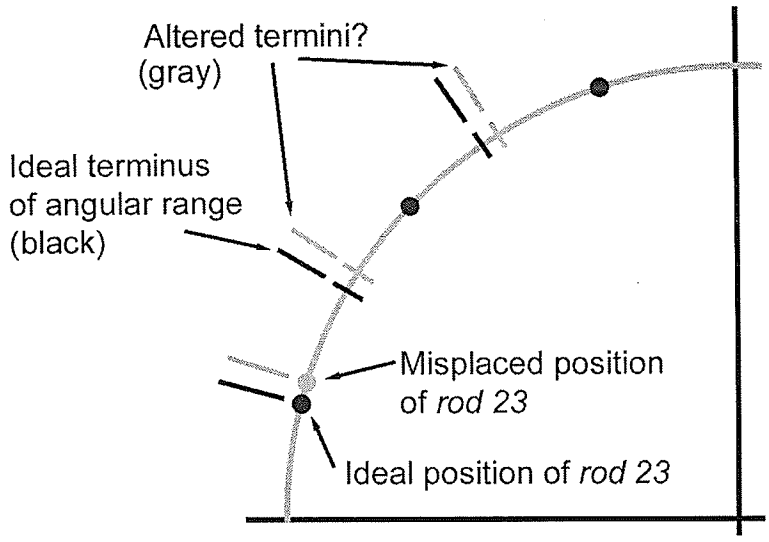

Figure 6.3 Misplacement of the canine rod (anterior misplacement shown) may propagate error throughout the entire system by altering the angular ranges.

For a single rod, the error in measurement of the proportion of retractive force to that rod depends on the amount that the rod is misplaced mesially or distally. In **Figures 6.4a – c**, the errors in proportion of retractive force associated with misplacement of each rod are presented. Absolute errors in measurement are presented in functions of deviations from ideal positions in degrees. Absolute error refers to the difference in retractive force: for example, if the canine was misplaced approximately 4.0° lower than ideal, the absolute error associated with that displacement is approximately 6% (see **Figure 6.4c**), which means that the proportion of retractive force would not be 13.7%, but would rather be 13.7% minus approximately 6% which is approximately 7.7%.

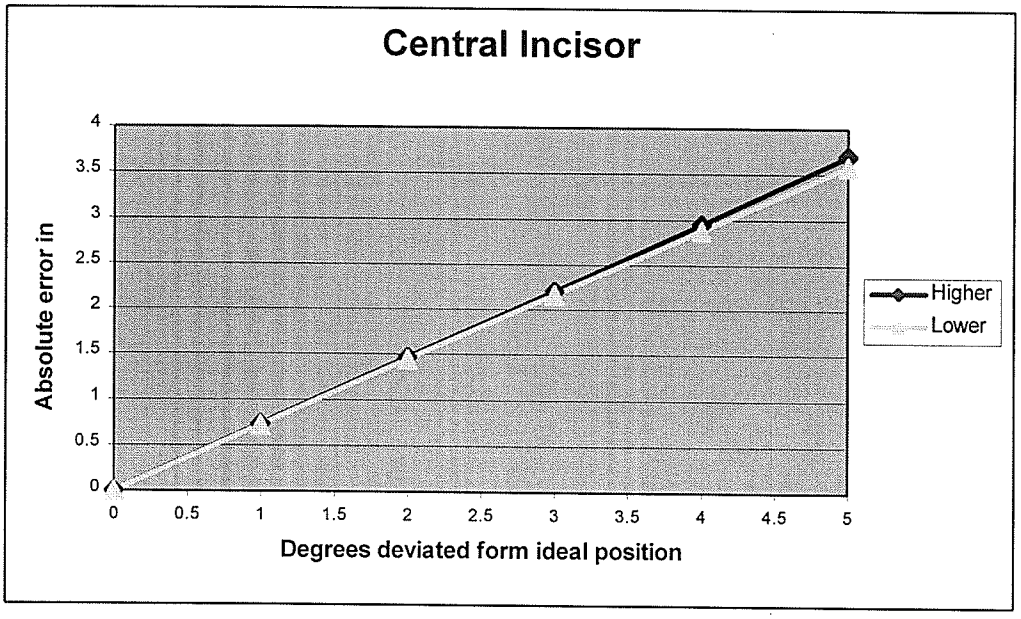

Figure 6.4a Absolute error associated with misplacement of central incisor rod in degrees, along semicircular archform.

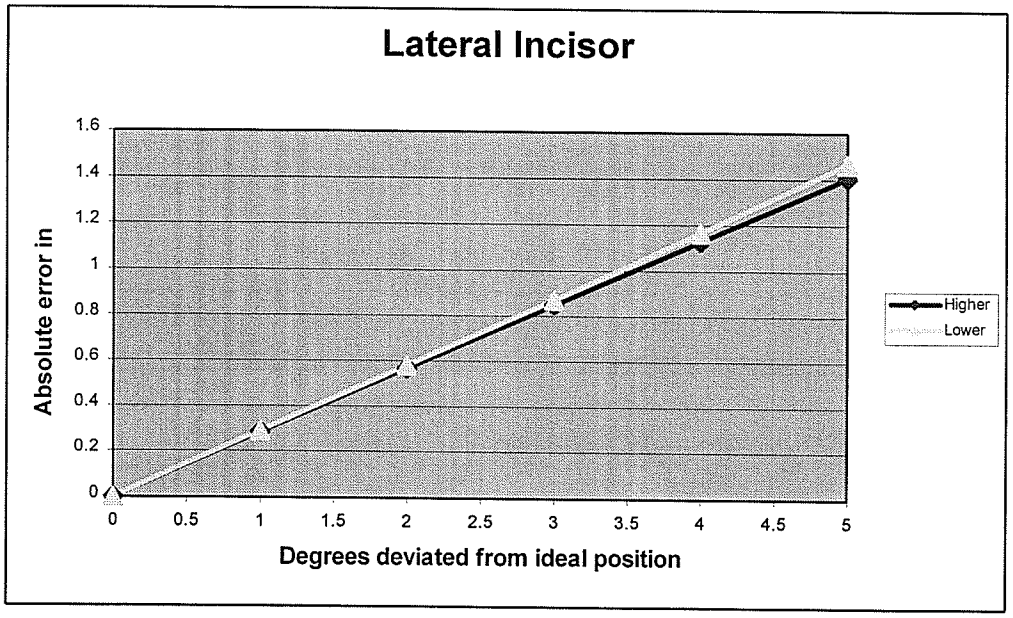

Figure 6.4b Absolute error associated with misplacement of lateral incisor rod in degrees, along semicircular archform.

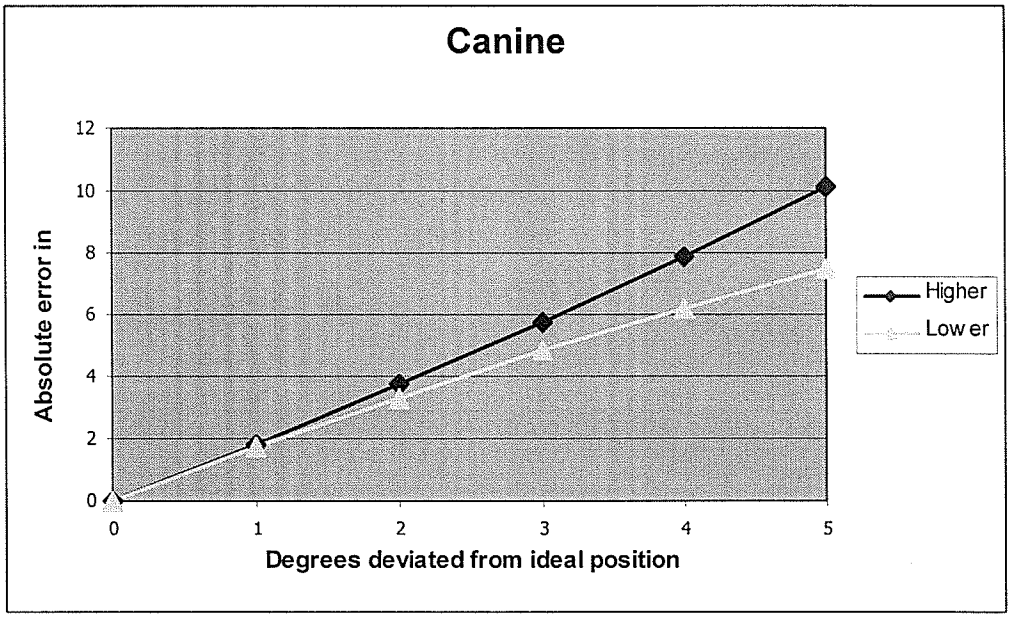

Figure 6.4c Absolute error associated with misplacement of canine rod in degrees, along semicircular archform.

It is worthwhile to note that the rod representing the canine is affected by positional changes the most, followed by the central incisor rod, then the lateral incisor rod. The reason for the canine rod being affected the most could be because it is the rod located closest to $\theta = \mathbf{0}°$, at which point the value of $\mathbf{cos}\theta$ is at its maximum, and the rate of change of $\mathbf{cos}\theta$ is zero. The measurement error associated with any positional change of a rod is amplified by a factor of $\mathbf{cos}\theta$. The value of $\mathbf{cos}\theta$ is at its minimum at $\theta = \mathbf{90}°$, which suggests that positional changes would affect the central incisor rod the least since it located closest to $\theta = \mathbf{90}°$.

Another reason why the measurement error of the lateral incisor rod is the lowest could be because the angular ranges for the central incisor and canine rods each have a fixed

terminus. If the position of the rod representing the central incisor deviates, only the terminus between the central incisor and the lateral incisor somehow adjusts to change the angular range from one side only. If the position of the rod representing the lateral incisor deviates, both termini of its angular range change, and the angular range loses from one terminus while gaining from the other to make the difference minimal. The entire angular range of the lateral incisor rod could shift accordingly.

To say that a change in the position of one rod will affect the entire system is sensible, but questionable. In actual fact, it is impossible to theoretically determine whether or not errors due to positional changes are propagated. A method to test the effects in positional changes would be to construct an apparatus similar to that displayed in **Figure 3.5**, intentionally change the position of one rod, and measure the effects. If the percentage of the retractive force that is taken away from the range of one rod is transferred to that of the adjacent rod, then the effects are limited to the ranges of those two rods, and not propagated to the third rod on that side of the semicircle. It is sensible to say this because the positions of the other two rods are considered ideal and the terminus of the angular ranges of those two rods is the same, then the third rod would not be affected. Whether or not this is the case requires further testing.

The preceding discussion is based on the premise that the system has the ability to automatically adjust around altered positions of rods by changing the positions of termini between angular ranges. Keeping in mind that the positions of the termini are assigned values in the theoretical model, the fact that the measured values agree well with the

theoretical model is truly surprising, since the way in which the rods interact with each other in the system is unknown.

Comparison of the actual positions of the rods to the ideal positions of the rods in the drilling diagram used to construct the apparatus (see **Figure 3.5**) revealed that each rod was placed to within 0.25mm of its ideal position. The estimates of the total errors in the system which could be attributed to positional errors of the rods are presented in **Table 6.1**.

This section of the discussion addresses the errors associated with the initial positions of the rods in relation to each other. It has been observed that the spatial relation of the rods do change during deflection, and thus, the extrapolation of this line of thinking is exceedingly difficult to apply to the situation during deflection since the termini of the angular ranges do effectively change during deflection.

Rod	Range of error
Central Incisor	0.36% - 0.37%
Lateral Incisor	0.142% - 0.144%
Canine	0.86% - 0.91%

Table 6.1 Measurement errors of the system associated with errors in placement of the various rods along the semicircular archform.

6.5.2 ERRORS ASSOCIATED WITH LOADING AND RECOVERY TIMES

Creep of the acrylic rods was unlikely to have occurred during measurements. As demonstrated in **Figure 5.9**, after a load of 96.96 ± 0.3g was applied for 30 minutes and then removed, all rods eventually returned to their zero points. Since during the measurement procedure (see **Section 3.2.2.5**) the light points were observed to return to their zero positions within a three minute interval between consecutive measurements, we can assume that there was no measurable rod creep or viscoelastic deformation remaining when the measurement commenced.

It is therefore unlikely that the effects of creep or viscoelastic deformation of the acrylic rods made any contribution to the error of the measurements.

6.5.3 ERRORS DUE TO FRICTION

The only sliding part of the apparatus was the archwire as it applied force to the acrylic rods. For both the flexible and rigid archwires, a petroleum-based lubricant (WD-40®; WD-40 Products Canada Ltd., Etobicoke, ON) was used to lubricate the points of contact of the archwire(s) and the rods. In the case of the flexible archwire, the dental floss was impregnated with WD-40®. For the rigid archwire, WD-40® was liberally applied (via collimated spray) to the inside of the semicircle cut from the plastic. Acrylic (methylmethacrylate) is said to have good chemical resistance to oils (vegetable, animal and mineral).[80]

Any friction in the system manifested itself in the measurements as a deviation of a point from the average line of deflection for the data set. In **Figure 6.5**, a data set (i.e., one trial of ten trials) of measurements from testing with the flexible archwire is presented. The gray lines represent the average line of displacement for each rod, and were determined by linear regression of all the data points for each rod over all ten trials. Each individual point in **Figure 6.5** represents a deflection of each rod for a particular load. The points on the semicircle (the outermost points) are referred to *point 1* for each rod but are actually the zero points for each rod with no load applied. The innermost points are referred to as *point 5*. *Point 2* for each rod is the deflection with one weight; *point 3* is with two weights, etc. For *rod 11* (the blue series), *point 2* deviates laterally from the average line of deflection. This deviation is due to friction between the floss and the rod for *rod 11*, which has prevented it from moving medially during measurement (one would expect medial collapse of all rods for a flexible archwire such as dental floss). Similar deviations of individual data points from average lines of deflection could be due to the effects of friction.

The friction associated with *point 2* for *rod 11* likely has a negligible effect on the measurement of the retractive force, since this rod is close to $\theta = \mathbf{90°}$ and $\mathbf{cos}\theta$ is minimum at this value, as described in **Section 6.5.1** above, and the deviation away from the average line of deflection is more horizontal than vertical.

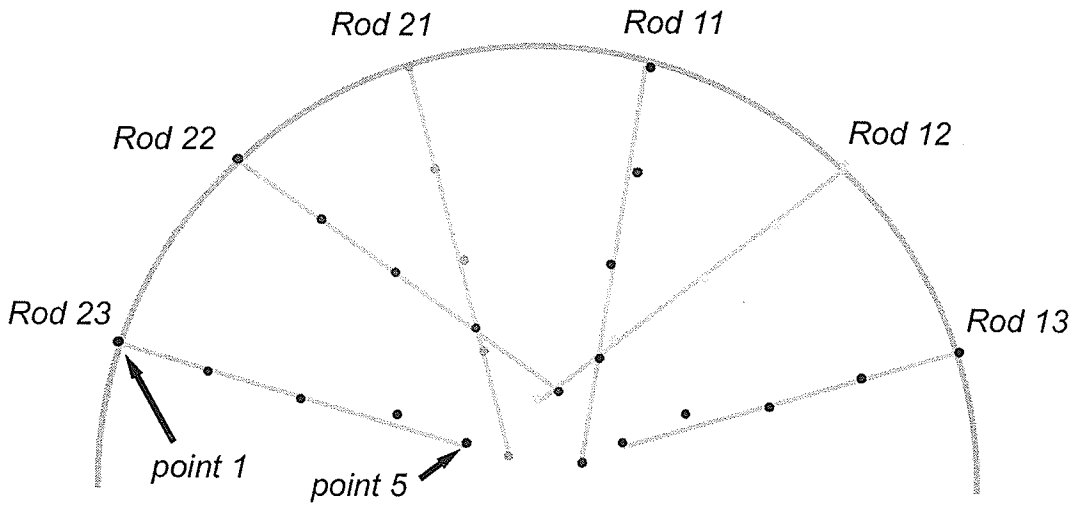

Figure 6.5 Data set for testing with a flexible archwire, showing individual data points. Average lines of deflection are the solid lines.

However, the friction associated with *point 4* of *rod 13* and *point 4* of *rod 23* is likely to have a greater effect on the measurement since the deviation away from the average line of deflection is more vertical than horizontal. These deviations of *point 4* of *rods 13* and *23* represent friction between the floss and the rods which prevented these rods from being deflected vertically as much as they should have been. The friction causes the rods to "hang" vertically, thus minimizing the measurement and inflating the error associated with the data set.

6.5.3.1 INTERPRETING THE RAW DATA

The crux of interpreting **Figure 6.5** is to realize that it depicts deflections of the light points on the measurement screen rather than actual deflections of the acrylic rods. The horizontal distance between the light emitters and the measurement screen amplifies the

amount of any deflection of the rods. **Figure 6.6** helps illustrate this point. At the top of this figure is a diagram of the apparatus with no applied load and the light emitters on. The rods are unbent, and the light points on the measurement screen 2.50m away are at their zero positions. At the bottom of this figure is a diagram of the apparatus with an applied load (via a flexible archwire), showing the paths of the light beams. Note the cross-over of the beams between the emitters and the screen. If you were to look at the light points on the screen at face value, it would appear that the central incisor rods have bent below the level of the lateral incisor rods – an event that is impossible using the flexible archwire. The appearance of the light points on the screen may be misleading, but it is important to realize that they are amplified deflections rather than actual deflections.

A vertical deflection of 1.0cm measured at the screen corresponds to a vertical deflection of approximately 0.338mm of the rod at the tip of the light emitter. A deflection of the rod is approximately 3.38% of the deflection of the measured value at the screen. In other words, the distance between the rod and the screen amplifies the deflection by a factor of approximately 29.5 for measurement at the screen. For *point 4* of *rod 23*, its vertical deviation from the average line of deflection is approximately 1.25mm, which corresponds to a vertical deflection of 0.0424mm or 42.4 m. For*rod 23*, this difference corresponds to an absolute error of approximately 1.9% associated with this data point.

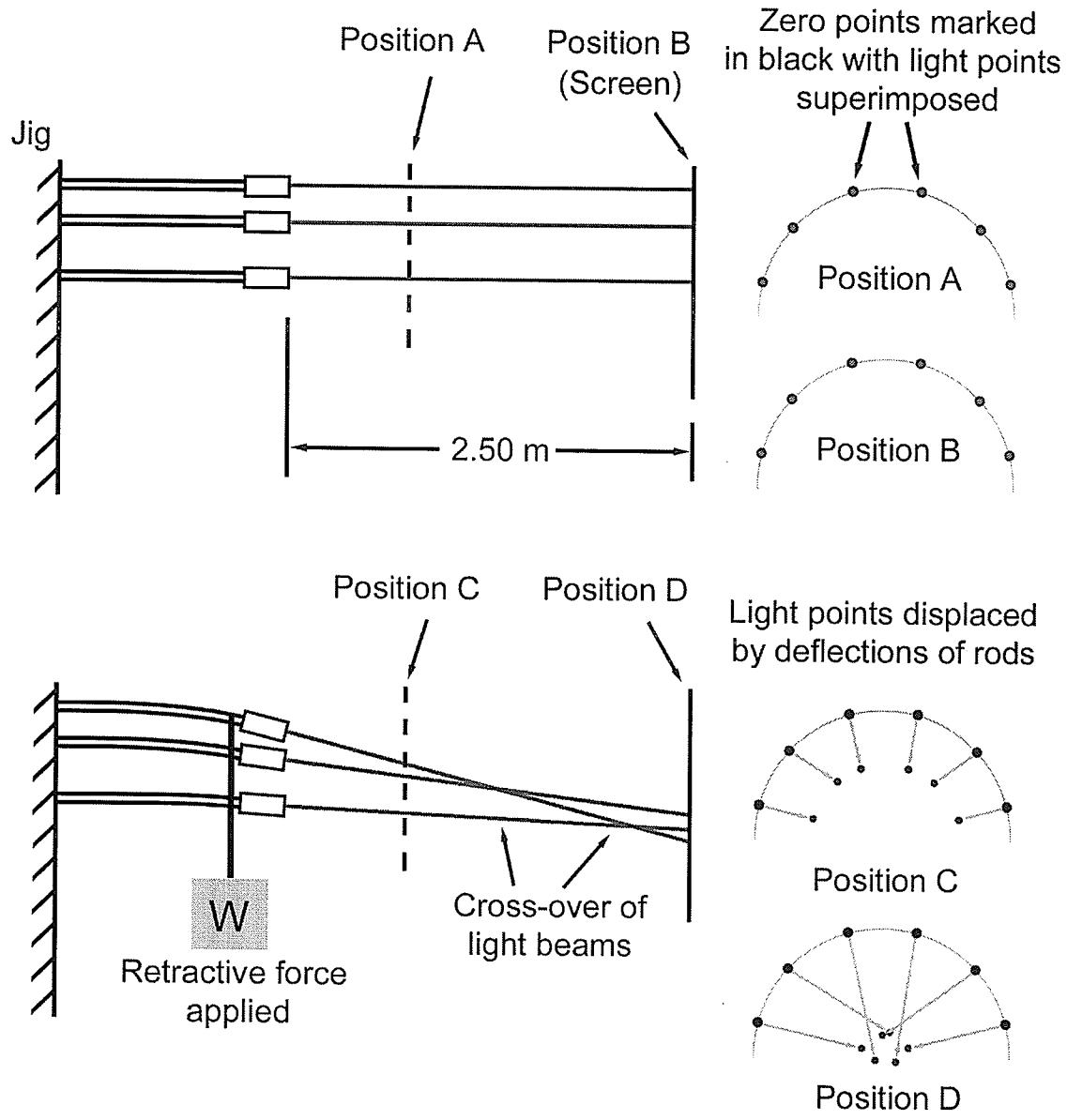

Figure 6.6 Schematic diagram (not to scale) illustrating the crossover effect when the measurement screen is a long distance from the light emitters. The upper part of the diagram shows the apparatus with the rods in an unloaded state. The light points at an arbitrary Position A between the emitters and Position B (the measurement screen) are the same and duplicate the rod positions in the arch. The bottom part of the diagram shows a sufficient load W placed on the rods to cause significant deflections. Because the distribution of the vertical load is not uniform, the light points observed at Position C describe a convex arc whereas at Position D the light points of the central incisor rod have been displaced more than those of the other two rod pairs and fall below the convex arc containing the other light points.

Since it is expected (based on the theoretical model) that the magnitudes of the retractive components are different for the various rods, it is thus expected that the rods will deflect different amounts which is ultimately reflected in the amount of displacement of the light points on the measurement screen. With this in mind, and remembering that any displacement of the light points on the screen is 1/29.5 of the amount of deflection of the rod at the tip of the light emitter, it is erroneous to assume that the light point displacements (as illustrated by *point 5* for each rod in **Figure 6.5**) should stay in a perfectly circular pattern. At some distance between the light emitters and the measurement screen, the light beams may cross each other for a particular load.

Whether or not the magnitude of the friction of the system is significant is questionable. What is clear is that friction has a greater effect on the measurements of the canine rod than it does with the lateral incisor rod or the central incisor rod, due to increased vertical components of deviation from average lines of deflection as they go from a more vertical orientation (as for the central incisor rod) to a more horizontal orientation (as for the canine rod).

6.5.4 ERRORS ASSOCIATED WITH OSCILLATIONS IN THE SYSTEM

There is an effect tied into the effects of friction in the system, namely, the effects of oscillations in the system. An attempt was made to apply the archwire with weights as consistently as possible during measurements, there were occasions when the dangling weights oscillated similar to the way a pendulum does. Since there is friction in the system, the amount of friction could have been lessened to a small degree as the

weight(s) were at their greatest lateral point in their swing(s). The decreased friction may have been enough to allow the rod's friction-restrained-resistance-to-deflection (i.e., the rods want to deflect but are restrained by the friction [resistance]) to express itself a small degree, thus allowing the rod to "creep laterally" a small amount. Also, when the archwire and weights were applied and the rods steadied themselves, it was observed that if one rod was tapped, the deflections of the remaining rods decreased and the configuration of the light points changed. It was also observed that any effects that such oscillations and tapping had were manifested to the greatest extent in the deflections of the canine rods. This observation was true for testing with flexible and rigid archwires.

6.5.5 ERRORS IN AMOUNT OF CONTACT WITH THE ARCHWIRE

For testing with the rigid archwire, simultaneous contact of all rods with the plastic of the rigid archwire was essential. If one rod did not contact the plastic, there would be a lag between application of force and deflection of that rod. The total deflection of that rod would be significantly less than its corresponding contralateral rod, as would the proportion of retractive force to that rod.

The semicircular arch form that was cut out of the plastic of the rigid archwire was done such that simultaneous contact of the plastic with all rods was attained. This was verified by suspending the archwire over the rods and placing it such that it just contacted the central incisor rods. Then the archwire was gently tapped and deflections of the light points on the measurement screen were observed. Of one point did not deflect, the archwire corresponding with that rod was sectioned and its position was adjusted directly

horizontally and vertically until contact was verified as described above, and finally was fused to the remainder of the archwire with Weld-On™ acrylic solvent.

What could not be elucidated was the degree of contact between the rods and the acrylic of the rigid archwire. Whether or not one rod had a stronger contact with the archwire than the other rods could not be determined. Intuitively, since the rigid archwire is designed to hang and use gravity to produce the retractive force, and since the lateral incisor rod, and more so, the canine rods are situated in the arch to contact the archwire at increasingly vertical tangents, it is sensible to assume that the central incisor rods would have the greatest degree of contact of any of the rods. It is difficult to ascertain whether or not differing degrees of contact contributes more or less to errors in measurement.

6.6 CORRELATION WITH *IN VIVO* SITUATIONS

The most obvious difference between *in vivo* and *in vitro* situations is that the *in vivo* situation is a biomechanical system. Within such a system, there are myriad variables and the effects of all the variables cannot be modeled in *in vitro* experimentation.

Several variables which exist clinically were eliminated in this investigation. Differing root sizes and shapes were eliminated in order to allow each rod to behave similarly so different responses to the same load could be identified. No brackets were used to engage the archwires to the rods, thus eliminating the effects of tying in to the brackets, as well as bracket friction and bracket torque. None of the moments that normally exist at a bracket could be expressed. The absence of brackets also permitted the retractive

effect of the archwire alone to be exerted on the teeth, by allowing the archwire to make point contact with the rods. Furthermore, the retractive effects would have been exaggerated if the rods were engaged to the archwires, which would have defeated the purpose of this investigation.

It can be argued that the loads applied to the rods may not be similar to what is commonly used clinically. To counter any such argument, *any* load less than that required to plastically deform the rods or debond the styrene tabs could be used in this investigation to determine the proportion of the retractive force delivered to any rod in the system.

Most importantly, a variable that exists in *in vivo* situations which was omitted experimentally was the presence of interproximal contacts. There were no contacts between adjacent rods similar to interproximal contacts which (may) exist between the anterior teeth during *en masse* retraction. The distribution of retractive force may actually even out among anterior teeth through interproximal contacts. A way of adapting the experimental apparatus and method to simulate interproximal contacts would be to physically attach the rods to the archwires. However, as mentioned above, doing this would have defeated a purpose of this investigation, since the proportions of retractive forces to the rods would have been exaggerated.

Results of this investigation show that the proportion of retractive force delivered to the rods is greatest at the central incisor rods (55.0%) and smallest at the canine rods

(13.7%). If this is true clinically, it would imply that *en masse* retraction is not accomplished by a posteriorly directed pull on the canines and lateral incisors, but rather by a posteriorly directed push which is transmitted from the central incisors through the lateral incisors and canines via interproximal contacts. Assuming that the retractive force on central incisors remains disproportionately high, then a modification of the archwire might be advisable to attain a more even distribution of retractive force in clinical situations. The fact remains that clinical accomplishment of space closure during *en masse* retraction of anterior teeth occurs successfully every day. However, interpretation of these results may lead one to believe that with an uneven distribution of retractive force among anterior teeth, lack of modification of mechanics leaves these teeth, particularly the canines, as excellent anchorage teeth for posterior protraction.

The concept of optimal force implies that a force exists for a particular tooth that will effect orthodontic movement of that tooth through bone most efficiently. This concept rests on the assumption that the (optimal) force depends on the amount of root surface of a tooth for efficient movement. The optimal force for a relatively larger rooted tooth like a canine will likely be higher than the optimal force for a tooth like a lateral incisor to achieve the same rate of orthodontic movement. Does this mean that an even distribution of retractive force among anterior teeth during *en masse* retraction is at all desirable? Of the six anterior teeth, the canines have the largest roots, followed by the central incisors, and finally the lateral incisors. At the very least, it would appear obvious that if optimal forces were desired in *en masse* retraction, the greatest proportion of retractive force should be directed to the canines and the smallest proportion be directed to the lateral

incisors. It is stressed that in the absence of archwire engagement and interproximal contacts, such a distribution of force was not noted in this investigation.

6.7 ELLIPTICAL ARCHWRIES

An argument can be made that the majority of anterior archforms correspond to elliptical rather than perfectly circular forms. In the frame of reference of **Figure 4.12**, an anterior archform arch may be termed more-or-less "tapered" if it corresponds to an ellipse with its major axis lying in the vertical plane, whereas an anterior archform may be more-or-less termed "square" if it corresponds to an ellipse with its major axis lying in the horizontal plane.

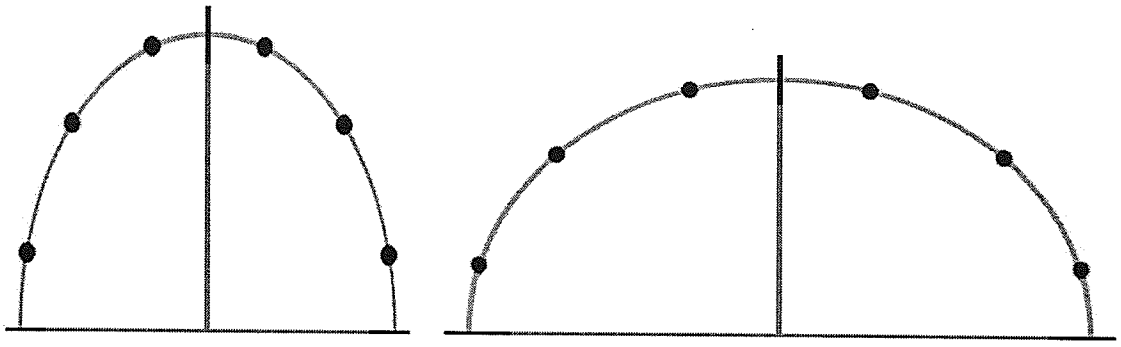

Figure 6.7 Elliptical anterior archforms which could be used for testing in an investigation similar to this one. A "tapered" archform may be elliptical with its major axis in the vertical plane, as in the diagram on the left. A "square" archform may be elliptical with its major axis in the horizontal plane, as in the diagram on the right.

Even if they were valid, the theoretical models developed in this investigation cannot be applied directly to analyze elliptical archforms for the sole reason that they rely on a constant radius which only exists on a circle. In ellipses, the "radius" changes as a

function of θ, and has a maximum value when parallel with the major axis and a minimum value when parallel with the minor axis.

However, educated guesses can be made. For example, for a circular infinitely flexible archwire, the retractive component will be maximum at θ = **90°** (that is, when the retractive force is directed vertically), and will be minimum at θ = **0°** (when the retractive force is directed horizontally). Please refer to **Figure 4.9** which demonstrates this and shows that the change in the retractive component obeys a *sine* function, or stated in other words, the change follows a *sinusoidal* curve as θ changes, with a constant radius. For a change of retractive component which obeys a *sine* function, the rate of change of that component will obey a *negative cosine* function.

In the case of ellipses, again, the retractive component will be maximum at θ = **90°** (retractive force is directed vertically), and will be minimum at θ = **0°** (retractive force is directed horizontally). The crux of analyzing force distribution for a flexible elliptical archwire is to realize the change in "radius" with the angle θ. Since the radius is not constant and changes as function of θ, the rate of change of the retractive component will not follow a sinusoidal curve, but will follow a *sigmoidal* curve. The differences in sinusoidal and sigmoidal curves are presented in **Figure 6.8**.

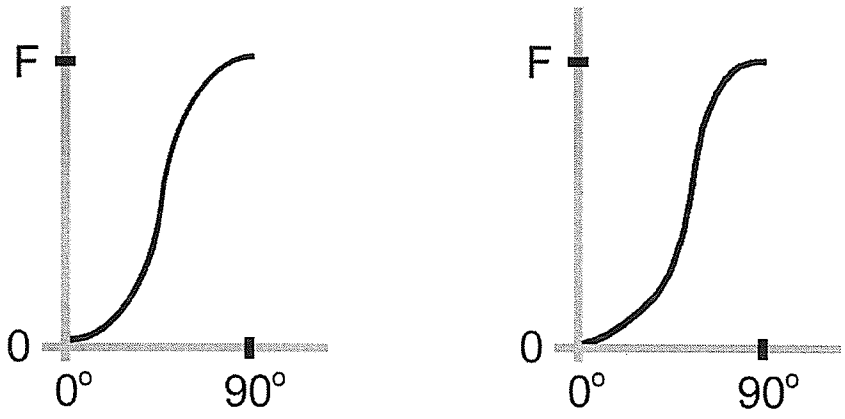

Figure 6.8 Sinusoidal (left) and sigmoidal (right) rates of change in the retractive component of an applied retractive force with an infinitely flexible archwire of circular (left) and elliptical (right) shape.

If the elliptical archform is changed from having its major axis in the vertical plane to the horizontal plane, then the expected difference in the sigmoidal change of retractive component is presented in **Figure 6.9**.

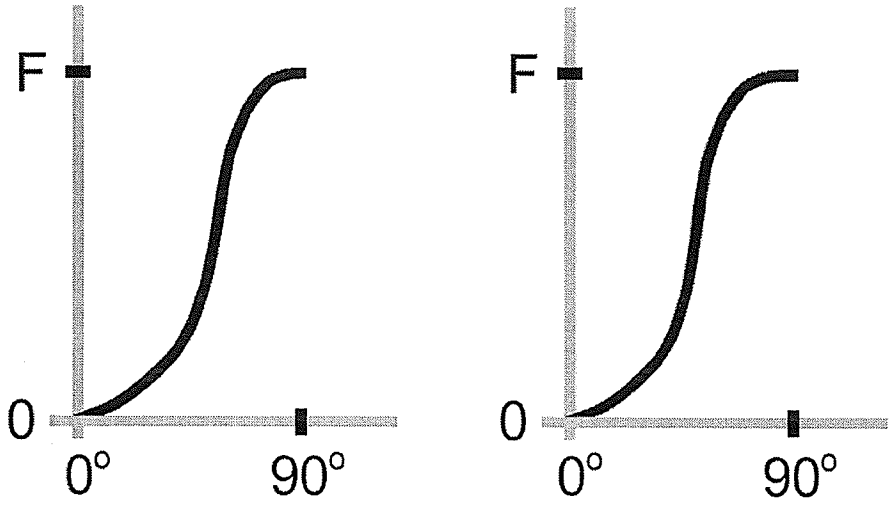

Figure 6.9 Sigmoidal changes in retractive component of an infinitely flexible archwire of elliptical shape with its major axis vertical (left) and horizontal (right).

For the diagram on the right in **Figure 6.9**, the initial slope (that is, the part closest to the origin) is less steep, whereas there is more of a plateau of the final part at $\theta = \mathbf{0°}$. The reason for the plateau (which is *not* horizontal) is because the "radius" changes less for every $\mathbf{d\theta}$ in region of θ approaches **90°**, and there is less of a curvature of the surface of the ellipse here than in any other region of the ellipse. This in turn implies that this region of the surface is "flattest" and the change in the retractive component at every adjacent $\mathbf{d\theta}$ would be minimum.

The area of greatest change of radius per $\mathbf{d\theta}$ is in the region of θ approximating the minor axis, or θ approaches **0°** for a horizontal ellipse. This means that one expects a rapid change in the retractive component for every $\mathbf{d\theta}$ near $\theta = \mathbf{0°}$, which explains the relatively drastic slope near the origin in the diagram on the right of **Figure 6.9**.

Thus, it is expected that the distribution of retractive force will produce a higher proportion to the central incisors when the flexible elliptical archform is horizontal than when it is vertical.

6.8 SUMMARY

The experimental results appeared to agree well with the predictions of the theoretical models for distribution of retractive force. Upon evaluation of the experimental results, it is apparent that the models were invalid or incomplete in their present form since they did not accommodate any explanation for medial movement of the rods, the changes in spatial orientation of the rods and geometry of the flexible archwire during deflection, and the effects of friction in the system. The theoretical model for the infinitely rigid

archwire did not predict the significant medial components of force that the rigid archwire produced on the rods. The theoretical model for the infinitely flexible archwire, however, does appear to give a good indication of the general direction and magnitude of the forces developed by a flexible archwire, although it is incomplete in its present form. It is expected that revised theoretical models will include predictions for amounts of retractive force that agree with the present theoretical models, since these amounts were verified by experimentation. Further experimentation in these regards is clearly indicated.

It appears that testing with the rigid archwire was more prone to experimental error than was testing with the flexible archwire. Errors such as degree of contact of the rods with the rigid archwire, oscillations and friction appeared to play a greater role in rigid testing than in flexible archwire testing.

While the experimental results seemed to generate more questions than answers, the null hypothesis that there is an even distribution of retractive force during *en masse* retraction has been disproved. The distribution of retractive force is shown by both the theoretical and experimental models to be markedly uneven. The retractive force applied by the archwire alone on the canine rods (representing the anterior tooth with typically the largest root surface area) is less than one third that applied to the lateral incisor rod (representing the anterior tooth with typically the smallest root surface area). This result seems to have implications for anchorage control as well as the need for improved appliance design to effect efficient *en masse* anterior retraction.

CHAPTER 7

CONCLUSIONS AND RECOMMENDATIONS

7.1 CONCLUSIONS

The conclusions that can be drawn from this *in vitro* investigation are the following:

1. For an anterior semicircular section of archwire with a constant radius, when a posteriorly directed retractive force is applied to the archwire, the posteriorly directed component of the retractive force has a distribution of approximately 55.0% to the central incisors, approximately 31.2% to the lateral incisors, and approximately 13.7% to the canines. This is true only when the archwire makes point contacts with bodies representing anterior teeth in such a way that there is negligible friction between the archwire and the bodies, and the archwire is not tied to the bodies in any way.
2. In a clinical application, friction effects may alter the force distribution and direction greatly.
3. The distribution of retractive force is the same for any archwire, since the distribution was found to be statistically similar for a very flexible and a very rigid archwire, under the conditions mentioned in #1 above.
4. The magnitudes of the medially directed components of the retractive force vary, with the greatest magnitudes associated with very flexible archwires, and the smallest magnitudes associated with very rigid archwires.
5. Deflection of acrylic rods is an acceptable way to measure retractive components *in vitro* since they were shown to produce consistent and reproducible results, and, depending on the lengths of the rods, can be tested within a range well below their elastic limit.

6. Creep and viscoelastic deformation of the acrylic rods did not have a detectible effect on measurements during this investigation.
7. The current clinical belief of anterior force equalization among the six anterior teeth during *en masse* retraction may not be valid.

7.2 RECOMMENDATIONS

For future experimentation, the following recommendations are suggested:

1. Develop theoretical model for a flexible archwire to accommodate the dynamics during rod deflection, the associated friction, the resistance of the rods to deflection and non-equidistant placement of the rods.
2. Use apparatus similar to that used in this investigation, with interproximal contacts modeled by round discs placed on each rod. The discs would represent teeth, and make point contacts with each other. Contacts should be passive; the laser point should not change from the positions when the discs are not on the rods. There would be an amount of weight of each disc that would have to be accounted for. This situation would represent the six anterior teeth, with no interproximal spaces, being retracted *en masse* by a round wire with frictionless brackets.
3. If light emitters are to be used for displaying deflection of acrylic rods, the emitters should be attached to the rods in such a way that they can be removed and replaced to allow a consistent location of the light point on the screen corresponding to a particular rod. In this investigation, if an emitter had to be

replaced, the clip that was used to hold the emitter to the end of the rod needed modifications which were time-consuming and frustrating.

4. Additional testing should be done with apparatus similar to that used in this investigation using square, tapering and elliptical archforms.
5. Additional testing should be done with anatomically correct tooth models in a typodont-style (wax "alveolus") apparatus using flexible and rigid archwires. Using such models incorporates variables such as interproximal contacts, root form and length, and may give a better indication of what happens clinically. It is unlikely that light deflection could be employed in this situation. Displacement of incisal edges would be a better measurement, but calibration of force *versus* displacement would be difficult and may be inconsistent since displacement will vary with wax temperature, alveolar wax height, presence of adjacent teeth, etc.

CHAPTER 8

ACKNOWLEDGEMENTS

I would like to thank a number of people for their contributions towards this thesis:

The Alpha Omega Foundation for their gracious donation which funded this investigation.

Dr. Jay T. Winburn III for his initial ideas for this investigation and insight into interpreting the results.

Dr. Billy Wiltshire for his guidance through the difficult times, and also for his encouragement, interest, and . . . . refereeing.

Dr. Peter Williams for his critical thinking and help in making sense of the inexplicable, which was always delivered with a smile.

My classmates, Dr. Pascal Carrière and Dr. Warren Cohen, without whose help and friendship I could not have survived graduate school.

Most of all, to my wife, Melissa. It seemed that she had to take a back seat to this work, but she was beside me at every moment. And now she gets her husband back!

REFERENCES

1. Lee BW. Relationship between tooth-movement rate and estimated pressure applied. J Dent Res 1965; 44: 1053.

2. Quinn RS, Yoshikawa DK. A reassessment of force magnitude in orthodontics. Am J Orthod 1985; 88: 252 – 260.

3. Burstone CJ, Baldwin JJ, Lawless DT. The application of continuous forces to orthodontics. Angle Orthod 1961; 31: 1 – 14.

4. Hocevar RA. Understanding, planning and managing tooth movement: Orthodontic force system theory. Am J Orthod 1981; 80: 457 – 477.

5. Storey E. The nature of tooth movement. Am J Orthod 1973; 63(3): 292 – 313.

6. Sandstedt C. Einige beiträge zur theorie der zahnreglierung. Nordisk Tandläka Tidsskrift 1904; 4, as cited in Schwarz AM. Tissue changes incidental to orthodontic tooth movement. Int J Orthodontia 1932; 28(4): 331 – 352.

7. Schwarz AM. Tissue changes incidental to orthodontic tooth movement. Int J Orthodontia 1932; 28(4): 331 – 352.

8. Storey E, Smith R. Force in orthodontics and its relation to tooth movement. Aust J Dent 1952; 56: 11 – 18.

9. Smith R, Storey E. The importance of force in orthodontics. The design of cuspid retraction springs. Aust J Dent 1952; 56: 291 – 304.

10. Oppenheim A. A possibility for physiologic orthodontic movement. Theoretical part. Am J Orthodontics and Oral Surg 1944; 30: 277 – 328.

11. Oppenheim A. A possibility for physiologic orthodontic movement. Practical part. Am J Orthodontics and Oral Surg 1944; 30: 345 – 368.

12. Hixon EH, Atikian H, Callow GE, McDonald HW, Tacy RJ. Optimal force, differential force and anchorage. Am J Orthod 1969; 55: 437 – 457.

13. Stoner MM. Force control in clinical practice. Am J Orthod 1960; 46: 163 – 186.

14. Nickolai RJ. On optimum orthodontic force theory as applied to canine retraction. Am J Orthod 1975; 68: 290 – 302.

15. Haack DC, Weinstein S. Geometry and mechanics as related to tooth movement studied by means of two-dimensional model. J Am Dent Assoc 1963; 66: 157 – 164.

16. Begg PR. Differential force in orthodontic treatment. Am J Orthodontics 1956; 42: 481 – 510.

17. Hixon EH, Aasen TO, Arango J, Clark RA, Klosterman R, Miller SS, Odom WM. On force and tooth movement. Am J Orthod 1970; 57: 476 – 489.

18. Weinstein S. Minimal forces in tooth movement. Am J Orthod 1967; 53: 881 – 903.

19. Lee BW. The force requirements for tooth movement part I: Tipping and bodily movement. Aust Orthod J 1995; 13: 238 – 248.

20. Burstone CJ, Pryputniewicz RJ. Holographic determination of centres of rotation produced by orthodontic forces. Am J Orthod 1980; 77: 396 – 409.

21. Pilon JJGM, Kuijpers-Jagtman AM, Maltha JC. Magnitude of orthodontic forces and rate of bodily tooth movement. An experimental study. Am J Orthod Dentofac Orthop 1996: 110: 16 – 23.

22. Burstone JC. Biomechanics of Tooth movement. In Kraus BS, Ridel RA, eds. Vistas in Orthodontics. Philadelphia: lea & Feibiger, 1962.

23. Neuger RL. The measurement and analysis of moments applied by a light-wire torquing auxiliary and how these moments change magnitude with respect to various changes in configuration and application. Am J Orthod 1967; 53: 492 – 513.

24. Reitan K. Some factors determining the evaluation of forces in orthodontics. Am J Orthod 1957; 43: 32 – 45.

25. Boester CH, Johnston LE. A clinical investigation of the concepts of differential and optimal force in canine retraction. Angle Orthod 1974; 44: 113 – 119.

26. Ouchi K, Watanabe K, Koga M, Isshiki Y, Kawada E, Oda Y. The effects of retraction forces applied to the anterior segment of orthodontic arch wires: Differences in wire deflection with wire size. Bull Tokto Dent Coll 1998; 39: 183 – 188.

27. Andreasen GF, Zwanziger D. A clinical evaluation of the differential force concept as applied to the edgewise bracket. Am J Orthod 1980; 78: 25 – 40.

28. Yamaguchi K, Nanda RS, Morimoto N, Oda Y. A study of force application, amount of retarding force, and bracket width in sliding mechanics. Am J Orthod Dentofac Orthop 1996; 109: 50 – 56.

29. Mitchell DL, Boone RM, Ferguson JH. Correlation of tooth movement with variable forces in the cat. Angle Orthod 1973; 43: 154 – 161.

30. Rajcich MM, Sadowsky C. Efficacy of intraarch mechanics using differential moments for achieving anchorage control in extraction cases. Am J Orthod Dentofac Orthop 1997; 112: 441 – 448.

31. Halderson H, Johns EE, Moyers R. The selection of forces for tooth movement. A summary of our present knowledge. Am J Orthod 1953; 39: 25 – 35.

32. Salzman JA. Principles of Orthodontics. 2nd ed. Philadelphia: JB Lippincott Company; 1950.

33. Steiner CC. Force control in orthodontia. Angle Orthod 1932; 2: 252 – 259.

34. Clifford PM, Orr JF, Burden DJ. The effects of increasing the reverse curve of Spee in a lower archwire examined using a dynamic photo-elastic gelatine model. Eur J Orthod 1999; 21: 213 – 222.

35. Caputo AA, Chaconas SJ, Hayashi RK. Photoelastic visualization of orthodontic forces during canine retraction. Am J Orthod 1974; 65: 250 – 259.

36. Chaconas SJ, Caputo AA, Hayashi RK. Effects of wire size, loop configuration and gabling on canine-retraction springs. Am J Orthod 1974; 65: 58 – 66.

37. Tanne K, Sakude M, Burstone CJ. Three-dimensional finite element analysis for stress in the periodontal tissue by orthodontic forces. Am J Orthod Dentofac Orthop 1987; 92: 499 – 505.

38. White TR, Caputo AA, Chaconas SJ. The measurement of utility archwire forces. Angle Orthod 1979; 49: 272 – 281.

39. Murphy NC, de Alba JA, Chaconas SJ, Caputo AA. Experimental force analysis of the contraction utility arch wire. Am J Orthod 1982; 82: 411 – 417.

40. Koenig HA, Burstone CJ. Analysis of generalized curved beams for orthodontic applications. J Biomechanics 1974; 7: 429 – 435.

41. Burstone CJ. Rationale of the segmented arch. Am J Orthod 1962; 48: 805 – 822.

42. Eden JD, Waters NE. An investigation into the characteristics of the PG canine retraction spring. Am J Orthod Dentofac Orthop 1994; 105: 49 – 60.

43. Timoshenko S. Strength of Materials. 3rd ed. New Jersey: Van Nostrand, 1955.

44. Yang TY, Baldwin JJ. Analysis of space closing springs in orthodontics. J Biomechanics 1974; 7: 21 – 28.

45. Halliday R, Resnick R. Fundamentals of Physics. 3rd ed. New York: John Wiley & Sons, 1988. Ch. 7, p 132.

46. Haskell BS, Spencer WA, Day M. Auxiliary springs in continuous arch treatment: Part I. An analytical study employing the finite-element method. Am J Orthod Dentofac Orthop 1990; 98: 387 – 397.

47. Raboud DW, Faulkner MG, Lipsett AW, Haberstock DL. Three-dimensional effects in retraction appliance desicn. Am J Orthod Dentofac Orthop 1997; 11: 378 – 392.

48. Haack DC. The science of mechanics and its importance to analysis and research in the field of orthodontics. Am J Orthod 1963; 49: 330 – 344.

49. Kalra V. Simultaneous intrusion and retraction of the anterior teeth. J Clin Orthod 1998; 32: 535 – 540.

50. Golledge P. Useful clinical technique for upper canine retraction and retention. Br J Orthod 1973; 1: 31 – 32.

51. Gjessing P. Biomechanical design and clinical evaluation of a new canine-retraction spring. Am J Orthod 1985; 87; 353 – 362.

52. Gjessing P. Controlled retraction of maxillary incisors. Am J Orthod Dentofac Orthop 1992; 101 : 120 – 131.

53. Daskalogiannakis J. McLachlan KR. Canine retraction with rare earth magnets: An investigation into the validity of the constant force hypothesis. Am J Orthod Dentofac Orthop 1996; 109: 489 – 495.

54. Samuels RHA, Rudge SJ, Mair LH. A clinical study of space closure with nickel-titanium closed coil springs and an elastic module. Am J Orthod Dentofac Orthop 1998; 114: 73 – 79.

55. Samuels RHA, Rudge SJ, Mair LH. A comparison of the rate of space closure using a nickel-titanium spring and an elastic module: A clinical study. Am J Orthod Dentofac Orthop 1993; 103: 464 – 467.

56. Sonis AL, Van der Plas E, Gianelly A. A comparison of elastomeric auxiliaries versus elastic thread on premolar extraction site closure: An *in vivo* study. Am J Orthod 1986; 89: 73 – 78.

57. Perez CA, de Alba JA, Caputo AA, Chaconas SJ. Canine retraction with J hook headgear. Am J Orthod 1980; 78: 538 – 547.

58. Carr WK. Simultaneous en masse retraction of maxillary anteriors with lingual root torque. J Clin Orthod 1971; 5: 200 – 212.

59. Güray E, Orhan M. "En Masse" retraction of maxillary anterior teeth with anterior headgear. Am J Orthod Dentofac Orthop 1997; 112: 473 – 479.

60. Fastlicht J. Efficient canine retraction with the universal appliance. Am J Orthod 1973; 64: 270 – 277.

61. Siatkowski RE. Continuous arch wire closing loop design, optimization, and verification. Part I. Am J Orthod Dentofac Orthop 1987; 112: 393 – 402.

62. Siatkowski RE. Continuous arch wire closing loop design, optimization, and verification. Part II. Am J Orthod Dentofac Orthop 1987; 112: 487 – 495.

63. Burstone CJ, Koenig HA. Optimizing anterior and canine retraction. Am J Orthod 1976; 70: 1 – 19.

64. Marcotte MR. Prediction of orthodontic tooth movement. Am J Orthod 1976; 69: 511 – 523.

65. Vanderby Jr. R, Burstone CJ, Solonghe DJ, Ratches JA. Experimentally determined force systems from vertically activated orthodontic loops. Angle Orthod 1977; 47: 272 – 279.

66. Kusy RP, Tulloch JFC. Analysis of moment/force ratios in the mechanics of tooth movement. Am J Orthod Dentofac Orthop 1986; 90: 127 – 131.

67. Sved A. The application of engineering methods to orthodontics. Am J Orthod 1952; 38: 399 – 421.

68. Smith RJ, Burstone CJ. Mechanics of tooth movement. Am J Orthod 1984; 85: 294 – 307.

69. Hatasaka HH. A radiographic study of roots in extraction sites. Angle Orthod 1976; 46: 64 – 68.

70. Farrant SD. An evaluation of different methods of canine retraction. Br J Orthod 1976; 4: 5 – 15.

71. Staggers JA, Germane N. Clinical considerations in the use of retraction mechanics. J Clin Orthod 1991; 25: 364 – 369.

72. Modern Plastics Encyclopedia 1982 - 1983. Vol. 59, No. 10A. McGraw-Hill, Inc. pp. 18 – 22.

73. Harper CA. ed. Handbook of Plastics, Elastomers, and Composites. 3rd ed. New York: McGraw-Hill, 1996. Ch. 1, p. 1.44.

74. Deanin RD, Driscoll SB. Cost per unit property of plastics. Mod Plast 1973. p. 1.16.

75. Frados J. Plastics Engineering Handbook of the Society of the Plastics Intustry, Inc. 4th ed. New York: Van Nostrand Reinhold Company, 1976. Ch. 3, p.58.

76. Materials Safety Data Sheet information for methylene chloride.

77. Materials Safety Data Sheet information for trichloroethylene.

78. Materials Safety Data Sheet information for methyl methacrylate.

79. Materials Safety Data Sheet information for Weld-On™.

80. CRC Handbook of Chemistry and Physics. 56th ed. Weast RC, ed. Cleveland: CRC Press, 1976. p. C-788.

81. Dorland's Illustrated Medical Dictionary. 28th ed. Philadelphia: W. B. Saunders Company, 1994.

82. Stewart J. Single Variable Calculus. Early Trancendentals. 2nd ed. Pacific Grove: Brooks/Cole Publishing Company, 1991. Review and Preview, p. 43.

83. Adams RA. Single-Variable Calculus. Revised Edition. Don Mills: Addison-Wesley Publishers Limited, 1986. Ch. 3, pp. 110 – 121.

84. Halliday D, Resnick R. Fundamentals of Physics. 3rd ed. New York: John Wiley & Sons, 1988. Ch. 3.

85. Wiltshire WA. Pre-clinical graduate orthodontic technique course workbook. University of Manitoba, 1999.

86. Moyers RE. Handbook of orthodontics. 4th ed. Chicago: Year Book medical Publishers, Inc., 1988. Ch. 11, p. 230.

87. Siatkowski RE. Optimal orthodontic space closure in adults. Dent Clin N Amer 1996: 40; 837 – 873.

88. Brinson HF. The visco-elastic behavior of a ductile polymer. In Deformation & Fracture of High Polymers. Kausch HH, Hassel J-A and Jaffee RL, eds. Battelle Institute Materials Science Colloquia, New York: Plenum Press, September 1972.

APPENDIX 1 CALIBRATION DATA

Rod 11

Deflection of light point to nearest 1/4mm.

Load (g)	Trial 1	Trial 2	Trial 3	Trial 4	Trial 5
0	0.00	0.00	0.00	0.00	0.00
16.16	24.00	23.00	24.25	24.25	24.75
32.32	48.00	47.75	47.50	47.00	47.50
48.48	70.50	69.50	70.00	70.25	71.00
64.64	93.00	93.75	93.00	93.50	94.75
80.8	117.50	117.75	116.50	116.50	120.00
96.96	141.00	141.25	142.00	142.00	144.00
113.12	164.50	165.00	165.00	165.50	167.75

Load (g)	Trial 6	Trial 7	Trial 8	Trial 9	Trial 10
0	0.00	0.00	0.00	0.00	0.00
16.16	24.00	24.00	24.75	24.75	23.00
32.32	47.00	47.50	47.00	48.75	46.00
48.48	70.25	70.75	70.25	71.00	70.25
64.64	93.50	94.50	94.25	94.50	94.00
80.8	117.25	118.25	118.00	119.00	118.25
96.96	141.00	142.75	142.25	143.00	143.00
113.12	165.00	167.00	167.00	168.25	166.50

Load (g)	Mean	SD	Minimum	Maximum
0	0.00	0.00	0.00	0.00
16.16	24.08	0.646034915	23.00	24.75
32.32	47.40	0.728392446	46.00	48.75
48.48	70.38	0.460223376	69.50	71.00
64.64	93.88	0.626387349	93.00	94.75
80.8	117.90	1.0749677	116.50	120.00
96.96	142.23	0.982132035	141.00	144.00
113.12	166.15	1.318669363	164.50	168.25

Slope	y-Intercept
1.465110797	-0.116666667

Rod 12

Deflection of light point to nearest 1/4mm.

Load (g)	Trial 1	Trial 2	Trial 3	Trial 4	Trial 5
0.00	0.00	0.00	0.00	0.00	0.00
16.16	23.75	23.00	23.75	23.25	24.50
32.32	47.25	46.50	46.75	46.50	47.75
48.48	69.75	70.50	70.00	70.00	70.00
64.64	93.75	94.25	93.50	93.25	95.75
80.80	117.25	119.00	117.25	117.50	119.75
96.96	141.00	143.25	142.00	142.50	143.00
113.12	164.25	166.25	166.75	166.00	168.00

Load (g)	Trial 6	Trial 7	Trial 8	Trial 9	Trial 10
0.00	0.00	0.00	0.00	0.00	0.00
16.16	23.25	23.50	24.50	24.75	23.25
32.32	47.25	47.50	47.00	48.00	47.00
48.48	71.25	70.50	70.75	71.50	71.00
64.64	93.25	93.75	94.25	94.50	94.50
80.80	118.25	118.00	119.25	119.25	118.25
96.96	142.50	142.75	143.50	143.75	142.25
113.12	166.50	167.00	167.00	168.25	166.50

Load (g)	Mean	SD	Minimum	Maximum
0.00	0.00	0.00	0.00	0.00
16.16	23.75	0.623609564	23.00	24.75
32.32	47.15	0.502770104	46.50	48.00
48.48	70.53	0.594535299	69.75	71.50
64.64	94.08	0.755075419	93.25	95.75
80.80	118.38	0.899459714	117.25	119.75
96.96	142.65	0.801040989	141.00	143.75
113.12	166.65	1.106797181	164.25	168.25

Slope	y-Intercept
1.472090847	-0.364583333

Rod 13

Deflection of light point to nearest 1/4mm.

Load (g)	Trial 1	Trial 2	Trial 3	Trial 4	Trial 5
0	0.00	0.00	0.00	0.00	0.00
16.16	24.00	23.25	23.75	23.50	24.25
32.32	47.00	45.00	46.25	46.25	46.00
48.48	70.00	69.50	68.75	69.00	69.00
64.64	92.50	91.50	91.75	92.00	92.00
80.8	115.75	115.00	114.25	114.50	115.75
96.96	139.25	140.50	138.25	140.00	138.75
113.12	163.75	162.25	162.00	163.50	162.00

Load (g)	Trial 6	Trial 7	Trial 8	Trial 9	Trial 10
0	0.00	0.00	0.00	0.00	0.00
16.16	24.00	23.50	23.25	24.25	23.00
32.32	46.00	46.25	45.50	47.00	45.50
48.48	68.75	69.25	69.00	69.00	68.25
64.64	92.25	92.00	92.75	92.50	91.00
80.8	114.25	116.00	114.75	115.00	114.25
96.96	137.75	139.25	138.25	138.25	139.50
113.12	162.00	161.50	162.00	164.00	163.00

Load (g)	Mean	SD	Minimum	Maximum
0	0.00	0.00	0.00	0.00
16.16	23.68	0.441745276	23.00	24.25
32.32	46.08	0.635194633	45.00	47.00
48.48	69.05	0.468448977	68.25	70.00
64.64	92.03	0.519748871	91.00	92.75
80.8	114.95	0.674948558	114.25	116.00
96.96	138.98	0.877575574	137.75	140.50
113.12	162.60	0.883490552	161.50	164.00

Slope	y-Intercept
1.432328501	-0.09375

Rod 21

Deflection of light point to nearest 1/4mm.

Load (g)	Trial 1	Trial 2	Trial 3	Trial 4	Trial 5
0	0.00	0.00	0.00	0.00	0.00
16.16	24.00	23.50	24.25	24.00	25.00
32.32	48.00	47.00	47.50	47.00	48.50
48.48	72.00	71.00	71.00	70.75	72.00
64.64	95.00	95.00	94.75	94.75	96.00
80.8	119.50	119.75	119.25	118.25	121.00
96.96	144.00	143.50	143.75	144.00	145.00
113.12	168.25	168.25	168.00	167.00	170.00

Load (g)	Trial 6	Trial 7	Trial 8	Trial 9	Trial 10
0	0.00	0.00	0.00	0.00	0.00
16.16	24.00	24.25	25.25	25.25	24.00
32.32	48.00	48.25	47.00	49.00	48.00
48.48	71.50	72.00	71.75	72.50	72.00
64.64	95.00	97.00	96.00	96.75	96.00
80.8	119.75	121.00	120.00	122.00	121.00
96.96	143.00	145.00	144.00	146.25	141.25
113.12	168.25	169.00	168.25	171.00	170.50

Load (g)	Mean	SD	Minimum	Maximum
0	0.00	0.00	0.00	0.00
16.16	24.35	0.603232036	23.50	25.25
32.32	47.83	0.687689368	47.00	49.00
48.48	71.65	0.567646212	70.75	72.50
64.64	95.63	0.835414069	94.75	97.00
80.8	120.15	1.094176504	118.25	122.00
96.96	143.98	1.330465666	141.25	146.25
113.12	168.85	1.259409032	167.00	171.00

Slope	y-Intercept
1.488850336	-0.15625

Rod 22

Deflection of light point to nearest 1/4mm.

Load (g)	Trial 1	Trial 2	Trial 3	Trial 4	Trial 5
0	0.00	0.00	0.00	0.00	0.00
16.16	24.50	23.50	24.00	24.00	25.00
32.32	48.00	47.25	48.25	47.75	48.00
48.48	72.00	71.25	72.00	71.25	72.00
64.64	95.50	95.00	95.50	95.25	96.75
80.8	119.25	119.00	119.00	118.75	120.25
96.96	143.50	143.50	142.75	144.25	144.00
113.12	167.25	167.00	168.00	168.25	169.00

Load (g)	Trial 6	Trial 7	Trial 8	Trial 9	Trial 10
0	0.00	0.00	0.00	0.00	0.00
16.16	24.25	24.50	24.75	25.50	24.25
32.32	48.00	48.75	47.75	49.50	48.50
48.48	71.25	72.50	72.00	72.50	72.25
64.64	95.75	96.50	96.00	97.25	96.50
80.8	118.25	120.25	120.25	121.50	121.00
96.96	144.00	144.50	144.25	146.00	145.75
113.12	167.00	170.00	168.50	171.00	169.50

Load (g)	Mean	SD	Minimum	Maximum
0	0.00	0.00	0.00	0.00
16.16	24.425	0.565808173	23.50	25.50
32.32	48.175	0.62416611	47.25	49.50
48.48	71.9	0.48876261	71.25	72.50
64.64	96	0.726483157	95.00	97.25
80.8	119.75	1.054092553	118.25	121.50
96.96	144.25	0.993031274	142.75	146.00
113.12	168.55	1.33749351	167.00	171.00

Slope	y-Intercept
1.48647454	0.05625

Rod 23

Deflection of light point to nearest 1/4mm.

Load (g)	Trial 1	Trial 2	Trial 3	Trial 4	Trial 5
0	0.00	0.00	0.00	0.00	0.00
16.16	24.00	23.00	23.50	23.25	24.50
32.32	47.50	45.75	47.75	46.50	47.75
48.48	71.25	69.50	70.50	70.00	71.00
64.64	94.75	91.75	93.00	93.25	94.00
80.8	118.50	116.25	117.25	115.50	118.75
96.96	142.00	140.00	140.00	140.50	141.00
113.12	164.50	164.50	164.50	163.50	165.00

Load (g)	Trial 6	Trial 7	Trial 8	Trial 9	Trial 10
0	0.00	0.00	0.00	0.00	0.00
16.16	23.50	24.00	23.50	24.50	23.25
32.32	46.25	47.25	47.00	47.25	46.50
48.48	69.75	70.00	69.50	71.00	69.00
64.64	91.75	93.00	90.75	94.00	93.25
80.8	115.50	116.50	116.25	117.00	117.00
96.96	138.25	140.00	138.75	141.00	140.50
113.12	162.75	164.25	163.50	164.00	164.50

Load (g)	Mean	SD	Minimum	Maximum
0	0.00	0.00	0.00	0.00
16.16	23.70	0.524404424	23.00	24.50
32.32	46.95	0.674948558	45.75	47.75
48.48	70.15	0.756453715	69.00	71.25
64.64	92.95	1.217921727	90.75	94.75
80.8	116.85	1.106797181	115.50	118.75
96.96	140.20	1.09163486	138.25	142.00
113.12	164.10	0.668746755	162.75	165.00

Slope	y-Intercept
1.446620108	0.041666667

APPENDIX 2 EXPERIMENTATION DATA

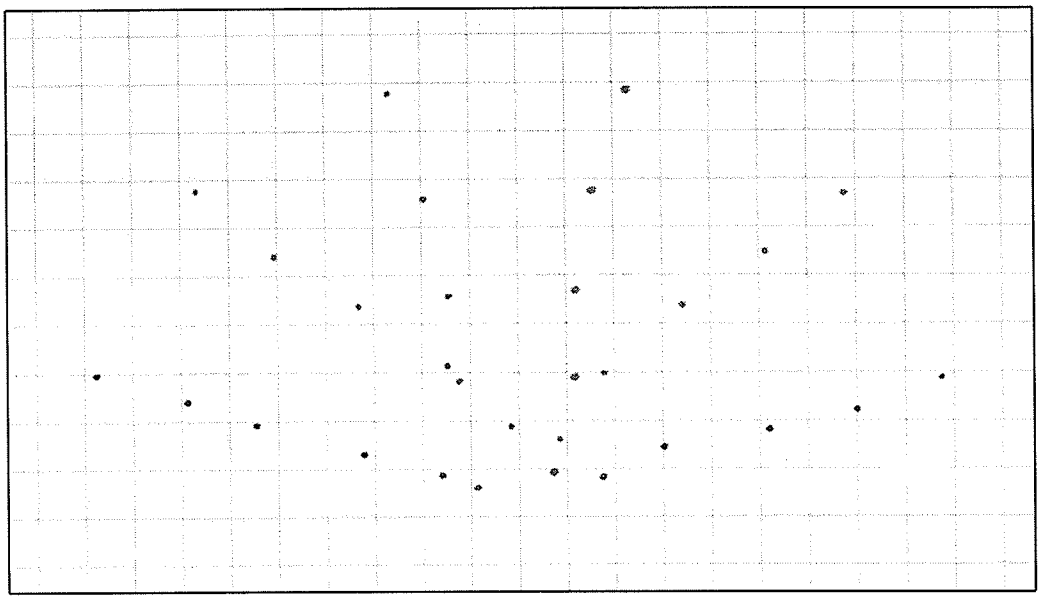

Flexible – Trial 1

		Displacement (mm)	
Rod	Load (g)	Vertical	Horizontal
11	16.16	13.20	4.50
	32.32	26.56	6.64
	48.48	37.66	6.58
	64.64	50.30	9.72
12	16.16	7.43	10.52
	32.32	14.41	21.20
	48.48	23.09	31.58
	64.64	31.87	37.59
13	16.16	3.96	11.16
	32.32	6.48	22.61
	48.48	9.07	36.67
	64.64	12.85	44.68

		Displacement (mm)	
Rod	Load (g)	Vertical	Horizontal
21	16.16	13.95	4.70
	32.32	26.79	7.86
	48.48	37.87	9.08
	64.64	52.17	11.45
22	16.16	8.59	9.96
	32.32	15.13	20.62
	48.48	23.04	32.50
	64.64	31.13	40.52
23	16.16	3.64	11.98
	32.32	6.75	20.93
	48.48	10.57	35.02
	64.64	13.33	45.37

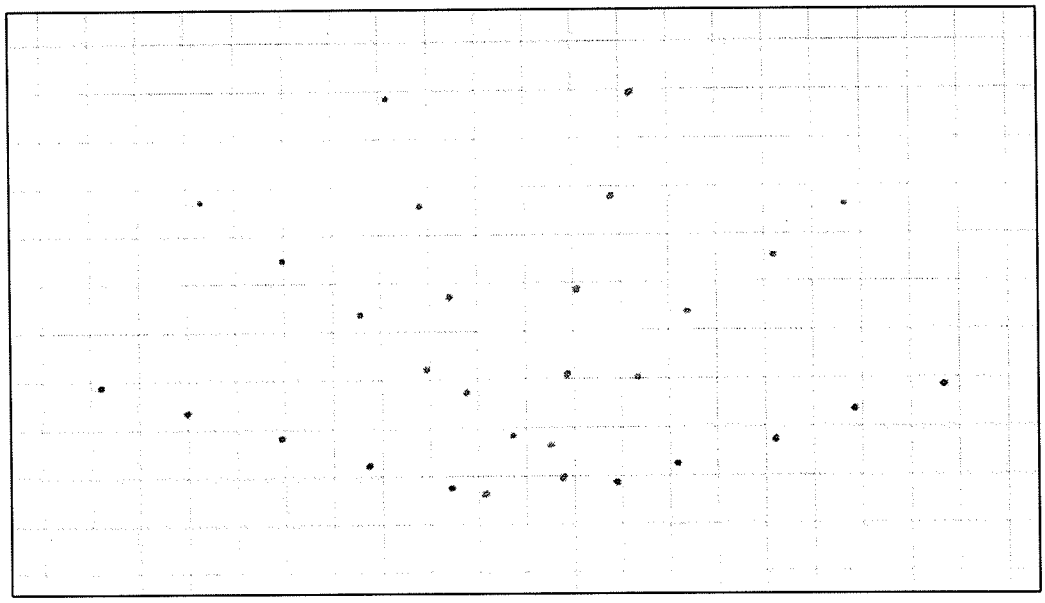

Flexible – Trial 2

		Displacement (mm)	
Rod	Load (g)	Vertical	Horizontal
11	16.16	13.62	2.63
	32.32	25.95	7.40
	48.48	37.23	8.60
	64.64	50.63	9.61
12	16.16	6.81	9.75
	32.32	13.89	21.33
	48.48	22.60	28.02
	64.64	31.28	39.15
13	16.16	3.01	11.86
	32.32	6.83	22.01
	48.48	10.15	35.26
	64.64	12.69	43.24

		Displacement (mm)	
Rod	Load (g)	Vertical	Horizontal
21	16.16	13.33	4.14
	32.32	25.65	7.38
	48.48	38.04	9.51
	64.64	51.38	12.16
22	16.16	7.57	10.78
	32.32	14.84	21.15
	48.48	22.30	21.15
	64.64	30.57	40.91
23	16.16	3.53	11.47
	32.32	7.12	23.68
	48.48	10.69	35.15
	64.64	13.66	45.80

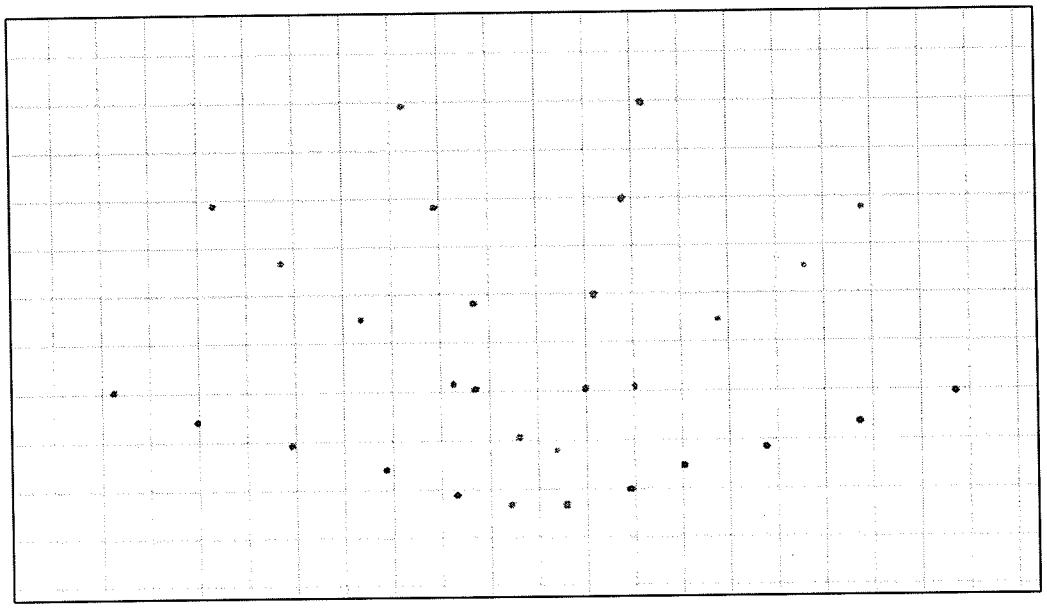

Flexible – Trial 3

		Displacement (mm)	
Rod	Load (g)	Vertical	Horizontal
11	16.16	13.39	2.17
	32.32	26.27	6.47
	48.48	38.47	7.66
	64.64	53.35	10.72
12	16.16	7.84	7.54
	32.32	14.64	18.88
	48.48	23.56	30.06
	64.64	31.77	40.42
13	16.16	3.55	12.83
	32.32	6.80	25.50
	48.48	9.14	35.81
	64.64	12.41	43.61

		Displacement (mm)	
Rod	Load (g)	Vertical	Horizontal
21	16.16	12.88	3.96
	32.32	25.41	8.79
	48.48	36.71	9.16
	64.64	51.52	13.49
22	16.16	7.48	8.76
	32.32	14.98	19.25
	48.48	23.52	19.25
	64.64	30.54	39.65
23	16.16	3.81	10.80
	32.32	6.91	22.87
	48.48	10.06	35.49
	64.64	13.46	44.81

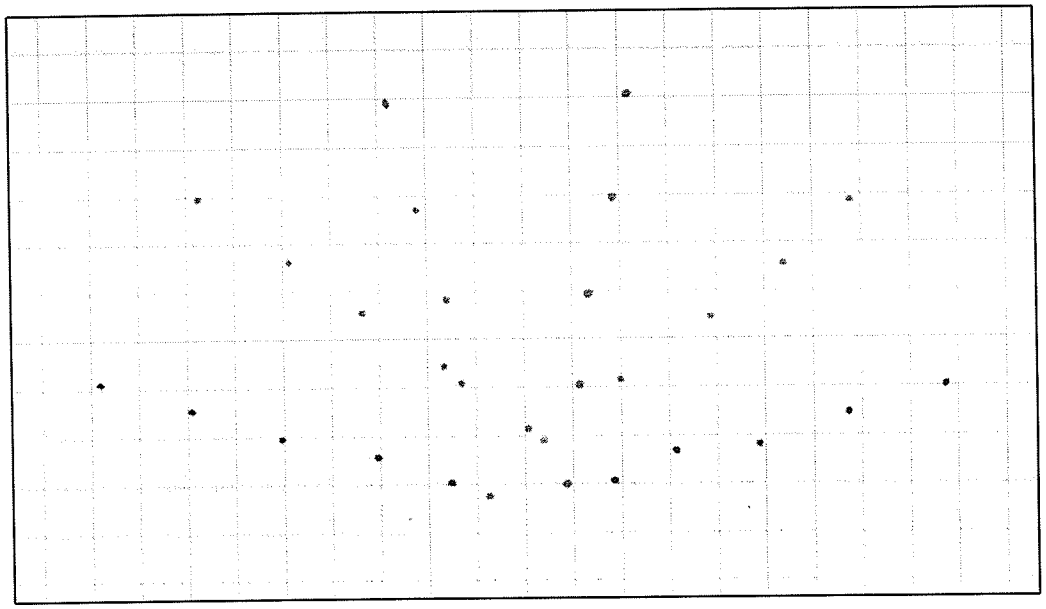

Flexible – Trial 4

		Displacement (mm)	
Rod	Load (g)	Vertical	Horizontal
11	16.16	14.02	2.15
	32.32	26.54	5.36
	48.48	38.43	7.01
	64.64	51.64	8.33
12	16.16	7.62	8.63
	32.32	14.60	18.34
	48.48	22.83	30.38
	64.64	30.77	40.16
13	16.16	3.23	12.77
	32.32	6.96	24.95
	48.48	8.14	35.77
	64.64	12.01	44.03

		Displacement (mm)	
Rod	Load (g)	Vertical	Horizontal
21	16.16	13.31	3.78
	32.32	25.39	7.43
	48.48	36.45	9.01
	64.64	51.16	13.06
22	16.16	8.19	11.46
	32.32	14.87	20.90
	48.48	22.19	20.90
	64.64	30.35	42.72
23	16.16	3.86	12.05
	32.32	7.22	23.91
	48.48	9.32	36.79
	64.64	13.10	46.13

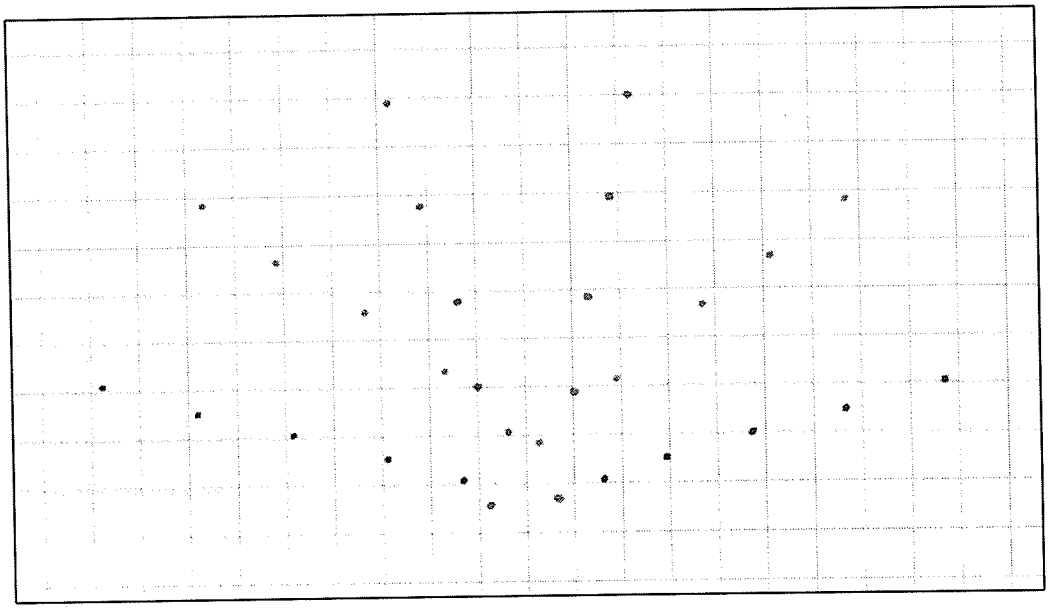

Flexible – Trial 5

		Displacement (mm)	
Rod	Load (g)	Vertical	Horizontal
11	16.16	13.33	2.61
	32.32	26.48	5.65
	48.48	39.11	7.93
	64.64	52.60	10.15
12	16.16	7.46	10.33
	32.32	13.90	19.21
	48.48	23.20	30.67
	64.64	31.57	40.92
13	16.16	3.31	13.01
	32.32	6.50	25.28
	48.48	9.22	36.80
	64.64	12.13	44.95

		Displacement (mm)	
Rod	Load (g)	Vertical	Horizontal
21	16.16	13.41	4.05
	32.32	26.03	8.46
	48.48	37.37	11.01
	64.64	52.72	12.65
22	16.16	7.61	9.39
	32.32	14.29	20.81
	48.48	22.04	20.81
	64.64	30.21	39.53
23	16.16	3.79	12.34
	32.32	6.54	24.90
	48.48	9.93	37.30
	64.64	12.84	47.39

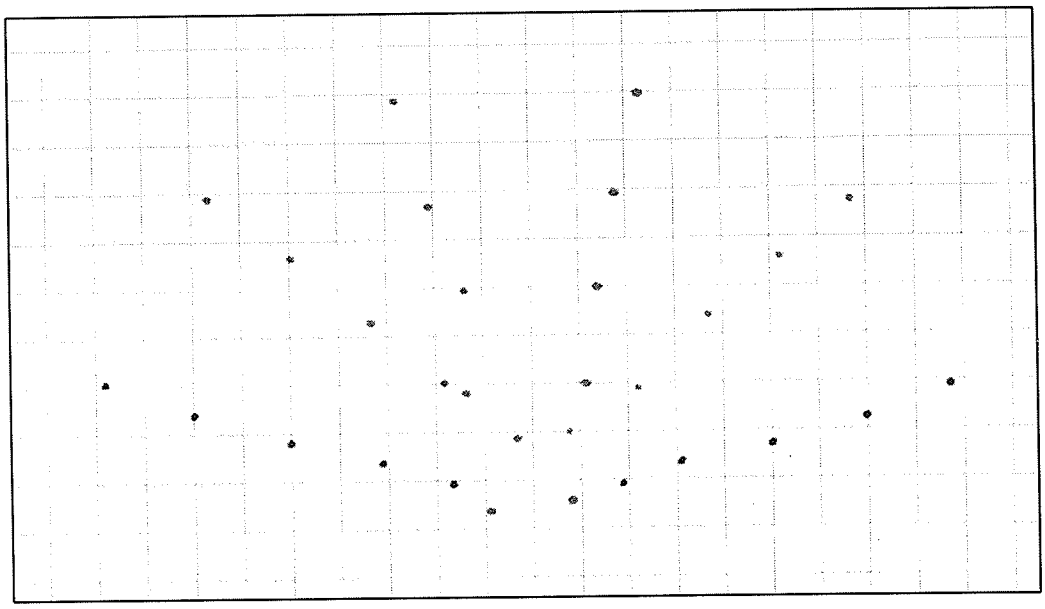

Flexible – Trial 6

		Displacement (mm)	
Rod	Load (g)	Vertical	Horizontal
11	16.16	13.22	3.40
	32.32	25.72	5.85
	48.48	37.96	7.32
	64.64	53.71	9.20
12	16.16	6.92	9.62
	32.32	14.69	19.38
	48.48	24.16	28.24
	64.64	29.80	37.60
13	16.16	4.15	11.09
	32.32	7.52	23.38
	48.48	9.75	35.70
	64.64	12.53	43.71

		Displacement (mm)	
Rod	Load (g)	Vertical	Horizontal
21	16.16	13.77	4.21
	32.32	24.30	8.30
	48.48	37.98	8.66
	64.64	54.12	11.64
22	16.16	7.38	10.55
	32.32	15.92	20.88
	48.48	24.04	20.88
	64.64	31.21	40.02
23	16.16	4.26	11.61
	32.32	7.92	23.76
	48.48	10.52	36.05
	64.64	13.51	45.40

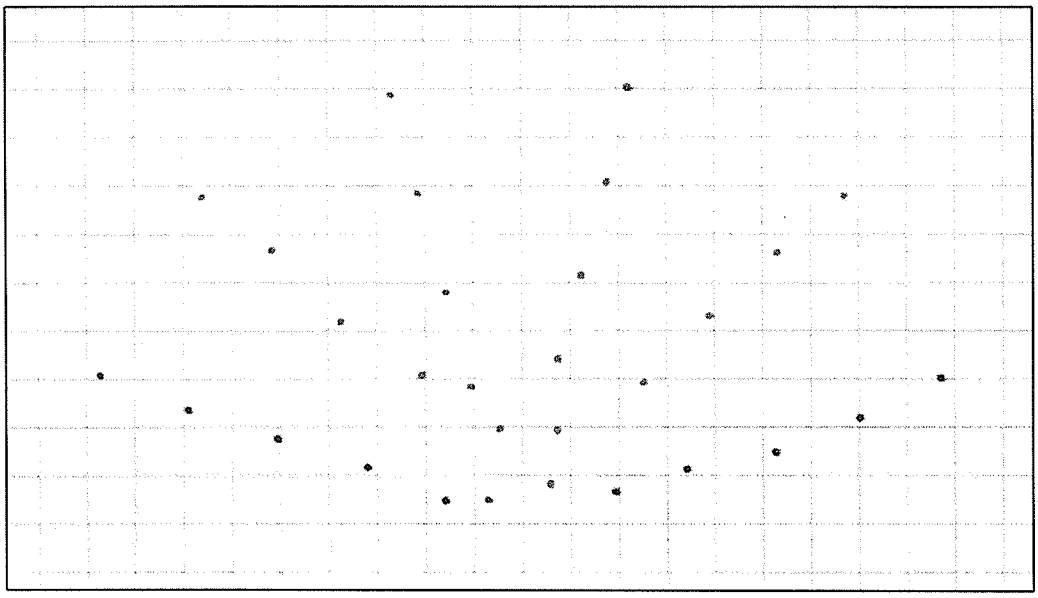

Flexible – Trial 7

		Displacement (mm)	
Rod	Load (g)	Vertical	Horizontal
11	16.16	12.38	2.91
	32.32	24.83	6.03
	48.48	35.90	9.26
	64.64	52.04	10.42
12	16.16	7.25	9.00
	32.32	15.62	17.98
	48.48	24.36	26.66
	64.64	30.82	37.61
13	16.16	4.99	10.46
	32.32	9.27	21.79
	48.48	12.02	33.68
	64.64	14.81	43.18

		Displacement (mm)	
Rod	Load (g)	Vertical	Horizontal
21	16.16	12.42	3.75
	32.32	25.09	6.76
	48.48	37.67	10.03
	64.64	52.39	12.25
22	16.16	7.17	9.31
	32.32	16.50	18.16
	48.48	23.27	18.16
	64.64	30.45	38.54
23	16.16	4.68	11.35
	32.32	8.28	22.87
	48.48	11.88	34.63
	64.64	16.16	45.05

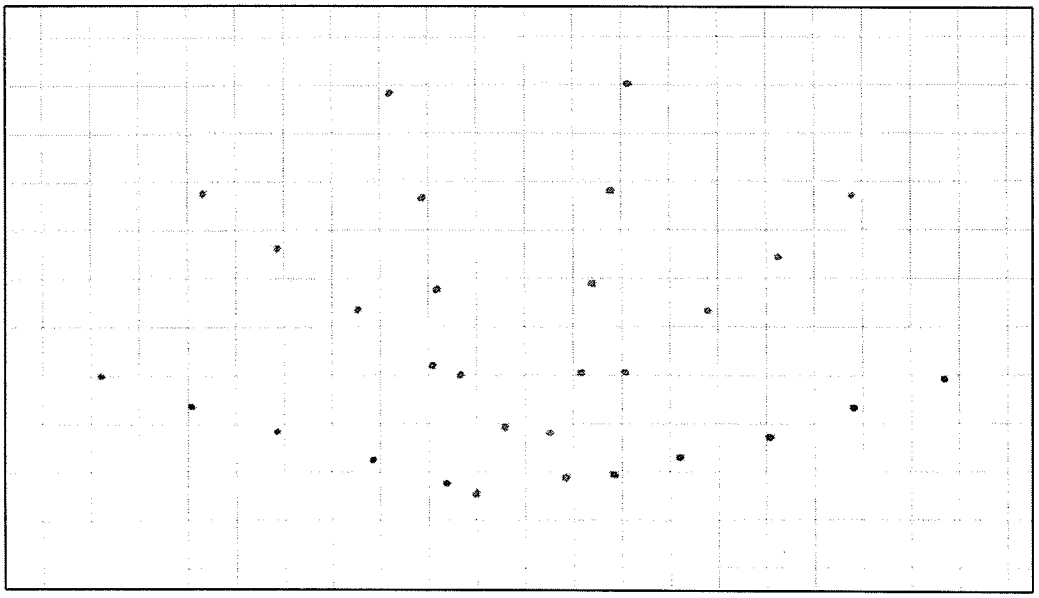

Flexible – Trial 8

		Displacement (mm)	
Rod	Load (g)	Vertical	Horizontal
11	16.16	14.26	2.68
	32.32	26.58	4.64
	48.48	38.10	6.43
	64.64	51.95	8.27
12	16.16	7.85	6.43
	32.32	14.93	18.93
	48.48	22.66	29.47
	64.64	30.69	39.42
13	16.16	3.57	12.04
	32.32	6.96	23.16
	48.48	9.92	35.04
	64.64	12.12	43.43

		Displacement (mm)	
Rod	Load (g)	Vertical	Horizontal
21	16.16	13.28	4.06
	32.32	25.08	5.64
	48.48	36.20	8.90
	64.64	51.61	11.03
22	16.16	7.32	9.90
	32.32	15.04	20.54
	48.48	22.42	20.54
	64.64	30.37	39.80
23	16.16	3.80	11.75
	32.32	6.96	23.03
	48.48	10.53	35.58
	64.64	13.67	45.27

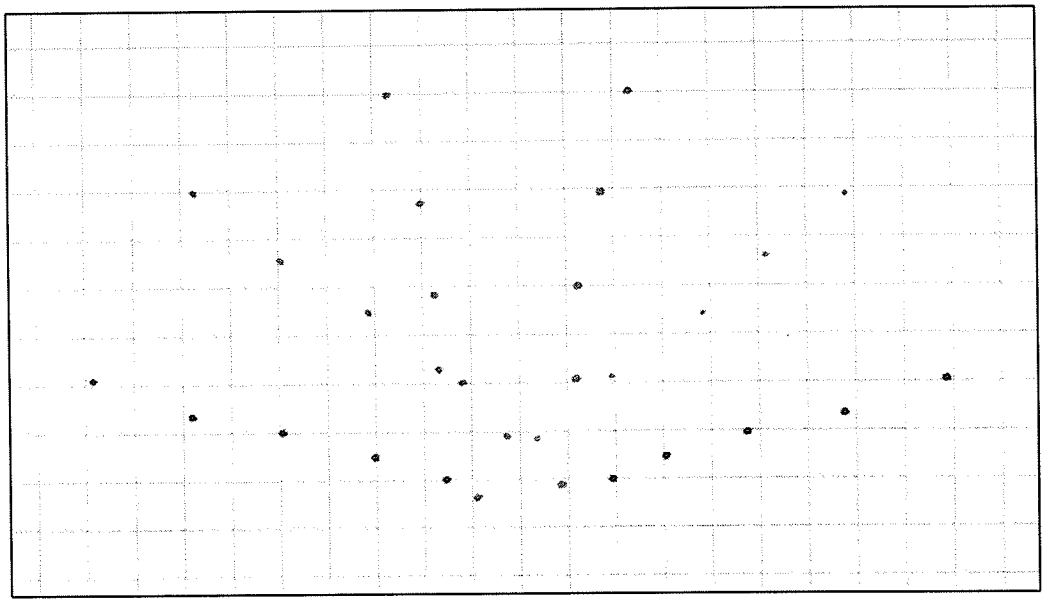

Flexible – Trial 9

		Displacement (mm)	
Rod	Load (g)	Vertical	Horizontal
11	16.16	13.74	4.04
	32.32	26.34	7.18
	48.48	38.38	7.58
	64.64	52.25	9.64
12	16.16	8.06	10.72
	32.32	15.53	19.13
	48.48	23.40	41.67
	64.64	31.89	41.67
13	16.16	4.14	13.25
	32.32	6.65	26.37
	48.48	9.71	36.58
	64.64	12.88	44.31

		Displacement (mm)	
Rod	Load (g)	Vertical	Horizontal
21	16.16	14.30	4.20
	32.32	26.27	5.82
	48.48	37.75	9.44
	64.64	52.83	11.10
22	16.16	9.25	11.44
	32.32	15.88	22.57
	48.48	23.55	22.57
	64.64	31.94	41.03
23	16.16	4.72	12.53
	32.32	6.73	24.26
	48.48	10.47	36.49
	64.64	13.33	45.87

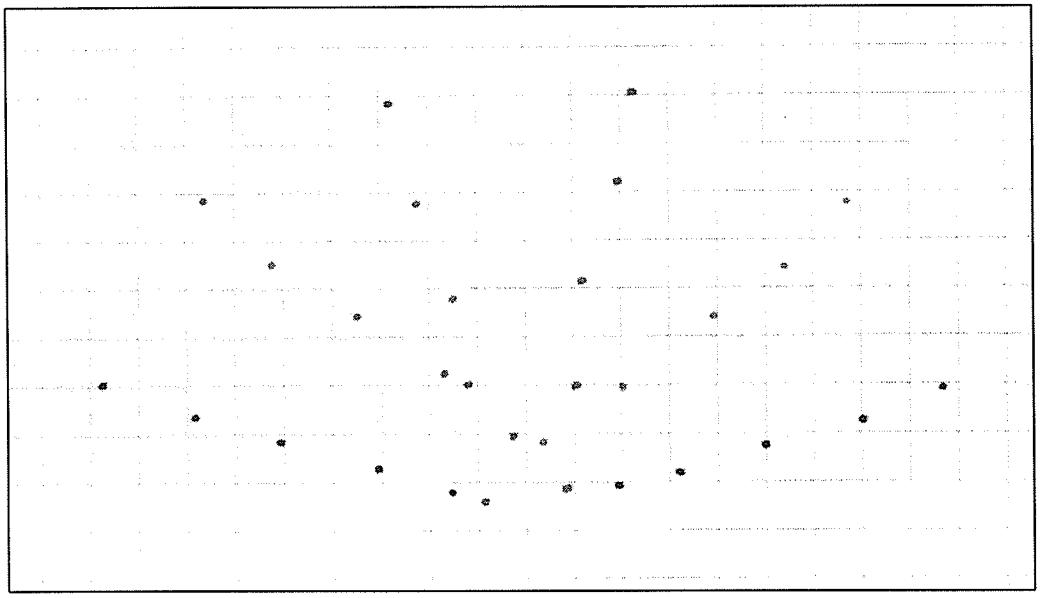

Flexible – Trial 10

		Displacement (mm)	
Rod	Load (g)	Vertical	Horizontal
11	16.16	11.97	2.20
	32.32	25.11	6.97
	48.48	38.64	7.64
	64.64	51.92	9.32
12	16.16	8.49	8.32
	32.32	14.72	17.82
	48.48	24.18	29.83
	64.64	31.29	40.32
13	16.16	3.86	10.46
	32.32	7.30	23.74
	48.48	10.79	34.74
	64.64	12.37	42.72

		Displacement (mm)	
Rod	Load (g)	Vertical	Horizontal
21	16.16	12.89	3.48
	32.32	25.48	8.14
	48.48	36.49	9.94
	64.64	52.20	16.16
22	16.16	8.33	8.93
	32.32	15.45	20.22
	48.48	22.91	20.22
	64.64	30.99	40.47
23	16.16	4.35	11.96
	32.32	7.83	22.93
	48.48	11.01	35.67
	64.64	13.85	45.38

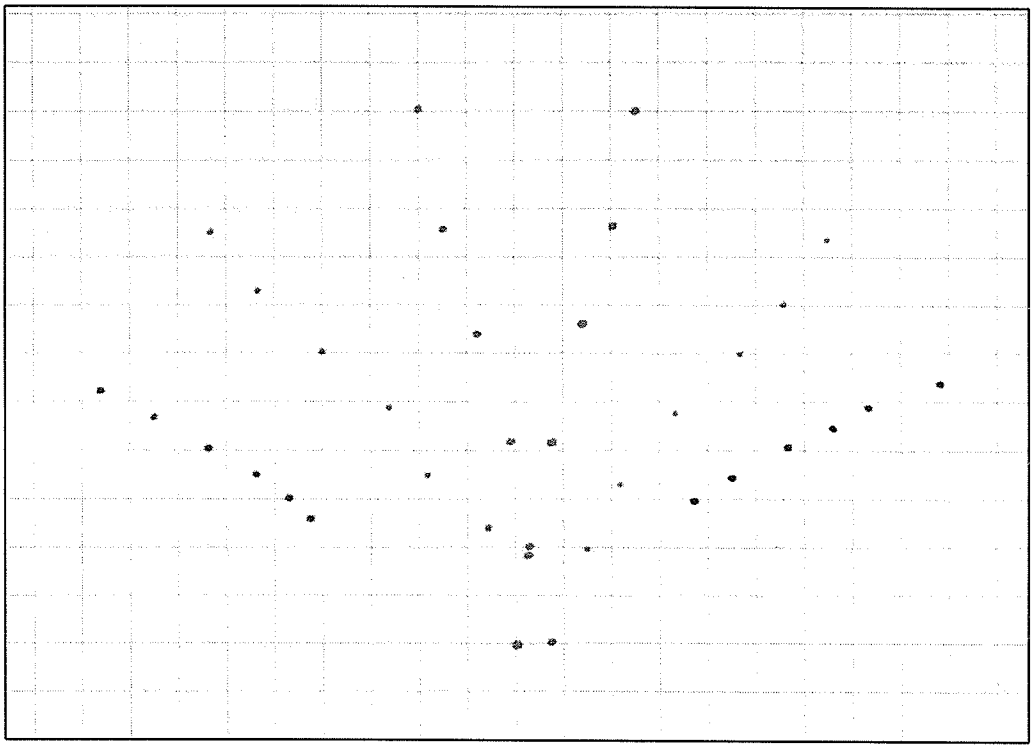

Rigid – Trial 1

		Displacement (mm)	
Rod	Load (g)	Vertical	Horizontal
11	22.30	15.12	3.04
	38.46	28.19	7.04
	54.62	43.42	10.87
	70.78	58.29	14.09
	86.94	15.85	15.85
12	22.30	8.42	5.79
	38.46	14.77	11.52
	54.62	22.73	19.99
	70.78	31.93	27.37
	86.94	31.58	31.58
13	22.30	3.36	9.60
	38.46	5.78	13.94
	54.62	7.97	20.27
	70.78	11.98	27.69
	86.94	32.86	32.86

		Displacement (mm)	
Rod	Load (g)	Vertical	Horizontal
21	22.30	15.97	3.84
	38.46	29.95	8.15
	54.62	43.59	12.48
	70.78	57.98	14.78
	86.94	17.87	17.87
22	22.30	7.93	6.23
	38.46	15.75	14.93
	54.62	23.30	23.72
	70.78	31.92	28.77
	86.94	36.83	36.83
23	22.30	3.43	5.93
	38.46	7.58	12.93
	54.62	10.85	19.06
	70.78	14.14	23.64
	86.94	26.45	26.45

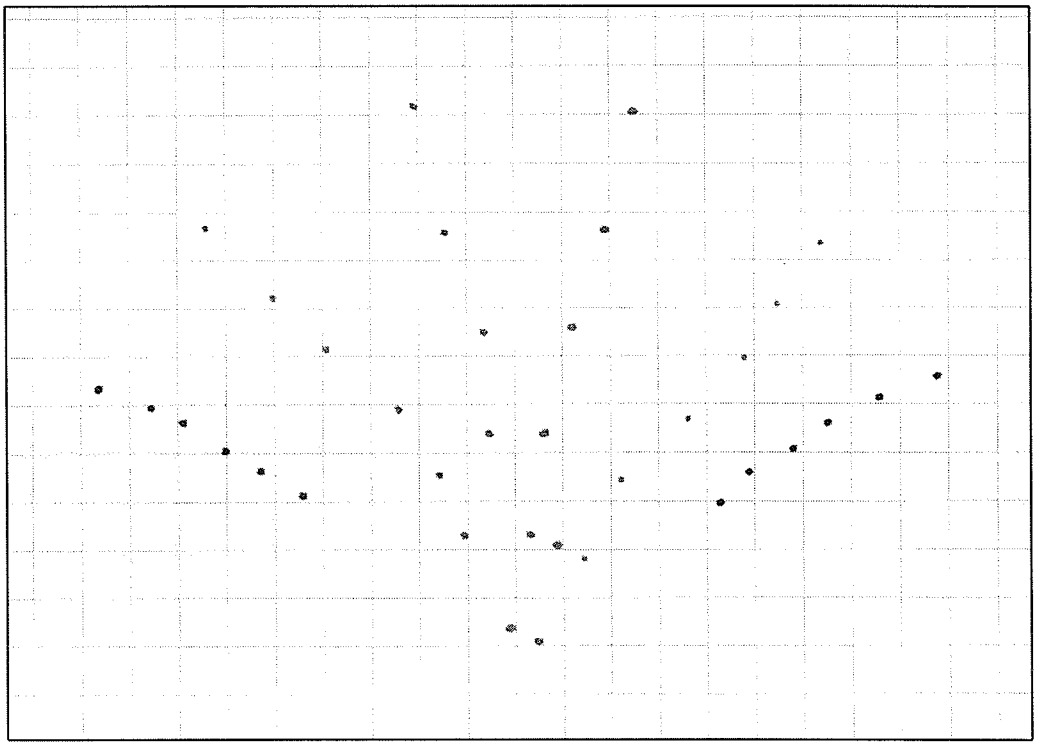

Rigid – Trial 2

		Displacement (mm)	
Rod	Load (g)	Vertical	Horizontal
11	22.30	15.40	3.56
	38.46	28.38	8.08
	54.62	42.23	11.55
	70.78	57.04	10.10
	86.94	67.81	15.90
12	22.30	8.37	5.66
	38.46	15.34	10.13
	54.62	23.62	17.51
	70.78	31.20	26.08
	86.94	41.50	31.35
13	22.30	2.76	7.50
	38.46	5.78	14.19
	54.62	9.24	18.90
	70.78	12.20	24.73
	86.94	16.19	28.14

		Displacement (mm)	
Rod	Load (g)	Vertical	Horizontal
21	22.30	16.75	3.99
	38.46	30.07	9.01
	54.62	43.26	9.64
	70.78	56.63	15.16
	86.94	70.72	16.19
22	22.30	9.17	8.55
	38.46	16.16	15.33
	54.62	23.97	24.69
	70.78	32.52	30.29
	86.94	40.72	33.96
23	22.30	2.58	6.86
	38.46	4.49	11.13
	54.62	8.04	16.53
	70.78	10.75	21.19
	86.94	13.87	26.43

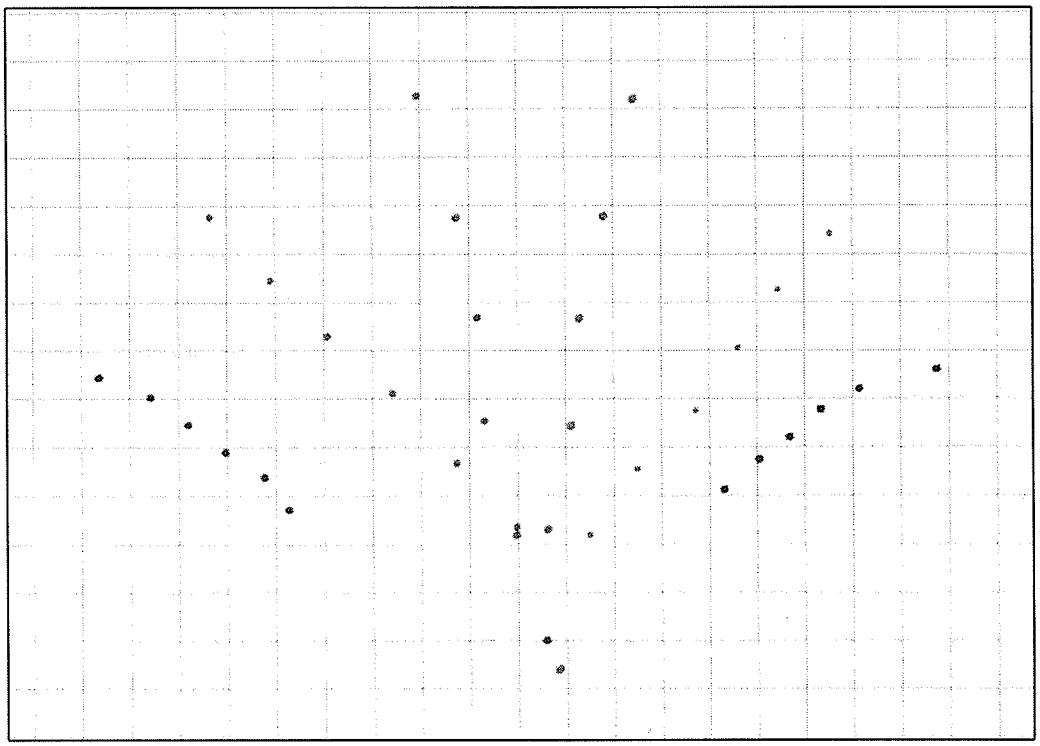

Rigid – Trial 3

		Displacement (mm)	
Rod	Load (g)	Vertical	Horizontal
11	22.30	15.45	3.72
	38.46	28.48	7.11
	54.62	42.96	8.28
	70.78	56.02	11.74
	86.94	74.77	9.68
12	22.30	7.75	6.99
	38.46	15.13	12.13
	54.62	23.26	17.87
	70.78	30.85	25.72
	86.94	39.18	32.13
13	22.30	2.49	9.95
	38.46	5.28	14.68
	54.62	8.73	18.92
	70.78	11.72	23.24
	86.94	15.29	27.74

		Displacement (mm)	
Rod	Load (g)	Vertical	Horizontal
21	22.30	16.07	5.50
	38.46	29.47	8.60
	54.62	43.02	9.11
	70.78	57.53	13.66
	86.94	71.58	19.40
22	22.30	8.16	8.31
	38.46	15.66	15.62
	54.62	23.35	23.99
	70.78	32.19	32.42
	86.94	40.70	40.27
23	22.30	2.34	6.46
	38.46	6.00	11.29
	54.62	9.74	16.19
	70.78	13.00	21.03
	86.94	17.26	24.27

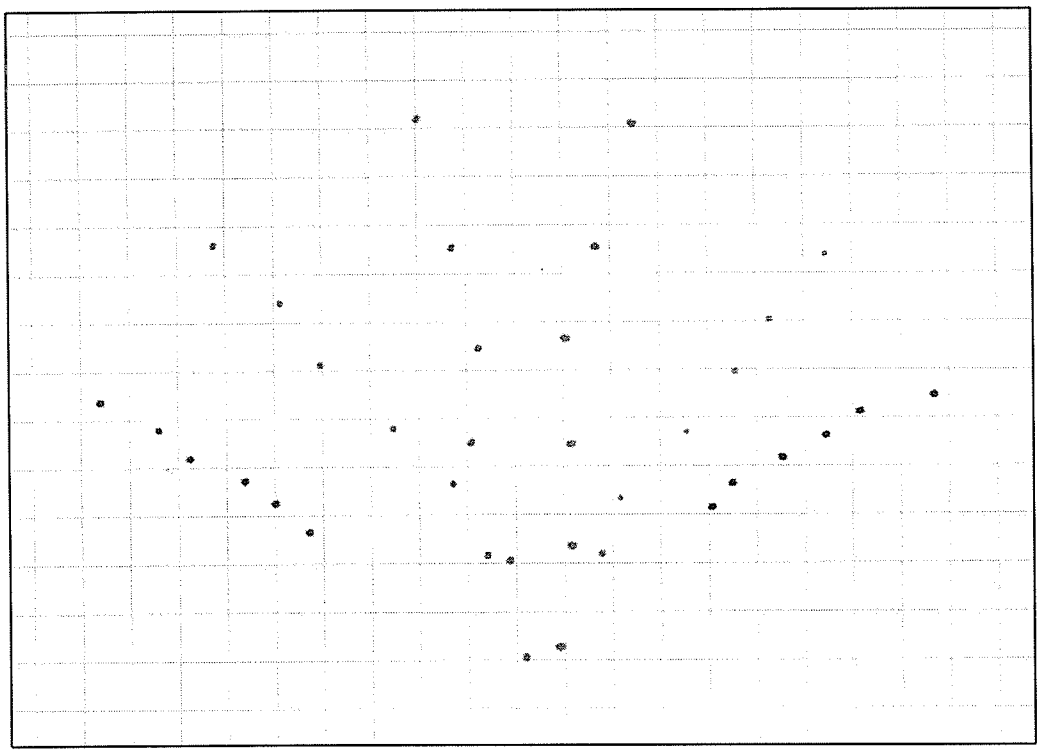

Rigid – Trial 4

		Displacement (mm)	
Rod	Load (g)	Vertical	Horizontal
11	22.30	16.40	5.32
	38.46	28.27	8.85
	54.62	42.14	7.94
	70.78	55.77	7.99
	86.94	68.49	9.88
12	22.30	8.51	7.34
	38.46	15.30	12.08
	54.62	23.40	18.32
	70.78	32.10	27.05
	86.94	39.11	29.31
13	22.30	1.97	9.50
	38.46	5.07	13.92
	54.62	7.99	19.89
	70.78	11.49	26.29
	86.94	14.60	29.09

		Displacement (mm)	
Rod	Load (g)	Vertical	Horizontal
21	22.30	16.62	4.50
	38.46	30.09	7.84
	54.62	42.73	6.99
	70.78	57.83	11.92
	86.94	70.77	13.61
22	22.30	7.78	8.42
	38.46	15.81	13.90
	54.62	24.22	23.50
	70.78	31.65	31.47
	86.94	40.78	36.37
23	22.30	3.50	7.41
	38.46	7.25	11.17
	54.62	10.07	18.66
	70.78	13.44	22.42
	86.94	17.13	27.12

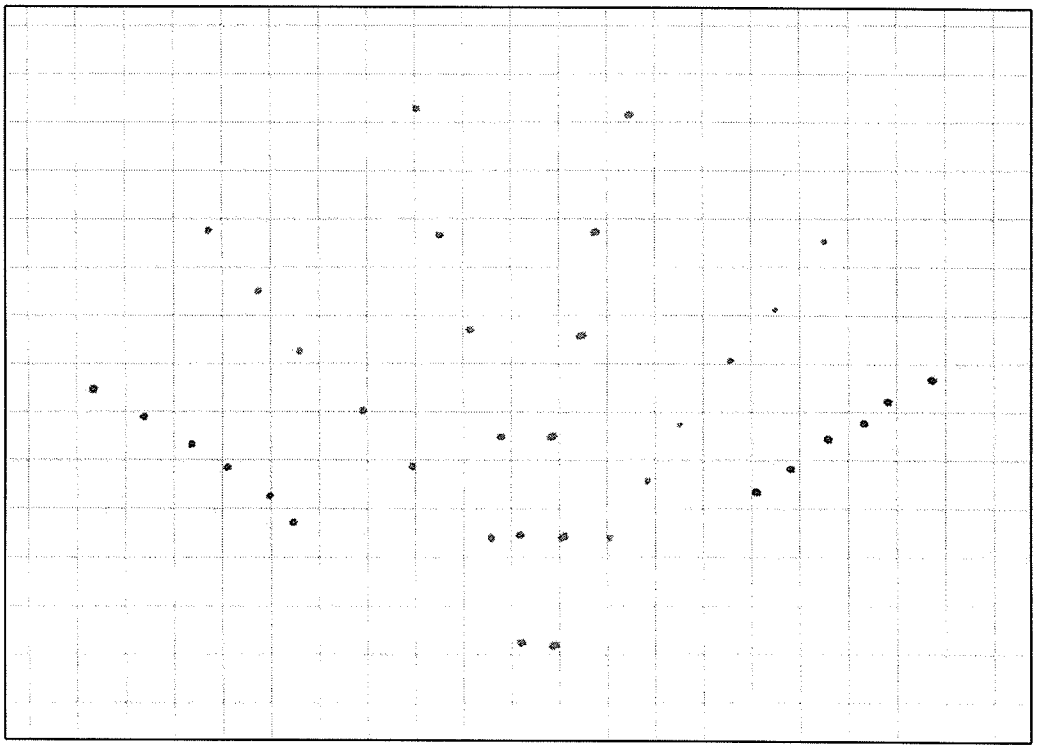

Rigid – Trial 5

		Displacement (mm)	
Rod	Load (g)	Vertical	Horizontal
11	22.30	15.06	4.16
	38.46	28.78	5.79
	54.62	42.52	9.65
	70.78	55.02	7.95
	86.94	69.40	9.02
12	22.30	9.08	6.26
	38.46	15.36	12.29
	54.62	23.92	18.82
	70.78	31.25	23.23
	86.94	38.74	28.13
13	22.30	2.63	5.69
	38.46	5.61	8.62
	54.62	7.52	13.45
	70.78	11.57	18.14
	86.94	14.55	22.82

		Displacement (mm)	
Rod	Load (g)	Vertical	Horizontal
21	22.30	16.52	3.33
	38.46	29.10	7.20
	54.62	43.37	11.33
	70.78	56.22	13.71
	86.94	70.13	13.95
22	22.30	8.28	6.35
	38.46	15.88	11.69
	54.62	23.93	19.97
	70.78	31.12	26.77
	86.94	40.83	37.17
23	22.30	3.45	6.45
	38.46	7.03	12.58
	54.62	10.41	17.00
	70.78	14.39	22.56
	86.94	17.58	25.86

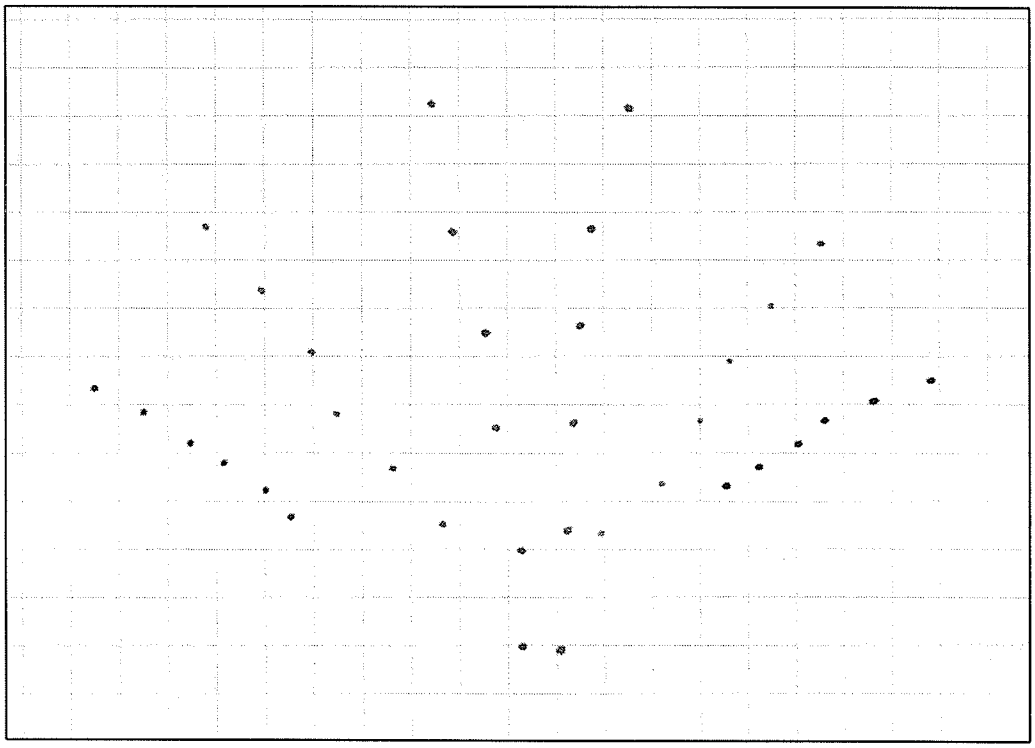

Rigid – Trial 6

		Displacement (mm)	
Rod	Load (g)	Vertical	Horizontal
11	22.30	15.47	4.81
	38.46	28.13	6.51
	54.62	41.18	7.53
	70.78	55.12	8.17
	86.94	70.99	9.32
12	22.30	8.33	6.69
	38.46	15.74	12.09
	54.62	23.51	16.22
	70.78	31.52	21.18
	86.94	38.23	29.45
13	22.30	2.38	7.82
	38.46	4.87	14.24
	54.62	8.27	17.53
	70.78	11.07	23.06
	86.94	13.60	27.40

		Displacement (mm)	
Rod	Load (g)	Vertical	Horizontal
21	22.30	17.33	2.83
	38.46	30.53	6.76
	54.62	43.02	8.12
	70.78	59.24	11.56
	86.94	71.73	11.91
22	22.30	8.44	7.02
	38.46	16.63	13.59
	54.62	24.77	16.62
	70.78	32.21	24.38
	86.94	39.48	30.94
23	22.30	3.83	6.86
	38.46	7.44	13.01
	54.62	10.27	17.55
	70.78	14.13	23.13
	86.94	17.05	26.29

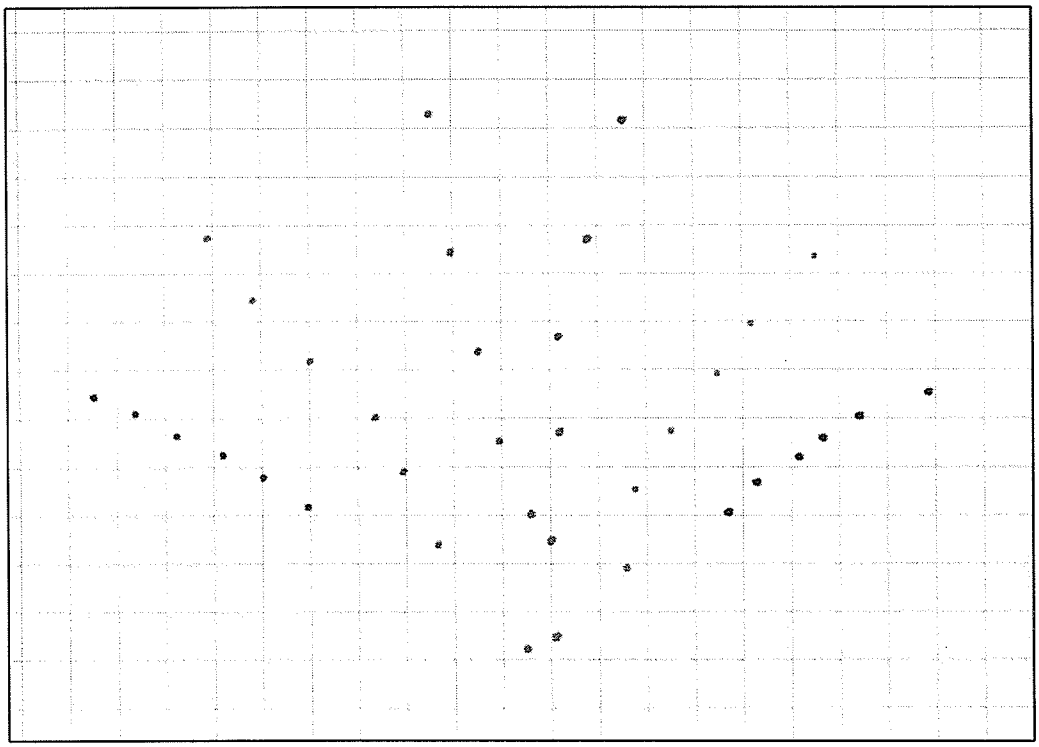

Rigid – Trial 7

		Displacement (mm)	
Rod	Load (g)	Vertical	Horizontal
11	22.30	15.07	5.05
	38.46	28.00	8.73
	54.62	40.67	8.71
	70.78	54.91	9.80
	86.94	67.51	8.76
12	22.30	9.14	8.28
	38.46	15.67	12.81
	54.62	22.97	18.87
	70.78	30.68	23.75
	86.94	40.83	24.76
13	22.30	3.05	9.25
	38.46	5.61	14.03
	54.62	8.27	17.48
	70.78	11.60	22.99
	86.94	15.50	26.53

		Displacement (mm)	
Rod	Load (g)	Vertical	Horizontal
21	22.30	18.28	2.82
	38.46	31.16	6.39
	54.62	43.30	9.09
	70.78	52.46	13.04
	86.94	70.21	12.55
22	22.30	8.18	5.83
	38.46	16.05	13.28
	54.62	23.35	21.50
	70.78	30.64	25.28
	86.94	40.17	29.91
23	22.30	2.40	5.76
	38.46	5.55	10.88
	54.62	8.02	17.22
	70.78	10.67	22.45
	86.94	14.71	28.55

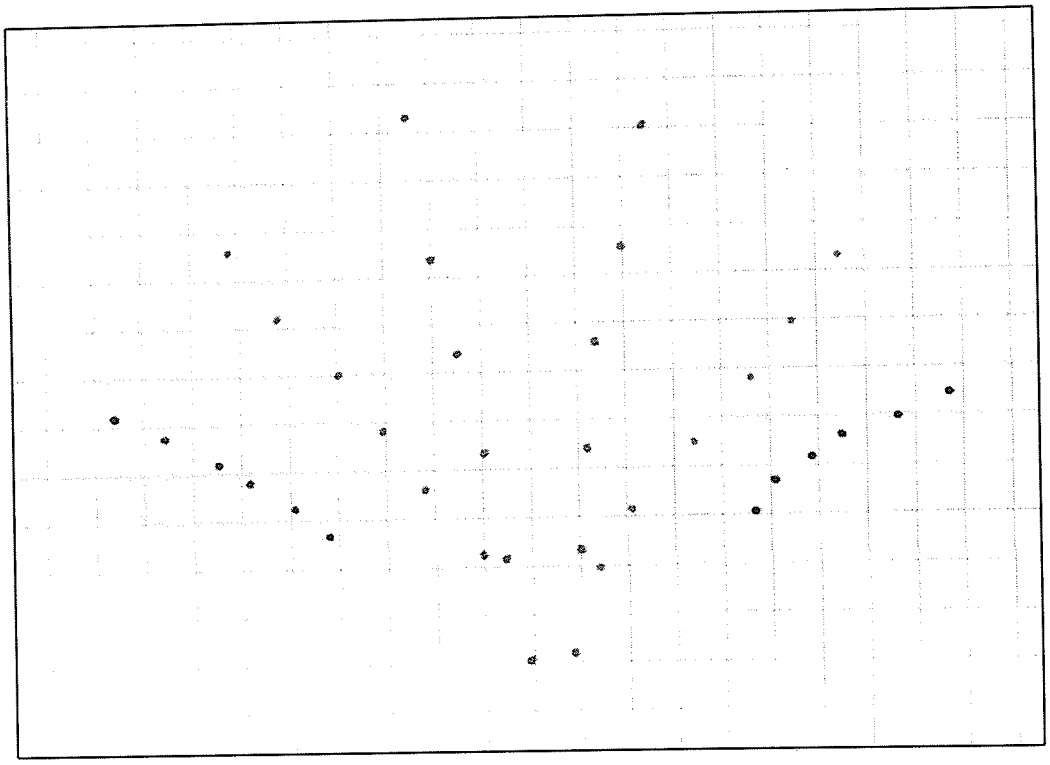

Rigid – Trial 8

		Displacement (mm)	
Rod	Load (g)	Vertical	Horizontal
11	22.30	15.88	3.21
	38.46	28.33	6.95
	54.62	42.25	8.14
	70.78	55.68	9.28
	86.94	68.72	11.07
12	22.30	8.64	6.20
	38.46	16.22	11.73
	54.62	24.32	19.33
	70.78	33.13	27.85
	86.94	40.55	32.50
13	22.30	3.13	6.77
	38.46	5.44	14.18
	54.62	8.21	18.05
	70.78	11.53	22.83
	86.94	15.59	25.82

		Displacement (mm)	
Rod	Load (g)	Vertical	Horizontal
21	22.30	18.87	2.83
	38.46	31.44	5.96
	54.62	44.36	9.29
	70.78	57.91	11.90
	86.94	71.45	14.87
22	22.30	9.01	6.43
	38.46	16.82	14.41
	54.62	24.14	20.33
	70.78	31.91	25.78
	86.94	40.39	33.04
23	22.30	2.63	5.36
	38.46	6.21	12.46
	54.62	8.89	22.48
	70.78	12.58	22.48
	86.94	15.85	27.30

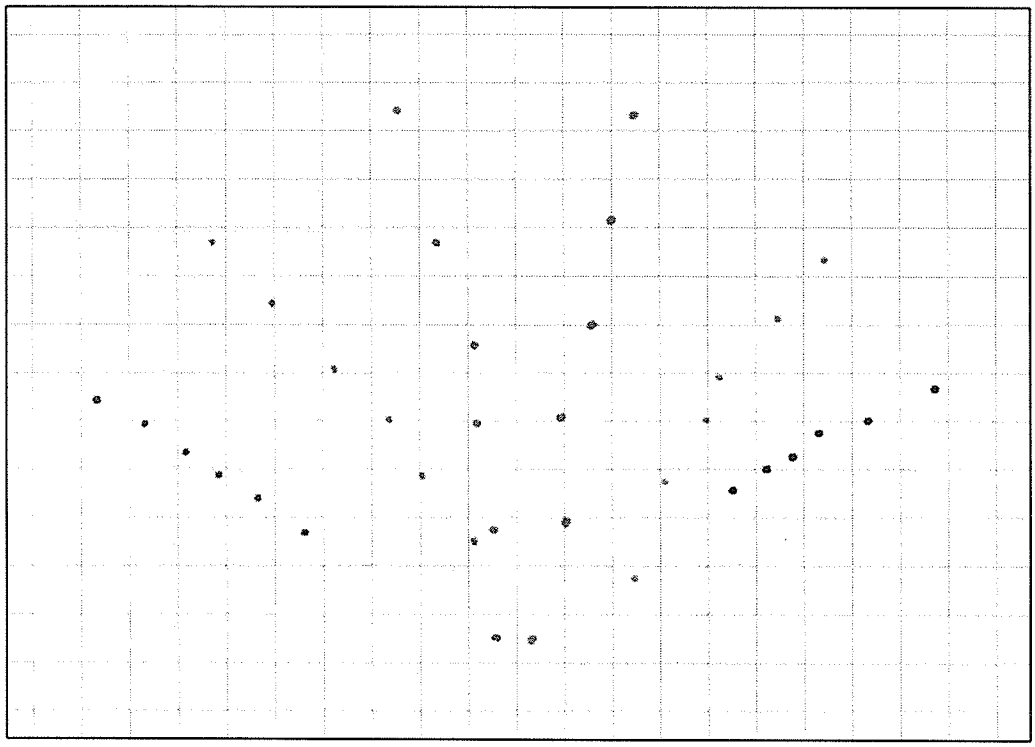

Rigid – Trial 9

		Displacement (mm)	
Rod	Load (g)	Vertical	Horizontal
11	22.30	13.68	3.45
	38.46	27.42	6.10
	54.62	39.43	10.03
	70.78	53.34	9.51
	86.94	68.60	13.97
12	22.30	7.98	6.02
	38.46	15.65	13.81
	54.62	21.44	15.52
	70.78	29.28	20.99
	86.94	42.17	25.08
13	22.30	4.00	8.68
	38.46	5.53	15.25
	54.62	8.89	18.69
	70.78	10.52	22.42
	86.94	13.08	26.55

		Displacement (mm)	
Rod	Load (g)	Vertical	Horizontal
21	22.30	17.58	5.21
	38.46	30.73	9.75
	54.62	41.31	10.32
	70.78	55.30	12.62
	86.94	69.46	12.77
22	22.30	8.10	7.77
	38.46	16.69	16.17
	54.62	23.76	23.15
	70.78	30.89	27.75
	86.94	39.44	34.72
23	22.30	3.22	6.52
	38.46	6.73	11.75
	54.62	9.97	15.83
	70.78	12.85	21.31
	86.94	17.63	27.25

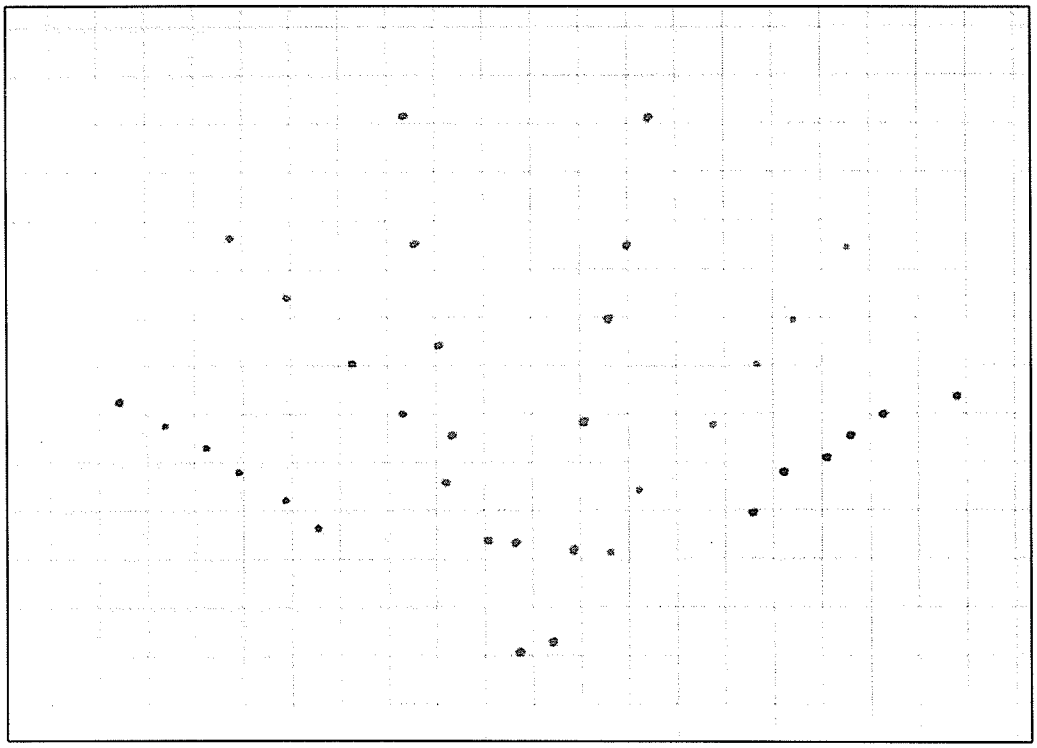

Rigid – Trial 10

		Displacement (mm)	
Rod	Load (g)	Vertical	Horizontal
11	22.30	16.43	3.07
	38.46	26.22	5.43
	54.62	39.81	8.46
	70.78	56.46	13.13
	86.94	68.34	13.13
12	22.30	9.54	7.04
	38.46	15.28	11.76
	54.62	23.21	17.86
	70.78	32.03	27.61
	86.94	40.25	31.13
13	22.30	2.54	9.44
	38.46	5.26	14.16
	54.62	8.07	17.32
	70.78	10.24	23.07
	86.94	14.95	26.83

		Displacement (mm)	
Rod	Load (g)	Vertical	Horizontal
21	22.30	16.64	1.72
	38.46	29.93	4.42
	54.62	41.99	6.13
	70.78	56.10	14.47
	86.94	70.38	14.82
22	22.30	7.81	7.47
	38.46	16.40	16.23
	54.62	23.16	22.72
	70.78	31.82	28.59
	86.94	39.72	34.16
23	22.30	3.50	6.08
	38.46	6.48	11.47
	54.62	9.64	15.90
	70.78	13.06	21.78
	86.94	16.54	26.16

APPENDIX 3 SCHEMATIC DIAGRAMS OF APPARATUS

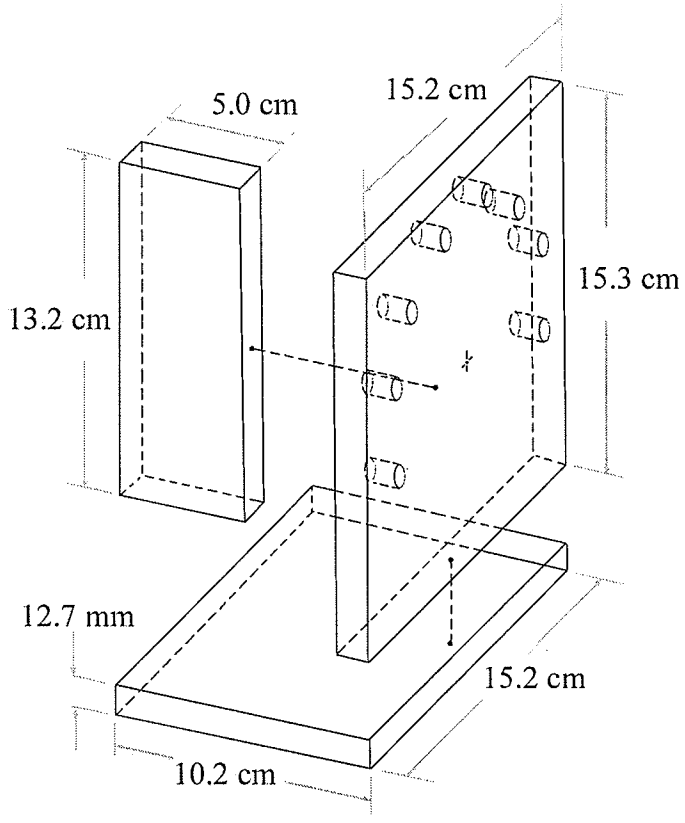

Exploded diagram of jig.

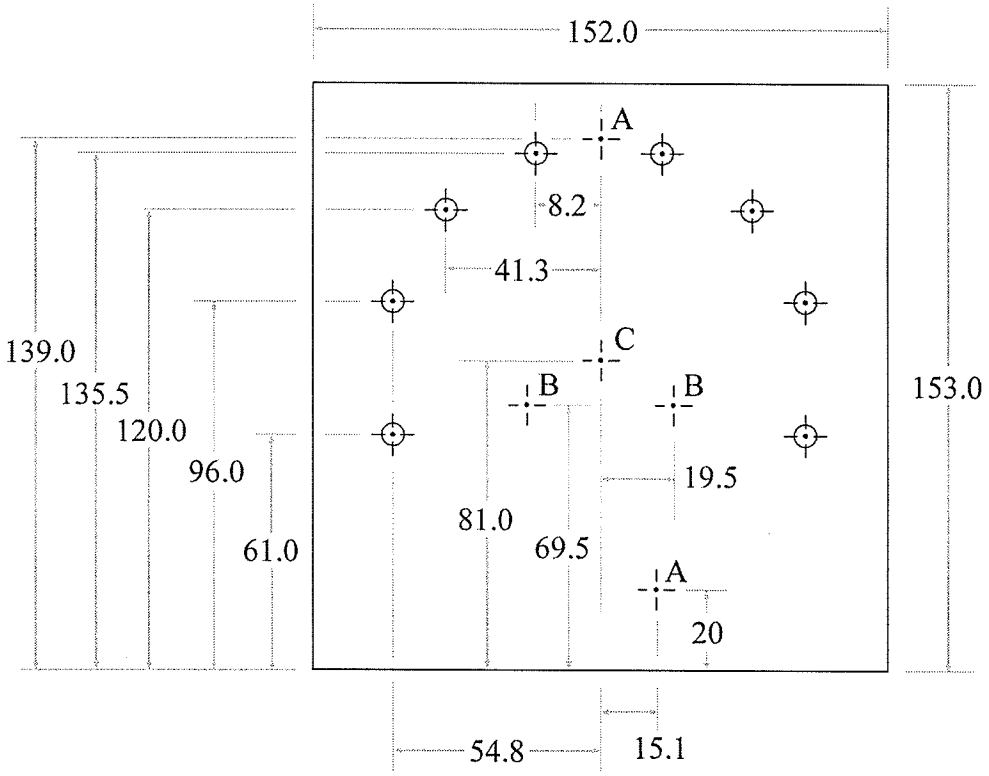

Drilling diagram of apparatus. All measurements are in millimeters. Holes indicated by the letter **A** are 1/8 inch (3.18 mm) in diameter for the light emitter reference points. Holes indicated by the letter **B** are 1/16 inch (1.59 mm) in diameter for the securing screws of the guide jig (used to steady the rods representing premolars distal the canine rods). The letter **C** indicates the centre of the semicircle on which the central incisor, lateral incisor and canine rods are located.